Role of HIPP cells in the dentate gyrus during fear memory formation

Dissertation

zur Erlangung des akademischen Grades

doctor rerum naturalium

(Dr. rer. nat.)

genehmigt durch die Fakultät für Naturwissenschaften

der Otto-von-Guericke-Universität Magdeburg

von   DVM, M.Sc. Syed Ahsan Raza

geb. am   20.11.1984   in   Lahore, Pakistan

Gutachter: Prof. Dr. Oliver Stork

Prof. Dr. Michael Koch

eingereicht am: 27.08.2017

verteidigt am: 31.01.2018

…. Philosophers suggested that the way the mind creates ideas is by forming associations between events

(Fanselow and Wassum, 2016)

Declaration of Authorship – *Erklärung*

Hiermit erkläre ich, Syed Ahsan Raza, dass ich die von mir eingereichte Dissertation zum dem Thema

'Role of HIPP cells in the dentate gyrus during fear memory formation'

selbständig verfasst, nicht schon als Dissertation verwendet habe und alle benutzten Quellen und Hilfsmittel vollständig angegeben habe.

Weiters erkläre ich, dass ich weder diese noch eine andere Arbeit zur Erlangung des akademischen Grades doctor rerum naturalium (Dr. rer. nat.) an anderen Einrichtungen eingereicht habe.

Unterschrift:

Ort, Datum: Magdeburg, 27.08.2017

Acknowledgements

This thesis represents a milestone for me which I achieved working for more than half a decade at OvGU within the *Genetics and Molecular Neurobiology* Laboratory. My experience at OvGU has been amazing during this tenure and I would like to thank a lot of people who one-way or another help me in achieving my goals till now.

First and formost, I would like to thank my advisor, Prof. Dr. Oliver Stork for providing me opportunity to work in his lab. I remember the day in May of 2011 when I was waiting for him at the main train station in Magdeburg and he received me with a big smile. Since that day, during my Master's thesis and during my PhD, he is been supportive in all aspects. I always love when he says 'go for it' to my scientific ideas. This amazing attitude as well as his tremendous patience helped me in developing the knowledge and skills that I possess now.

I am very grateful to my parents, my siblings and my wonderful wife, who have provided me through moral and emotional support in my life. A sincere gratitude to my friend Dr. Waqas Azeem, without him I would not have been in Europe.

A very special gratitude goes out to all my lab members. With a special mention to Dr. Anne Albrecht, who was an amazing help in this path and I literally followed her footsteps. Many thanks for reading and critically commenting on my thesis as well. I am very thankful to Dr. Jorge Bergado-Acosta for teaching me stereotaxy. I would like to specially mention Dr. Iris Müller and Dr. Jan Teuber for helping me in scientific endeavors but especially in everyday matters.

I would like to thank Deniz A. Madencioglu for proof reading my thesis and wonderful smiles she got. I am thankful to Dr. Gürsel Çalışakan for his scientific inputs in my thesis work. Many thanks to all past and present members in Stork's lab, Dr. Bettina Müller, Dr. Kiran Sandhu, Dr. Monica Santos, Daniel Lang, Emre Kul and Yunus E. Demiray, who created wonderful working environment in the lab.

I would like to thank Simone Stork, Franziska Webers and Antja K. von Hoff for perfect lab assistance and also many thanks to Theresa Porzucek and Annabella Bohnsted for an excellent animal care.

Last but not the least, to all people in science for their inspirational scientific work.

Summary

Role of HIPP cells in the dentate gyrus during fear memory formation

Syed Ahsan Raza DVM, MSc

Pavlovian fear conditioning employs the association of aversive and an elemental stimulus. As a result of this association, the elemental stimulus becomes a predictor of aversive reinforcement while the conditioning context becomes a partial predictor and processed in the background. By contrast, in the absence of such explicit predictor, the fear-eliciting context as a whole becomes a sole predictor and processed in the foreground. Thus, the salience of different contextual and elemental components of the reinforced stimulus configurations must be encoded. The dentate gyrus (DG) uniquely separates specific patterns and critically evaluates contextual background in classical conditioning paradigms. Altered background context conditioning has been implicated in disturbed specificity of trauma-related memories and their associated intrusive re-experiencing in posttraumatic stress disorder.

While cumulative evidence points out a pivotal role of the hippocampal formation and its cholinergic modulation in these processes, local circuits underlying this phenomenon are unknown. In this study, I provide evidence with pharmacogenetic inhibition that the neuropeptide Y (NPY)-positive hilar perforant path-associated (HIPP) cell mediates the devaluation of background context memory during fear conditioning. The expression of dominant negative CREB in HIPP cells reduces the expression of NPY and disrupts the adjustment of background salience. The NPY-dependent adjustment of the background context salience by HIPP cells is further confirmed with acute blockage of the NPY-Y1 receptor signaling in the DG during background context conditioning. No comparable effects of the HIPP cell manipulation are observed on foreground context memory, acquired during unpaired stimulus presentation or in the absence of an elemental predictor and when tested during retrieval session. I demonstrate that the HIPP cells are driven by cholinergic transmission via M1 muscarinic receptors and in this way contribute to the inhibitory effects of acetylcholine in the DG. Finally, I show that the HIPP cell specific knockdown of M1 receptors enhances the salience of background context. Collectively, the data furnish novel evidence for an adaptive local peptidergic circuit in the DG that mediates the cholinergic encoding of background context salience via NPY during acquisition of fear memory.

Zusammenfassung

Role of HIPP cells in the dentate gyrus during fear memory formation

Syed Ahsan Raza DVM, MSc

Klassische Furchtkonditionierung nach Pavlov beinhaltet die Assoziation eines diskreten und anfangs neutralen Reizes (konditionierter Reiz; meist ein Ton) mit einem furchtauslösenden, aversiven Reizes (unkonditionierter Reiz; meist ein elektrischer Fußschock). Nach wiederholter Paarung beider Reize wird ersterer Reiz zum Indikator des aversiven Stimulus und erlangt dadurch furchtauslösende Eigenschaften. Der Kontext, in dem diese Assoziation stattfindet, wird zwar auch erinnert, tritt jedoch in den Hintergrund, da dieser nicht primär den aversiven Reiz vorhersagt. Im Gegensatz dazu wird bei Fehlen eines diskreten Reizes der Konditionierungskontext als solcher zum Indikator des aversiven Stimulus, er tritt also in den Vordergrund. Dieses Paradigma wird daher auch Vordergrundkontextkonditionierung genannt. Die Gedächtnisbildung hängt also von der Salienz und dem Gleichgewicht dieser beiden Faktoren, konditionierter Stimulus und Kontext, ab. Aufgrund seiner herausragenden Rolle bei der Mustertrennung, wurde der Gyrus Dentatus (GD) des Hippocampus auch in diesem Zusammenhang als kritisch identifiziert.

Obwohl umfangreiche Literatur den Hippokampus und seine cholinerge Modulation als essentiell für diese Prozessen identifizert hat, ist die zugrundeliegende neuronale Verschaltung noch weitgehend unbekannt. Die Untersuchung dieser Mechanismen ist Gegenstand der vorliegenden Arbeit. Mithilfe pharmakogenetischer Intervention konnte ich nachweisen, dass Neuropeptid-Y (NPY)-positive, hiläre perforant-path assoziierte (HIPP) Zellen im dorsalen Gyrus Dentatus an der Unterdrückung des Hintergrundkontextes während der Furchtkonditionierung mitwirken. Die gezielte Expression von dominant negativem CREB in HIPP-Zellen reduzierte die NPY Expression und erhöhte die Salienz des Hintergrundkontextes. Diese NPY-abhängige Regulation des Hintergrundkontextes konnte ich in einem nächsten Schritt durch die akute Blockade des postsynaptischen NPY-Y1 Rezeptors im GD bestätigen. Keine vergleichbaren Effekte zeigten sich bei der Manipulaion von HIPP-Zellen in einem Vordergrundkonditionierungsparadigma oder bei der ungepaarten Präsentation des diskreten und des aversiven Reizes.

Des Weiteren konnte ich zeigen, dass die Aktivierung der HIPP-Zellen von cholinerger Transmission durch den M1-Rezeptor abhängt. HIPP-Zellen tragen zur

Acetylcholin-vermittelten Hemmung im GD bei. Dieses Ergebnis konnte ich weiter untermauern durch den HIPP-Zell-spezifischen knock down des M1-Rezeptors. Dies führte zu einer Erhöhung der Hintergrundkontextsalienz.

Zusammenfassend, konnte ich in meiner Dissertation einen lokalen, peptidergen Schaltkreis im Gyrus dentatus indentifizieren, der mithilfe von NPY-positiven HIPP-Zellen die Hintergrundkontextsalienz während der Furchtgedächtnisbildung vermittelt.

Table of Contents

Abbreviations

ACC	Anterior cingulate cortex
ACh	Acetylcholine
aCSF	Artificial cerebrospinal fluid
AMPA	α-amino-3-hydroxy-5-methyl-4-isoxazole propionic acid
BLA	Basolateral amygdala
BM	Basomedial amygdala
CA	cornu ammonis
Ca^{2+}	Calcium ions
CaMKII	Calcium/calmodulin dependent protein kinase II alpha
CeA	Central nucleus of amygdala
CeL	Lateral nucleus of amygdala
CeM	Medial nucleus of amygdala
Chat	Cholineacetyltransferase
Chrm1	Cholinergic muscarinic receptors type 1
Cl^-	Chloride ions
CNO	clozapine-N-oxide
CR	Conditional response
Cre	cAMP response elements
CREB	cAMP/Ca^{2+} response element binding protein
CS	Conditional stimulus
dB	Decibels
DG	dentate gyrus
DMEM	Dulbeccos Modified Eagles Medium
DREADD	Designer receptors exclusively activated via designer drug
EC	Entorhinal cortex
ERT2	Estrogen receptor type 2
GABA	Gamma amino butyric acid
GAD	Glutamic acid decarboxylase
GAPDH	Glyceraldehyde 3-phosphate dehydrogenase
GFP	Green fluorescent protein
HCO_3	Bicabonate ions
HICAP	Hilar commissural-association pathway-related cells

HIPP	Hilar inhibitory perforant path associated cells
HPA	Hypothalamic-pituitary-adrenal
I/O	Input-output
ICM	Intercalated cell mass
IL	Infra-limbic cortex
IPSPs	Inhibitory post-synaptic potentials
ISI	Inter-stimulus interval
KA	Kainate
kHz	Kilo hertz
LA	Lateral amygdala
LCM	Laser capture micro-dissection
LTP	Long-term potentiation
mA	Mili Ampere
mAChR	Metabotropic muscarinic receptors
MAPK	Mitogen activated protein kinase
MOPP	Molecular layer perforant path-associated cells
mPFC	Medial prefrontal cortex
nAChR	Ionotropic nicotinic receptors
NMDA	N-methyl-D-aspartate
NPY	neuropeptide Y
PBS	Phosphate buffer saline
PFA	Paraformaldehyde
PKA	Protein kinase A
PKC	Protein kinase C
PL	Pre -limbic cortex
PS	Population spike
PV	Parvalbumin
SST	Somatostatin
US	Unconditional stimulus

1. Introduction

Memories – the phenomenon of learning new information and storing it for subsequent recall – are stored in the mammalian nervous system as alterations in the strength of synaptic connections among neurons. This relates to the fact that exhibition of behavior by an animal is a result of underlying activity in its nervous system. Thus in simple terms, a change in animals' behavior pattern in response to an experience is referred as learning. Combining these terms, learning is when animal acquires new information and memory is when it recalls that information. In the area of neurobiology of learning and memory, the experimental animal, a rodent, is said to have a memory formation when it expresses a behavior in the recall (test) session different to what it showed during the learning (training) session (Sweatt, 2009). It can be viewed as a lasting trace of past experiences that influences current or future behavior.

Memories are classified according to many different criteria. The duration over which information in memory remains available lasts from seconds 'short-term memory' to years 'long-term memory' (Izquierdo et al., 1999). This distinction is based on the number of times an animal experiences a stimulus that modifies its behavior. A single stimulus is likely to last over short term while repetition of behavior-modifying stimuli could even prolong over life span of an animal. The biological processes that lead to establishing a memory include acquisition and consolidation. During acquisition, the new information is encoded which is then stabilized and stored via a consolidation process. Recall of this stored information at a later time point is termed as retrieval (Dudai, 2004). Another process where the learned response is gradually reduced is termed as extinction (Maren et al., 2001). Long-term memory is often divided on the basis of its content and the level of consciousness during learning, and termed explicit/declarative (knowing what) vs. implicit/non-declarative (knowing how) memories (Squire et al, 1984). The explicit memories include conscious recollection of the facts and events e.g. in humans remembering faces, places, names, and/or dates while implicit memories include sensory or motor abilities and do not depend upon consciousness e.g. driving a car, playing football and/or spelling a word. Memories are also classified on their nature and referred as associative vs. non-associative memories (Fig. 1.1). The non-associative memories do not require an animal forming any association between one environmental stimulus to another and is more likely an unconscious learning which

includes habituation, dis-habituation and sensitization. The associative form of learning is more complex and importance of acquired associations in shaping behavior has been emphasized over time. Associations result from experiencing certain events in close temporal proximity. The establishment of association between two events takes place in two types of relationships, one when two stimuli are experienced close in time (Pavlov, 1927) and the other when a behavior is followed closely by a stimulus (Thorndike, 1898). The pioneering work in associative learning is lead by Ivan Pavlov where he trained a dog to associate a bell ring (neutral stimulus) with the food stimulus and over time the dog could form association between the bell and food. The bell becomes conditioned stimulus that produces a conditioned response in the dog in the form of salivation. This type of learning (Pavlovian/classical conditioning) is extremely important in any natural environment for survival. The other form of associative learning is instrumental conditioning in which the environment is arranged in a way that the animal has to show a necessary response in order to obtain some result such as avoiding a painful stimulus or receiving food. Importantly, the type of learning and memory that is considered to comprise conscious state consisting not only the associative but also non-associative components caused by exposure to real as well as imagined threats is termed as 'fear memory'. Learning motivated by fear is very prevalent and is the most powerful form of emotional learning that provides a lasting influence on the individuals and has a strong survival value (Costanzi et al., 2011). Building on the innate fear, learning motivated by fear gives the animal an ability to learn by experience that some circumstances predict danger and predominantly this type of learning is the key to its survival in the wild. Due to its prevalence and lasting nature, fear motivated learning is the most widely studied form of learning and memory.
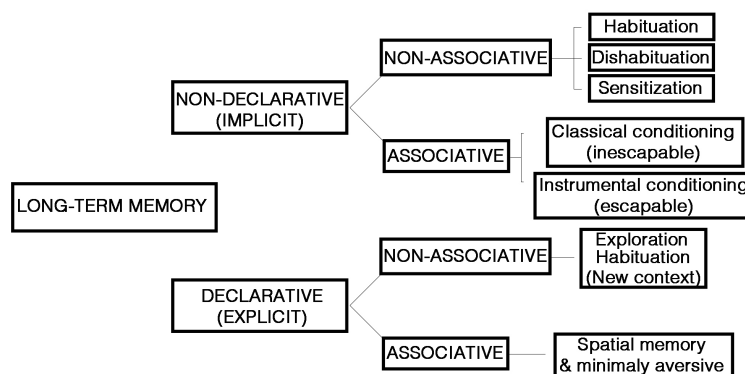

Fig. 1.1: Taxonomic classification of long-term memory types. A possible classification of long-term memory observed in rodents along with some examples of the behavioral tasks that

are related to these particular form of memories (Adapted with modifications from Jorge A. Quillfeldt, 2006).

1.1 Fear-motivated learning

In fear motivated learning, an individual learns to avert fear (humans) or learns to avert a putative fear like state (animals). There lies a high degree of emotional arousal between acquisition and consolidation of fear motivated learning that is known to enhance memory consolidation. Because of this emotional arousal, fear motivated learning give rise to one of the strongest, finely detailed and long lasting memories (Cahill and McGaugh, 1998; McGaugh, 2013). The lack of fear is inherently dangerous and potentially lethal. Fear conditioning is the fundamental form of learning in which animals learn to predict aversive events and showcase appropriate reaction to threats. It is studied via classical (Pavlovian conditioning) and/or instrumental (avoidance) conditioning. For the cause of simplicity and the relevance to the current study, only Pavlovian conditioning is discussed here.

1.1.1 Pavlovian fear conditioning

Pavlovian fear conditioning is a popular and powerful technique and is squarely seated at the interface of memory and emotion (LeDoux, 2000). This is employed largely for studying learning and memory in animal models, primarily because it not only attains behavior quickly but also the behavioral expression is consistent and easily measured, as well as depends on the well-characterized core neural circuits. Fear conditioning or sometimes called threat conditioning (LeDoux, 2014), occurs by pairing of an initially harmless conditional stimulus (CS, e.g. auditory tone, light or the environment as a whole) with an aversive unconditional stimulus (US, e.g. foot shock). As a result of this CS-US association, the CS acquires aversive properties and results in a fear response or conditioned response (CR) even when presented alone (Maren, 2001). In rodents, the CR is exhibited via a freezing behavior (complete immobility except for respiratory movement) (Blanchard and Blanchard, 1969) and is tested in the memory retrieval session by re-exposing the animal to the CSs. Freezing is a typical defensive behavioral representation of rodents' natural response to threats. In simple terms, rodents forge at night to reduce the encounter with predators but if there is an encounter with a predator, the rodent freezes to reduce the likelihood of an attack. However, if there is a predator-prey contact then rodents stop freezing and make strong efforts to escape. Thus, in fear conditioning the CR is one step lower than the actual response to the US (the post-encounter

3

phase when predator has been detected) (Fanselow, 1989). Thereof, the animal shows vigorous activity bursts at the presentation of foot shock while only a freezing response at the presentation of foot shock-paired CS. Other physiological responses in rodents at freezing include change in the heart rate, an increase in the blood pressure accompanied by shallow and rapid breathing, endocrine responses and decreased pain sensitivity (LeDoux, 2000) (Fig. 1.2).
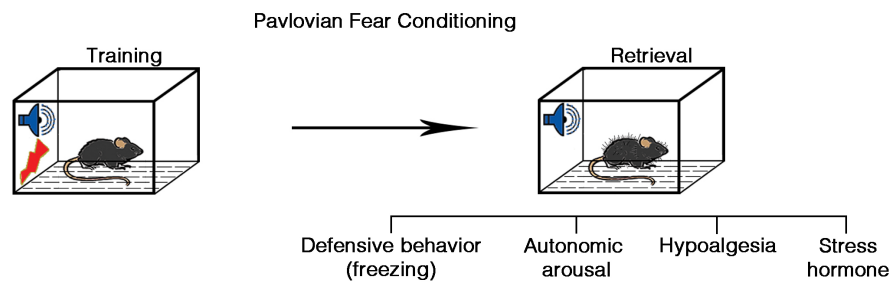
Fig. 1.2: Pavlovian conditioning paradigm with the depiction of conditional response in rodents. During conditioning, auditory tones and foot shocks are presented together and the animal forms association of the aversive stimulus with the tone as well as the conditioning context. On memory retrieval, the animal shows conditioning responses mainly characterize by freezing; however, other responses related to fear are also observed in the absence of foot shocks.

During Pavlovian conditioning, multiple forms of learning may occur (Fig. 1.3). The level of conditioning in different learning forms is based on the nature of a CS-US predictive relationship. The animal remembers an aversive event or the CS-US association, however on top of that it is also plausible to show that the animal forms independent memories of each of the single events or for components of the aversive event or episode. Generally, the situational cues also influence conditioning; one prominent example is the conditioning context, which naturally competes with the CSs (Rescorla and Wagner, 1972). Thus, a context that contains multiple cues with different sensory modalities such as odor, texture, shape and noise is also a significant contributor to the conditioning. Therefore, in the classical conditioning paradigm, a coincidence of the US in association with a discrete CS in a context that carries stable features results in a combined contextual and elemental CS conditioning. Herein, the best predictor gains association strength at the cost of other potential predictors. Thus, if the elemental CS lacks significant predictive value for the US, it would drive the associative strength of the context and the contextual information is processed as 'foreground context' and can provoke full conditional response upon subsequent exposure to the conditioning context. This type of

conditioning where the context becomes more salient and gains prediction is termed as the foreground (unpaired) context conditioning. By contrast, a systematic pairing of the elemental CS with the US results in an incidental learning of the conditioning context. As a result, the elemental CS achieves association strength and the contextual information is processes as 'background context'. This type of conditioning where the conditioning salience loads on the elemental CS which becomes a sole predictor while the subsequent conditioning context exposure alone evokes only a partial response is termed as the background (paired) context conditioning (Phillips and LeDoux, 1992). The abovementioned conditioning procedures thus result in either a predominant context-US or a CS-US association (Desmedt et al., 1999). In yet another conditioning paradigm, the combined contextual information gains association strength to the US in the absence of an elemental CS and in return generates full conditional response upon subsequent context exposure. Here the CS is not restricted to a single sensory modality but the conditioning context, as a whole along with other contextual sensory modalities, becomes the sole predictor of the US. This form of conditioning is named as the pure contextual conditioning. In short, the salience of training condition loads onto the CS in the background context conditioning while in the foreground and pure context conditioning, the context becomes the salience determinant.
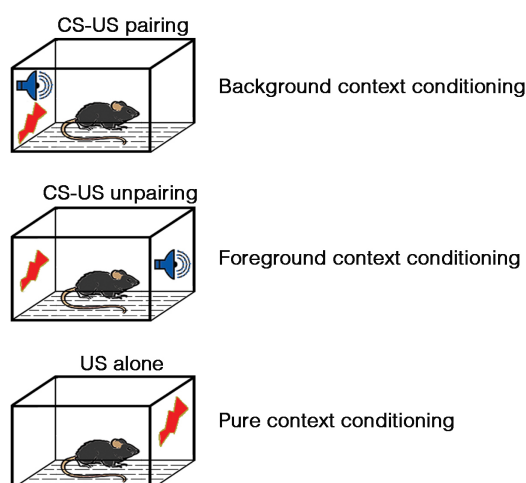
Fig. 1.3: Conditioning paradigms used in this work. These conditioning paradigms are widely used to study multiple forms of fear learning that depend on the associative strength of different stimuli.

Here it is worth mentioning that if a choice is given between two environments that provide equivalent intensity of foot shocks except that in one of the environments the foot shock is un-signaled and in the other the CS-tone (signaled) precedes a foot

shock; rodents choose the signaled shock environment. This occurs because a rodent would naturally prefer the least frightening context as the CS-tone overshadows the context in signaled (background) conditioning leading to a partial response (Lockard, 1963; Fanselow, 1980). Of note, the CSs condition better when they precede the US and the temporal association of the context-US requires some minimal time for conditioning to occur. The immediate delivery of the US upon placement of an animal in the context would be unable to produce conditioning and subsequent freezing response (Fanselow, 2010).

The neuronal basis of fear is well conserved across species and is supported by the animal and human studies (Phelps and LeDoux, 2005). In the past years, the neurobiological mechanisms of fear conditioning are extensively studied and a speedy progress is being made in the identification of fear memory circuits that control the elements of fear conditioning. It is true in part because it is easily implemented only by few CS-US presentations leading to the formation of lasting and quantifiable memory (Gale et al., 2004) and another important aspect of this paradigm's popularity is an indication that the human anxiety disorders typically results from abnormal fear learning regulation by irregular activity patterns in the cerebral networks and dysregulation of normal fear learning mechanisms (Bremner et al., 2003; Bouton et al., 2006; Graham and Milad, 2011).

1.2 Fear memory circuits

The modern work on the brain circuits involved in fear memory emerged from decades of lesion, pharmacological and genetic studies. Recent technical developments that include genetic rodent models, manipulation of specific neuronal elements, optogenetic manipulations and electrophysiological recordings of neuronal populations have largely enhanced the understanding of modern day neurobiology to not only dissect but also understand the function of individual neuronal circuits that regulate fear behaviors. Two brain regions that have gained particular importance, in recent years, are the amygdala and hippocampus. However, other brain regions are also important that have specific roles in the elements of fear learning (Kandel et al., 2014; Izquierdo et al., 2016).

1.2.1 Amygdala – a threat center

The amygdala, an almond shaped heterogeneous structure located in the medial temporal lobe, is a critical component of the neural circuitry underlying fear

learning. It is composed of distinct nuclei that differ on the basis of cell type, density, connectivity and neurochemical composition (LeDoux, 2000; Swanson, 2003). The main nuclei that play their part in a conditioned fear include the basolateral complex (BLA), which is subdivided in to the lateral (LA), basolateral (BL) and basomedial (BM) nuclei; the central nucleus (CeA) containing the lateral (CeL) and medial (CeM) sectors; and the intercalated cell mass (ICM). The main entry site of sensory inputs to the amygdala is the LA that receives auditory, gustatory, visual, olfactory and somatosensory information from the thalamus and cortex (Fig. 1.4). In case of a background context conditioning, the LA receives information about the CS via thalamic and cortical projections. This thalamo-cortical pathway is responsible for the transmission of rapid but crude information about fear eliciting stimulus, which is not filtered by conscious control. By contrast, the cortico-amygdala pathway is slower but provides detailed as well as sophisticated sensory information. The LA is the site of convergence for the CS-US association and plays a major role in learning related plasticity. A damage or disruption of the LA prevents fear conditioning (LeDoux, 2007) and is also a site of fear memory consolidation converting short-term memory to long-term memory (Dudai, 2004). The central nucleus, CeA, is the main source of the amygdala projections to fear effector structures in the brainstem including the hypothalamus, periaqueductal grey and motor vagal nuclei. The LA connects with the CeA directly and indirectly via the BLA and ICM. The CeA controls the expression of fear reactions including behavioral, autonomic and endocrine responses. The learning related plasticity in the CeA is based on LA's plasticity (LeDoux 2000, Maren, 2001). Experimental manipulations that increase inhibitory signaling in the amygdala showed anxiolytic effects and interfere in acquisition and expression of fear conditioning. By contrast, decrease in inhibitory signaling induces opposite effects (Ehrlich et al., 2009).
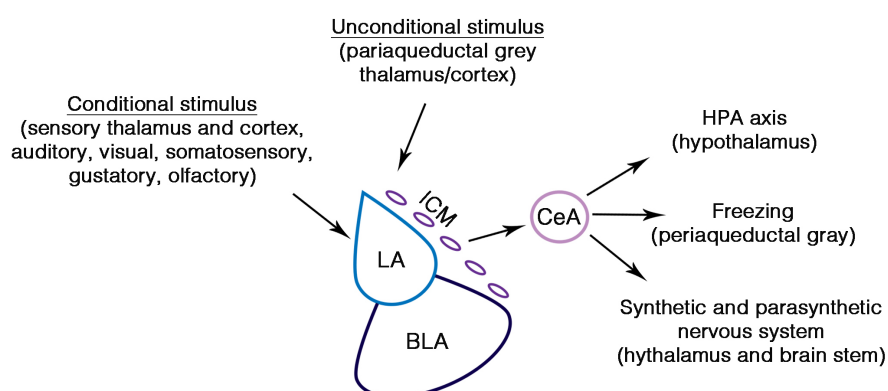

Fig. 1.4: Input and output of the amygdala nuclei. During Pavlovian conditioning, the CS and

US converge on the LA, which serve as the entry point to the amygdala. Processing of fear takes place in the amygdala nuclei and then the CeA projects to different brain areas to elicit specific conditioning responses. LA, lateral amygdala; BLA, basolateral amygdala; ICM, intercalated cell mass and CeA, central nucleus of amygdala (Adapted with modifications from Rodrigues et al., 2009).

1.2.2 Hippocampus – a contextual predictor

The hippocampus is located in the temporal lobe and ever since the case study of H.M., who famously lost his ability to form new declarative memories after surgical removal of the hippocampus, this structure has been at the forefront of research in the neurobiological basis of memory. The hippocampus is known to integrate multimodal information into higher-order representations of a context and is critical in the discrimination of similar contexts (Rudy, 2009). The role of the hippocampus in fear memory becomes evident with the experiments in rodents where loss of acquisition and expression of contextual fear conditioning is observed via electrolytic lesions of the hippocampus (Phillips and LeDoux, 1992; Maren et al., 2001). Recent advances that identify the place cells and grid cells in rodent hippocampal formation suggest a firm notion that the hippocampus provides the brain with a spatiotemporal framework to bind various cognitive, emotional and sensory components of a particular experience. Thus, via this complicated framework the experience is stored and can be later consciously retrieved in part or with all the components of that experience (Knierim, 2015).

The rodent hippocampus is a cashew shaped structure that lies beneath the neocortex. It is composed of two parts, the cornu ammonis (CA) and the cytoarchitecturally distinct dentate gyrus (DG). The CA is further divided into three subareas (CA1, CA2 and CA3) and together with the DG; they formulate the so-called tri-synaptic loop. Here the neuronal arrangement is highly organized and form multiple *strata* including the *startum oriens*, *pyramidale* and *radiatum*. The excitatory principle cells, pyramidal cells are located in the *stratum pyramidale* while the inhibitory neurons are found mainly in other two *strata* (Watson et al., 2012). The DG is also organized into different layers including the molecular layer, granular layer, and hilus. Here, the excitatory principle cells are called granule cells and are located in the granule cell layer while other excitatory cells called the mossy cells are found in the hilus. The inhibitory cells are located in the molecular layer and mainly in the hilus (Amaral et al., 2007).

The main input to the hippocampal formation arises from the entorhinal cortex (EC) that consists of medial and lateral parts. These carry spatial and high order information and project to the DG via the perforant pathway, the DG projects via the mossy fiber pathway to the area CA3 that in turn connects the area CA1 through the Shaffer collateral pathway. Finally the CA1 projects back to the EC completing the loop (Fig. 1.5). In addition to the CA1 connection, CA3 axons send collaterals that make synapses to other CA3 neurons as well. However, tracing studies have revealed more complex widespread connections among the hippocampus. The EC also projects directly to the CA3 and CA1 regions. The CA3 also provides feedback projection to the DG via mossy cells residing in the hilus. The hippocampus, in addition to major inputs from the EC (Kitamura et al., 2015), also receives inputs from the perirhinal, postrhinal cortex, medial septum, locus coeruleus, raphe nucleus, nucleus reuniens and amygdala. The CA1 and CA3 regions provide major output to the lateral septum via the fornix. The CA1 also projects to the nucleus accumbens, amygdala and prefrontal cortex (Knierim, 2015).
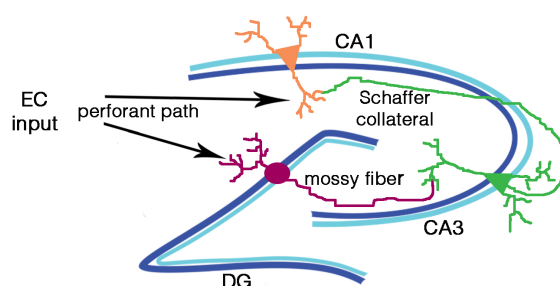
Fig. 1.5: A simplistic representation of the hippocampal tri-synaptic pathway. The entorhinal inputs (EC) via the perforant pathway reaches the dentate gyrus (DG) and targets the granule cells, which in turn through the mossy fibers provide input to the cornu ammonis (CA3) cells. The Schaffer collaterals provide communication from the CA3 to pyramidal cells in the area CA1. The EC also projects indirectly to the CA1.

One of the unique functions of the hippocampus is its ability to rapidly develop a unique representation of a spatial context within which an important event occurs. The recent advances with the lesion studies, pharmacological and optical manipulations shed light on the functional division of the hippocampus along its longitudinal axis referred as the dorso-ventral axis. In rodents, the dorsal and ventral hippocampi are differentially involved in spatial versus emotional memory and cognition. The dorsal hippocampus along with the subiculum forms a network with the retrosplenial and anterior cingulate cortex as well as ventral tegmental area and substantia nigra. It receives multimodal information via the EC and has a

preferential role in spatial learning and memory (Moser and Moser, 1998). The ventral hippocampus is interconnected with the hypothalamus, prefrontal cortex and amygdala and thus is involved in emotional behaviors like anxiety, stress and fear responses. Accordingly, an inactivation of the ventral hippocampus that is directly connected to the amygdala but not the dorsal hippocampus reduces the anxiety like behavior in rodents (Bannerman et al., 2004). Also, the ventral hippocampus controls individual stress responses via the hypothalamic-pituitary-adrenal (HPA) axis and participates in a glucocorticoids negative feedback loop (Jacobson and Sapolsky, 1991). Stress differentially influence synaptic plasticity in the ventral hippocampus compared to the dorsal hippocampus (Maggio and Segal, 2007). Moreover, this functional differentiation between the dorsal and ventral regions of hippocampus is also shown with different fear conditioning paradigms. Lesions of the dorsal hippocampus disrupt background context memory while lesions of the ventral hippocampus disrupt foreground context memory (Phillips and LeDoux, 1994). Similar observations are made by comparing the expression of neural activity markers along the dorso-ventral axis of the hippocampus in background vs. foreground context conditioning (Trifilieff et al., 2007).

The DG being a primary target of cortical inputs to the hippocampal formation is thought to rapidly compute distinct representations of the temporal and spatial relationships of comprising events by a process called pattern separation. By contrast, the CA3 is capable of using partial cues to retrieve previously stored representations by a process called pattern completion (O'Reilly and McClelland, 1994). Thus the DG is critically involved in the discrimination of similar contexts (Rudy, 2009) possibly via its pattern separation function. In aversive memory, impaired pattern separation could lead to fear generalization and anxiety disorders (Kheirbek et al., 2012; Maren et al., 2013). Moreover, immediate early gene expression studies show a sparse population (2-4%) of the DG granule cells that are activated in a given context (Schmidt et al., 2012). These activated DG granule cells are incorporated into memory engrams. The contextual function of the DG in fear memory formation is dependent upon granule cell ensembles that are incorporated into the context memory engrams (Liu et al., 2014) (Fig. 1.6). Thus, neuronal activity specifically in the dorsal DG is integral for encoding and formation of the context memory and for the discrimination of conflicting memories (Lee et al., 2004; Kheirbek et al., 2013). Correspondingly, stimulation of preformed granule cell

ensembles in the dorsal DG is not only necessary for particular context memory retrieval but also this stimulation can sufficiently activate a corresponding non-reinforced contextual memory (Ramirez et al., 2013; Denny et al., 2014). The contextual strength of fear memory is correlated with activated granule cells and their corresponding ensemble size in the DG (Stefanelli et al., 2016) and the output of these memory ensembles modulates the encoding of strength and specificity of contextual fear in the hippocampal CA3 area (McHugh et al., 2007; Denny et al., 2014; Bernier et al., 2017).
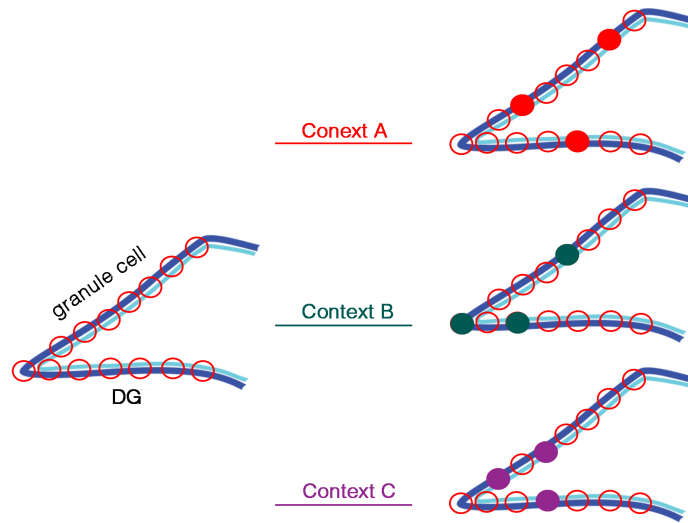
Fig. 1.6: A representative image of the dorsal dentate gyrus with granule cells. The exposure to a novel context activates granule cells that form memory ensembles of that particular context. Exposure to different contexts activates different granule cell ensembles. Note the percentage of active granule cells is always very low that represent context memory ensembles.

1.2.3 Other brain circuits of importance

Most of the circuit analysis suggested that the amygdala is a site of fear conditioning and the hippocampus has its peculiar role in fear conditioning, however, other brain areas are also involved in the regulation of fear and its formation.

A number of studies have attributed to the role of medial prefrontal cortex (mPFC) in fear conditioning. This structure is divided into four distinct regions that showcase different functions including the medial precentral cortex and anterior cingulate cortex (ACC, regulate motor behaviors), pre and infralimbic cortex (PL and IL, control emotional, mnemonic and cognitive processes) (Rozeske et al., 2015). The PL and IL receive afferent fibers from the amygdala and hippocampus and in return send projections back to these regions. It has been shown that the PL is involved in the expression of conditioned fear while the IL is involved in the expression of

11

extinction to a specific cue (Arruda-Carvalho and Clem, 2014; Cho et al., 2013). Even in the animals with a surgical removal of the hippocampus, the PL and IL take over and provide a compensation to the hippocampal functions in the acquisition and extinction of contextual conditioning (Zelikowsky et al., 2013).

There are other brain structures involved in the formation of fear memories. Recently it has been identified that the nucleus reuniens processes the information from the PFC to the hippocampus and determines memory attributes for contextual specificity (Xu and Südhof, 2013). Moreover, another structure the retrosplenial cortex is shown to independently produce context specific behavior in the absence of the hippocampus (Cowansage et al., 2014). Another study shows that the neurotoxic lesions to the perirhinal cortex 1 day after training disrupted the hippocampal contextual fear memory (Bucci et al., 2000). Excitotoxic lesions of the EC attenuate conditioning to the tone in unpaired foreground context conditioning (Majchrzak et al., 2006) and excitatory stellate neurons in the median EC drive contextual fear conditioning in the DG and area CA3 (Kitamura et al., 2015).

1.3 Neurotransmitter systems in fear memory

The communication between neurons within the brain is a basic mechanism of memory formation that is carried out by neurotransmitter molecules. When a neuronal membrane is depolarized, an action potential is generated that causes the voltage gated calcium channels to open in that neuron. The influx of calcium in this presynaptic neuron causes the stored neurotransmitters to be released into the synaptic cleft. These molecules then bind to their respective receptors on the postsynaptic neuron. Generally, each neurotransmitter binds to different subsets of receptors that are either ionotropic (ion channels) and/or G protein coupled metabotropic receptors (GPRCs). An information is stored when a group of neurons, fire together wire together, becomes connected and gains synaptic strength. The precise balance of the excitatory and inhibitory neurotransmitters in fear memory circuits is vital for fear memory formation.

Glutamate is the main excitatory neurotransmitter that uses three different ionotropic receptors named after their selective pharmacological agonists: N-methyl-D-aspartate (NMDA), α-amino-3-hydroxy-5-methyl-4-isoxazole propionic acid (AMPA) and kainate (KA). Glutamate also exerts its action via the metabotropic glutamate receptors (mGluR1-8) that act through the second messenger system.

Glutamate establishes excitatory postsynaptic potential (EPSP) and is involved in learning and memory because of its role in synaptic plasticity. The type of synaptic plasticity that occurs at the glutamatergic synapses is known as long-term potentiation (LTP). It is long being considered as a cellular model for experience dependent plasticity *in vivo* and *in vitro* and has been frequently studied during fear memory formation. Founding studies from Bliss and Lomo in 1973 show that high frequency electrical stimulations of the perforant path projecting from the EC to the hippocampus results in enhanced strength of underline synapses, furthermore, only the active synapses take part in this plasticity. Modern neuroscience believes that memories are actually acquired by initially using LTP-like mechanisms in different brain circuits; however, their ultimate storage depends upon the lasting and self-perpetuating biochemical as well as morphological changes in the given active synapses (Izquierdo et al., 2016). The LTP induction protocol varies from region to region within the hippocampus and also need different patterns of stimulation in the same region. For example, hippocampal CA1 stimulation upon 100 Hz exhibits the NMDA receptor dependent LTP. Depolarization of a postsynaptic membrane carrying NMDA receptors as well as concurrent glutamate release from the corresponding presynaptic terminal results in the activation of NMDA receptors, thus resulting in a postsynaptic Ca^{2+} influx which ultimately leads to LTP. This calcium signaling then activates intracellular signaling pathways (PKC, PKA, CaMKII and MAPK) that are implicated in the induction of LTP and also involves in its later stabilization. Later the activation of second messenger system also incorporates AMPA receptors in the synapse and results in a strengthened response (Johansen et al., 2011; Kandel et al., 2014). The importance of LTP in fear memory is observed with specific deletion of the NMDA receptors in the hippocampal sub-regions. The CA1 neurons lacking NMDA receptors produced decrease LTP and severe deficits in contextual fear conditioning (Shimizu et al., 2000) and the NMDA receptor deletion in the DG granule cells resulted in a loss of LTP at the perforant path synapses and the knockout animals were unable to differentiate between the fear training chamber and neutral chamber possibly disrupting pattern separation function of the DG (McHugh et al., 2007). These studies suggested that the downstream signaling events following LTP have important roles in the formation of lasting memories (Kandel et al., 2014).

As a consequence of new information, e.g. a threatening stimulus, the amygdala neurons undergo increased glutamatergic signaling (Lin et al., 2010) and form synapses among each other and in turn constitutes circuits to store this threatening information. This plasticity via glutamate neurotransmitter is modulated by the release of the inhibitory neurotransmitter molecule, gama-aminobutyric acid (GABA) often together with neuropeptide co-transmitters as well as under the influence of monoaminergic neurotransmitters such as dopamine, serotonin, norepinephrine and acetylcholine. Thus, in the above example, if the new information is not related to threat then the glutamatergic signaling within the amygdala nuclei is suppressed. This could be done alone by the GABA or with the concerted action of neuropeptides and neuromodulators. The imbalance between excitation and inhibition among neural circuits of fear memory has been hypothesized as one of the key molecular mechanisms responsible for different psychiatry disorders (Harrison, 2015; Cohen et al., 2015).

1.3.1 GABAergic system in fear memory

The inhibitory GABAergic system is identified by the glutamic acid decarboxylase (GAD) serving as a unique presynaptic marker and an enzyme for GABA synthesis. GAD has two isoforms; GAD_{65} and GAD_{67}, named after their approximate molecular weights and both are derived from two different genes. These two isoforms differ in their function as well as in their cellular localization. GAD_{67} is known to form the cytoplasmic GABA and satisfy neuronal metabolic needs while direct association of GAD_{65} with the membrane upon phosphorylation infers its role in vesicular release. Likewise, GAD_{67} is sequestered within the soma of GABAergic neurons producing tonic firing pattern and GAD_{65} is present in their nerve terminals producing sparse firing in activity dependent manner (Soghomonian and Martin, 1998). Chronic stress effects the expression pattern of both GAD_{65} and GAD_{67}, and the GAD_{65} deficient mice show increased anxiety-like behavior, generalized fear memory and resilience to stress at a young age (Kash et al., 1999; Bergado-Acosta et al., 2008; Müller et al., 2014).

Upon release within the synaptic cleft, GABA binds to either ionotropic $GABA_A$ receptors to conduct fast synaptic transmission or to slow metabotropic $GABA_B$ receptors that mediate a cascade of intracellular downstream events. However, both of these receptors contribute to the inhibitory postsynaptic potentials (IPSPs). The

GABA$_A$ receptors are pentameric (α, β and γ subunits in different combinations) and are mostly present at the postsynaptic sites. They are widely distributed throughout the brain; however, differential expression of their subunits is reported in stressful situations in the amygdala and hippocampus (Jakobson-Pick et al., 2010; Poulter et al., 2010). Upon GABA$_A$ activation, anions (HCO$_3$, and particularly Cl$^-$) conductance is increased that in turn hyperpolarize the cell leading to inhibition via fast IPSPs. The metabotropic GABA$_B$ receptors are located in the presynaptic site and exert slow G protein coupled response via second messenger system (cAMP and IP3) and mediate slow IPSPs through certain potassium channels (Brambilla et al., 2003).

A dysregulation of the GABAergic system is closely associated with the onset of a number of pathological conditions like schizophrenia, epilepsy, depression, bipolar disorder, autism and post-traumatic stress disorder (PTSD) (Graham and Milad, 2011; Bremner et al., 2007). Studies with fear conditioning indicate that the GABAergic transmission regulates fear behavior and the underlying plasticity. Increase in the GABAergic transmission via systemic and local treatments results in anxiolytic effects and interferes with the acquisition and expression of conditioned fear response, whereas decrease in the GABAergic transmission through pharmacological manipulations leads to anxiogenic-like effects and improve learning of the conditional fear. Moreover, the extinction of fear is also affected in a similar fashion (Ehrlich et al., 2009). The activity of GABA$_A$ within the hippocampus is reported to be important for the formation and expression of contextual fear memory (Möhler, 2007). A recent microRNAs screening study identifies miR-33 in the hippocampus that sets the bar for GABA$_A$ receptor mediated state dependent memory (Jovasevic et al., 2015). Genetic mouse models that are deficient for GABA$_A$ receptor subunits or GABA$_B$ receptors show anxiety and depression-like phenotype (Möhler et al., 2012). Correspondingly, a strong GABAergic regulation of the amygdala, a key structure in fear-motivated learning, has been identified. The activation of GABA$_A$ receptor in the LA impairs fear memory acquisition (Wilensky at al., 1999) while reduced GABA levels are reported in the BLA during fear conditioning (Stork et al., 2002).

Most of the GABAergic neurons retain their axons within their respective layers or at least within the local area and they are termed as short axon or local neurons or interneurons. There are other GABAergic neurons that have long axons and are called projection neurons (Tomioka et al., 2007). The GABAergic interneurons are

categorized according to their cellular morphology (Amaral, 1978), pattern of connectivity (Freund et al., 1990), contents of calcium binding proteins or neuropeptides (Somogyi et al., 1994; Sloviter et al., 1987; Gulyás et al., 1991), somatodendritic location (Scharfman, 1995) and their physiological characteristics (Sik et al., 1997; DeFelipe at al., 2013). An individual interneuron can completely block dendritic activity, change the phase of action potential firing at the soma or it can completely inhibit firing of action potential of a principle cell. Local inhibitory circuits formed by different interneurons tightly control the activity of memory circuits by shaping the signal propagation and contribute to the generation of synchronous activity between multiple principle neuron populations (Buzsaki, 2002). The hippocampus contains a heterogeneous population of interneurons located in different layers that differ in their firing properties, connectivity and their neurochemical signature. The advancement in this field leads to the identification of various subtypes e.g. calcium binding proteins expressing parvalbumin (PV), calretinin and calbindin interneurons and neuropeptide expressing somatostatin (SST), neuropeptide Y (NPY), cholecystokinin and vasoactive intestinal peptide expressing interneurons (Jinno and Kosaka, 2006).

1.3.1.1 GABAergic local circuits in the DG

The DG serves as the interface between the EC and hippocampus (Anderson et al., 1971) and the population activity within this region is tightly controlled by powerful inhibition via the GABAergic local interneurons (Nitz and McNaughton, 2004). There lies a set of diverse interneurons in the DG and around 21 cell types are alone found in the hilus (Amaral, 1978). Morphological studies have divided the DG interneurons into those that form synapses at dendrites or perisomatic regions (Fig. 1.7). Further, interneurons forming perisomatic synapses are divided into those that form synapses to axon initial segments or cell bodies and proximal dendrites of the granule cells (Houser, 2007). The PV+ basket cells constitute the axo-axonic and perisomatic targeting interneuron population and are known to provide a powerful feed-forward and feedback control over granule cells in the DG (Caroni, 2015). The molecular layer perforant path-associated (MOPP) cells located in the molecular layer are known to provide feed-forward inhibition to the granule cells (Li et al., 2013). On the other hand, the dendritic targeting interneurons of the DG can be classified as the hilar inhibitory perforant path associated cells (HIPP) and hilar commissural-association pathway-related cells (HICAP) (Han et al., 1993). The

somas of HICAP cells are located in the hilus and they project to the inner third of the molecular layer. These cells receive inputs from the granule cells and in return provide feedback inhibition to them at their excitatory inputs and are known to express cholecystokinin (Houser, 2007; Savanthrapadian et al., 2014).
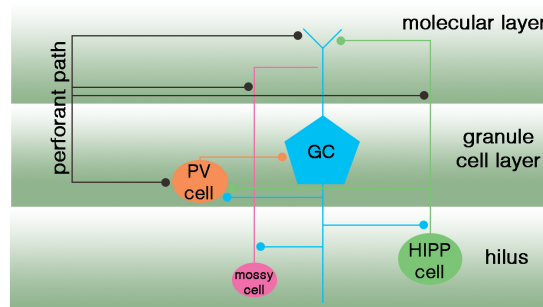
Fig. 1.7: A representative local DG circuit. The projections from the entorhinal cortex via the perforant path target the dendrites of granule cells (GC) in the molecular layer and parvalbumin-positive cells (PV) in the granule cell layer. The perforant path also targets the axons of HIPP cells and mossy cells both of which are located in the hilus. The PV+ cells provide inhibition to the GCs at their soma. The HIPP cells receive inputs from the GCs and in return they provide inhibition to them at their dendrites in the molecular layer. The HIPP cells also provide inhibition to the PV+ cells.

HIPP cells constitute another peculiar population of the GABAergic local circuit interneurons. Their cell bodies are located in the hilus and they receive inputs from granule cells via the mossy fiber collaterals (Hosp, et al., 2014; Savanthrapadian et al., 2014) and directly from the perforant path (Myers and Scharfman, 2009). In return, they provide inhibition to the outer molecular layer of the DG on the apical dendrites of the granule cells. Interestingly, HIPP cells use SST and NPY as co-transmitters (Deller and Leranth, 1990). These HIPP cells are also known to frequently target the PV+ cells in the area (Savanthrapadian et al., 2014). HIPP cells with hilar location and distinct neurochemical content play key roles in negative feedback and feed-forward circuits in the DG, control granule cells and their excessive discharge to the area CA3. HIPP cells also restrict the formation of granule cell memory ensembles during fear conditioning (Stefanelli et al., 2016).

Considerable evidence suggests the involvement of GABAergic local circuits in the hippocampus in the formation of fear and anxiety. The PV+ cell recruitment enhances network activities in the DG that are ultimately important for long-term consolidation and PV+ cells are shown to effectively suppress recruited granule cells during learning and memory formation (Holtmaat and Caroni, 2016). Similarly, during cued conditioning, auditory CSs activate PV+ cells in the BLA that inhibit SST+

cells thereby disinhibiting excitatory neurons and facilitate the formation of fear memory (Wolf et al., 2014). The role of neuropeptides in learning and memory is also documented and the neuropeptide Y is considered as one of the most abundantly expressed peptide in the mammalian brain (Tatemoto et al., 1982). It exerts its functions via the GPCRs and in the brain specifically via Y1, Y2, Y4 and Y5. These NPY receptors are known to couple $G_{i/o}$ and inhibit adenylate cyclase enzyme, thus decrease the cAMP accumulation (Cabrele and Beck-Sickinger, 2000). In recent years, a lot of work has been done with studies on the NPY and its implication in anxiety and fear related memories (Tasan et al., 2015; Gøtzsche and Woldbye, 2016). Recently, it has been shown that the SST^{+} neurons in the DG that are known to coexist with the NPY^{+} cells, control the size of neuronal ensembles (Stefanelli et al., 2016) and SST[+] interneurons through activation by cholinergic inputs from the medial septum in the area CA1 fine-tune fear memories (Lovett-Barron et al., 2014). These observations point out to the involvement of cholinergic signaling in the hippocampus to modulate the formation of fear memories (Knox, 2016).

1.3.2 Neuromodulation – monoaminergic and cholinergic

Neuromodulators are small molecules utilized as transmitters and are superimposed on chemical synapses in the brain. These are synthesized in different brain areas while exert their functions in other brain regions providing modulation to the GABA and glutamate signaling, however they display fairly similar characteristics comparable to the GABA and glutamate. These include biogenic amines (dopamine, serotonin, norepinephrine, histamine) and acetylcholine (ACh). These molecules, mostly via the GPCRs, can silence as well as activate a whole circuit, change its frequency and control the generated activity patterns. These molecules are found throughout the entire brain and play critical roles as mediators of motivational and emotional states (Bargman and Marder, 2013). For simplicity, here only the cholinergic system with respect to Pavlovian fear conditioning is discussed.

The cholinergic system that uses acetylcholine as a neuromodulator has been implicated in a variety of cognitive functions including arousal, attention, vigilance, learning and even consciousness. The cell bodies of cholinergic neurons are located in the basal forebrain nuclei and the axons project to multiple brain regions where they exert their functions by the metabotropic muscarinic (mAChR) and ionotropic

nicotinic (nAChR) receptors. The medial septum (MS) projects (containing the cholinergic and GABAergic components) to the hippocampal formation and forms a septo-hippocampal loop that plays a key role in learning and memory (Everitt and Robbins, 1997; Khakpai et al., 2013; Knox, 2016). The cholinergic terminals from the MS terminate on the glutamatergic principle cells and GABAergic interneurons in the hippocampus, with a high density on the DG granule cells, basket cells and HIPP cells (Dougherty and Milner, 1999; Khakpai et al., 2013). The hippocampal cholinergic neurons are critical for Pavlovian fear conditioning, as increased levels of ACh is observed in the hippocampus after conditioning (Calandreau et al., 2006). Of note, the MS projections are an exclusive source of ACh in the hippocampus (Knox, 2016). The blockade of muscarinic signaling in the dorsal hippocampus disrupts the acquisition as well as the consolidation of fear memory (Rogers and Kesner, 2004; Wallenstein and Vago, 2001).

1.4 Mechanisms of gene expression and functions of CREB in fear learning

Neuronal plasticity in the CNS is extremely essential for the representation of novel information. During learning, experience dependent plasticity ranges from synthesis and insertion of synaptic proteins to the synchronization of the neuronal circuits and ultimately leading to discrete behaviors. The LTP is thoroughly studied during fear memory formation and employed as a cellular model for experience dependent plasticity *in vivo* and *in vitro*. The influx of Ca^{2+} ions within the cell is implicated in the induction of LTP and is known to activate intracellular signaling pathways (PKC, PKA, CaMKII and MAPK). These pathways are involved in stabilization of memory, are required for transcriptional activation of transcription factors e.g. $cAMP/Ca^{2+}$ response element binding protein (CREB) and are also modulated by neuromodulators. Among transcription factors, CREB is one of the important candidates that connect neuronal activation during learning with gene expression required for lasting memories (Alberini, 2009). The activity dependent intracellular signals lead to activation of protein kinases and ultimately result in addition of a phosphate group to CREB at serine 133. This phosphorylation at serine 133 recruits the CREB-binding protein and p300, where both have histone acetyltransferase activity, thus promoting targeted gene expression. However, phosphorylation independent mechanisms of the CREB dependent gene transcription also exist whereby a glutamine rich constitutive activation domain Q2 on the CREB stimulates transcription through its interaction with the transcription factor IID (Nakajima et

al., 1997). In general, the phosphorylated CREB targets the transcription of genes that contains cAMP response elements (CRE) in their promotor regions (Gonzalez and Montminy, 1989). These include other transcription factors (cFos), receptor subunits (GluR1), neurotransmitter synthesizing enzymes (tyrosine hydroxylase) and certain neuropeptides (NPY) (Carlezon et al., 2005; Hsieh et al., 2008) (Fig. 1.8). During fear memory formation, CREB phosphorylation has been observed in the amygdala and hippocampus and the involvement of CREB in classical fear conditioning is beginning to be explored. Recently, it has been shown that the overexpression of CREB in defined cellular populations control the fear memory formation and the subsequent increase in the cellular excitability with CREB enables these cells to become the part of memory engrams in the hippocampus (Park et al., 2016) as well as in the amygdala (Han et al., 2009; Zhou et al., 2009).
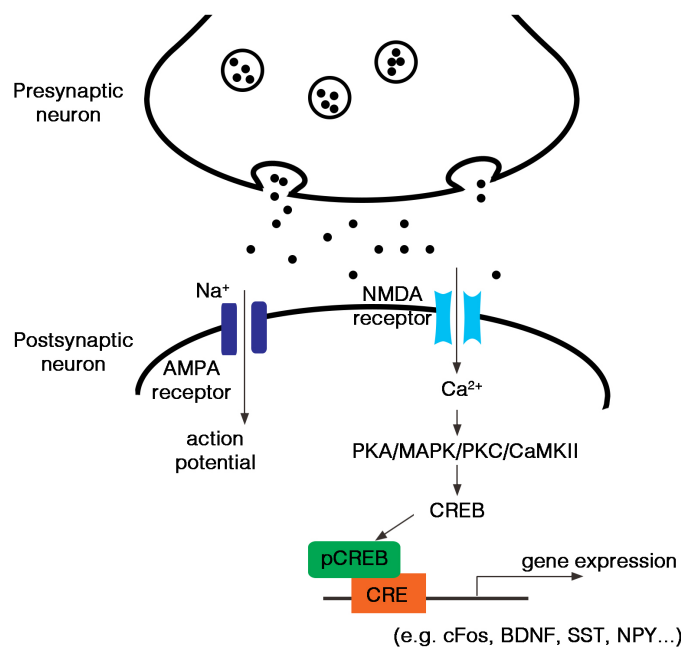
Fig. 1.8: Schematic of cellular signaling. A simple illustration shows a communication between the pre- and postsynaptic neurons with an intracellular cascade leading to the CREB dependent activation of gene expression. Neuropeptide Y is one of the candidate genes that show CRE element in its promoter sequence and thus is transcribed with the CREB activity.

1.5 Fear conditioning as a model to understand critical circuits involved in pathological fear

Circuits in the brain that are known to be involved in multiple psychiatric conditions mostly belong to the limbic system that is known to process emotions (Heimer and Van Hoesen, 2006). One of the strong candidate tool to study the limbic system particularly the amygdala, hippocampus and prefrontal cortex, and its involvement

in emotional learning is Pavlovian fear conditioning. It offers a unique opportunity to investigate the pathophysiology of fear and anxiety disorders. Fear refers to the ability to cope with danger while anxiety occurs when the organism fails to effectively cope with danger. Anxiety disorders are extremely common in the general population with a lifetime prevalence of 28.8% (Kessler et al., 2005) and could be marked by excessive fear in response to situations or specific objects likely in the absence of a true danger. As the involvement of excessive fear is a key component of anxiety disorders, the research on fear related circuits in the animal models, mainly rodents, has gain utmost importance. In recent decades, a comprehensive neurobiological analysis revealed important neural circuitry and synaptic mechanisms involved in fear conditioning. Along with the advancement in molecular techniques, the underlying intracellular processes in these fear related circuits are beginning to unravel. These developments have helped in great deal to understand the neurobiology of fear-based anxiety disorders, phobias, panic disorders, major depression and PTSD. These disorders are generated as a consequence of excessive fear experience and its inappropriate non-adaptive responses ultimately leading to pathogenesis.

The amygdala and hippocampus have their respective roles in components of fear processing. The perception of threat *per se* and/or the conditional stimulus that predicts the threat, contextual modulation of fear with its subsequent responses and initiation of effector components of fear are all identified with fear conditioning protocols. The key findings, that the amygdala is a threat center where the convergence of CS-US associations are processed in the LA and fear responses are instructed via the CeA, and the hippocampal involvement in contextual processing of fear and differentiation of normal and fearful contexts, all results with studies involving fear conditioning methods. These basic components of fear circuitry are thoroughly preserved across species and are also likely to support similar kind of functions in humans (Phelps and LeDoux, 2005).

More recently, with the help of classical fear conditioning, neural circuits of fear including their specific locations and dynamics of their connections at discrete cellular level are beginning to be discovered. This points out to the identification and manipulation of genetically marked cellular populations within the identified fear circuits in controlling specific fear responses. The cell-type specific identification of behavioral and molecular correlates of the individual population of neurons in

genetic mouse models during discrete conditioning events are paving the way to better understand the normal and pathological processes of fear, anxiety-related behaviors and associated disorders. In the future, the outcomes of this very basic technique and the identification of basic mechanisms in the cellular and molecular circuitry will provide unique avenues for the control and treatment of globally prevalent fear and anxiety related disorders.

1.6 Aim of the study

The emotional aspects of fear memories provide an organism with adaptive instincts with which it survives in the natural habitat by making precise decisions based on the predictions of the future threatening situations. Therefore, fear memories are widely accepted to remain lastingly intact and are known to be present in all species including humans. Even a slight disturbance in such a strong memory significantly leads to a pathological fear, which ultimately becomes the cause of many psychiatric conditions especially anxiety disorders such as phobias and PTSD. Classical fear conditioning is extensively used as a laboratory tool to understand the formation of fear memories at the level of involved brain circuits as well as following the cellular and molecular processes. In a simple conditioning paradigm, multiple stimuli that represent a context are well separated by distinct elemental stimulus and fear memory loads onto neuronal ensembles in the hippocampus and amygdala, respectively. Previous studies have shown the control of background context memory by cholinergic neuromodulation in the hippocampus, however the involvement of the local dentate gyrus circuit in the determination of contextual salience is not known. Therefore, I hypothesized that the hilar inhibitory perforant path (HIPP) cells in the DG circuit could be significant contributors to this salience determination.

First, I aimed at verifying fear conditioning protocols by which animals could clearly differentiate between elemental cue as sole predictor (background context conditioning-context in background) vs. context as a sole predictor (foreground context conditioning-context in foreground). Then I set to investigate the role of HIPP cells in determining the background context memory salience during conditioning with unique pharmacogenetic tools. Previous studies have shown the involvement of the transcription factor CREB in fear conditioning, however its role in HIPP cells signaling during background context conditioning is poorly understood. I tested intracellular signaling in HIPP cells with viruses overexpressing CREB and dominant negative CREB along with their involvement in fear memory. HIPP cells are GABAergic cells and are known to co-express NPY and SST. Thus, I confirmed the involvement of NPY-dependent HIPP cell signaling in the DG specifically during background context conditioning. Furthermore, the presence of muscarinic receptors is well documented on the HIPP cells, but their specific role is not investigated. Finally, I determined the control of HIPP cells with cholinergic

signaling from the medial septum in mediating the salience of background context conditioning.

2. Materials and Methods

2.1 Animals
2.1.1 Animal housing and welfare

All mice used in this study were bred and raised under standard laboratory conditions in the animal facility at the Institute of Biology, Otto-von-Guericke University Magdeburg. The weaned littermates were kept in groups of 2-6 individuals in type 2 long cages (Techniplast GmbH and Bioscape Ebeco GmbH, Germany) with a standard bedding material, on an inverse 12 h light/dark cycle. The lights are switched on at 7 pm with a 30 min dawn phase. The animals had *ad libitum* excess to standard pallet diet (Ssniff R/M-H V-1534, Ssniff spezialdiäten, Soest, Germany) and water. Room temperature (21° C) and moisture (50-60%) was regulated by an automated air conditioning system. The European regulations for animal experiments were followed for animal housing and animal experiments in this study and were approved by the Landesverwaltungsamt Saxony-Anhalt with a Permission number 45202-2-1177-UniMD.

2.1.2 Mouse lines
2.1.2.1 C57BL/6BomTac mice

The wild type C57BL/6 mice were purchased from Taconic (M&B Taconic, Germany) at an age of 6-7 weeks and bred in the animal facility at the Institute of Biology, Otto-von-Guericke University Magdeburg. The litters were weaned at an age of four weeks and were group housed, males and females separately, until the onset of different experiments. Only the male wild type C57BL/6 mice were used during this study. These wild type C57BL/6 mice allowed me to establish and optimize different forms of Pavlovian fear conditioning paradigms and were also used for pharmacological manipulations within the dorsal DG and for field potential recording under drug manipulations.

2.1.2.2 SST-Cre[ERT2] mice

The heterozygous male breeders were purchased from the Jackson laboratories (JAX® Bar Harbor, Maine, USA). The heterozygous SST-Cre[ERT2] mice (allelic symbol B6(Cg)-Sstt[m1(cre/ERT2)Zjh]/J) were bred with the wild type C57BL/6 female mice in the animal facility at the Institute of Biology, Otto-von-Guericke University Magdeburg. The breeding was continued as +/+ sibling × heterozygote. All the heterozygous SST-

Cre^{ERT2} mice used in this study were obtained from Institute's own breeding pairs. The heterozygous SST-Cre^{ERT2} mice have knock-in/knock-out allele that abolishes the gene function of somatostatin and expresses a CreERT2 fusion protein from the *SST* promotor/enhancer element. The fusion protein consists of a Cre recombinase that is joined to a triple mutated ligand-binding domain of the human estrogen receptor. The natural ligand estradiol at physiological concentrations cannot bind to this mutated receptor. However, the synthetic partial agonist tamoxifen binds to it and translocates the CreERT2 fusion protein to the nucleus where the Cre recombinase becomes active. This leads to a specific tamoxifen induced recombinase activity only in the SST$^+$ interneurons. During weaning of litters, tail biopsies were done and allele-specific polymerase chain reaction (PCR) with supplier's recommended protocol (Appendix, A2.0) was used to identify the mutant genotypes. Only the heterozygous male SST-Cre^{ERT2} mice were used in this study. These mice enabled the inducible expression of viral vectors in HIPP cells without disturbing the *NPY* gene function in these cells. These mice were also used to specifically investigate the CREB activity and mRNA expression in HIPP cells.

2.1.2.3 NPY-GFP mice

The male heterozygous breeders (B6.FVB-Tg(Npy-hrGFP)1Lowl/J) were purchased from the Jackson laboratories (JAX® Bar Harbor, Maine, USA) and were bred with the wild type C57BL/6 female mice in the animal facility at the Institute of Biology, Otto-von-Guericke University Magdeburg. The breeding was continued as +/+ sibling × hemizygote. The transgenic hemizygous mice express humanized Renilla Green Fluorescent Protein (hrGFP) under control of the mouse *NPY* promotor. During weaning of litters, tail biopsies were done and allele-specific PCR with supplier's recommended protocol (Appendix, A2.0) was used to identify transgenic animals. Since the transgene expression is consistent with the *NPY* gene in the brain tissue, thus the transgenic mice were used to visualize hilar NPY$^+$ cells allowing for studying physiological properties of HIPP cells with patch clamp recordings and immune staining for cholinergic fibers and Chrm1 receptors.

2.1.2.4 NPY-GFP × SST-Cre^{ERT2} double transgenic mice

The heterozygous SST-Cre^{ERT2} mice were bred with the NPY-GFP mice in our animal facility. The double mutants obtained with allele-specific PCR using the supplier's

recommended protocols (Appendix, A2.0), allowed me to confirm the specific co-expression of SST$^+$ and NPY$^+$ cells in the hilus as a molecular signature of HIPP cells.

2.1.2.5 PV-Cre mice

The homozygous male PV-Cre breeders were obtained from the Jackson laboratories (JAX® Bar Harbor, Maine, USA) and were bred with the wild type C57BL/6 female mice in the animal facility at the Institute of Biology, Otto-von-Guericke University Magdeburg. The breeding was continued as +/+ sibling × -/+ mutants. PV-Cre (B6;129P2-Pvalb$^{Tm1(Cre)Arbr}$/J) knock-in mice express a Cre recombinase under the *Pvalb* promotor/enhancer element and directs its expression in parvalbumin expressing neurons without disturbing the endogenous *Pvalb* expression. Recombination occurs in more than 90% of parvalbumin neurons such as interneurons in the brain and proprioceptive afferent sensory neurons in the dorsal root ganglia. During weaning of litters, tail biopsies were done and allele-specific PCR with supplier's recommended protocol (Appendix, A2.0) was used to identify the mutant genotypes. PV-Cre heterozygous male mice were used in this study that allowed me to manipulate PV$^+$ cells of the DG and study their role in the fear memory formation.

2.1.2.6 CamK2a-Cre mice

The homozygous CamK2a-Cre (Tg(Camk2a-cre)159Kln) also known as Cam-Cre mice were purchased from the Jackson laboratories (JAX® Bar Harbor, Maine, USA) and were bred in the animal facility at the Institute of Biology, Otto-von-Guericke University Magdeburg. The breeding was continued as +/+ sibling × -/+ mutant. Only the heterozygous mutants were used in this study. The mutants have the mouse calcium/calmodulin-dependent protein kinase II alpha (*Camk2a*) promoter driving the Cre recombinase expression and show 50% of recombination at an age of 8 weeks in the hippocampus, cortex and olfactory bulb. During weaning of litters, tail biopsies were done and allele-specific PCR with supplier's recommended protocol (Appendix, A2.0) was used to identify mutant genotypes. I use the mutant male mice to study the role of whole dorsal DG in the fear memory formation by manipulating it with conditional hM4Di viruses.

2.1.2.7 Chat-Cre

Also known as ChAT-IRES-Cre with an allelic symbol B6;129S6-Chat$^{tm1(creLowl)}$/J were purchased from the Jackson laboratories (JAX® Bar Harbor, Maine, USA) and were

bred as homozygotes in the animal facility at the Institute of Biology, Otto-von-Guericke University Magdeburg. Chat-Cre knock-in mice express the Cre recombinase under the promoter/enhancer element of the *Chat* gene in cholinergic neurons without disrupting endogenous cholineacetyltransferase expression. During weaning of litters, tail biopsies were done and allele-specific PCR with supplier's recommended protocol (Appendix, A2.0) was used to identify mutant genotypes. In this study, I used the homozygous Chat-Cre mice that allowed me to manipulate cholinergic projection neurons arising from the medial septum and study cholinergic modulation of HIPP cells within the dorsal DG with conditional hM3Dq viruses.

2.2 Behavioral experiments

In this study, 3-4 days before starting all behavior experiments, mice were separated and placed in individual cages. The experiments were carried out during the dark phase that corresponds to animals' active phase, between 10 am and 4 pm. In this study, all the experimental mutant mice were heterozygotes and were littermates while only Chat-Cre driver mice were homozygotes. Throughout this study, in parallel testing of randomly assigned experimental and control groups was done. During the experiments, I was blind to the group affiliation and handled the animals for two days before the start of the experiment.

2.2.1 Fear conditioning

Pavlovian fear conditioning is a well-established tool to decipher the underlying processes of emotional memory formation. Fear conditioning was conducted (Laxmi et al., 2003; Albrecht et al., 2010) in a soundproof rectangular conditioning chamber that contains an acrylic glass arena (16 cm × 32 cm × 20 cm) and a floor with the grids to deliver foot shocks (TSE System, Bad Homburg, Germany). The arena was equipped with a loudspeaker to provide the tone cues and a ventilator (background noise 70 dB SLP, light intensity < 10 lux). During this study, three types of fear conditioning protocols were employed. In all these protocols, mice were allowed to explore the conditioning chamber for 6 min twice daily for 2 days prior to the training, referred to as habituation. These habituation sessions provide a stable pre-training representation of contextual features without inducing latent inhibition (Albrecht et al., 2010). In one control experiment, a group of mice were not habituated to the conditioning chamber. On the 3rd day, different conditioning

protocols (Fig. 2.1) were used which always start with 2 min of the baseline context exposure.

In *background context condition*, after initial context exposure of 2 min, mice received three conditional stimuli (CS: 10 kHz tone for 9 s, 80 dB), each co-terminating with the unconditional stimuli (US foot shock: 0.4 mA for 1 s). The inter-stimulus interval (ISI) between each pairing was set at 20 s. For *foreground context conditioning*, an unpaired training protocol (Calandreau et al., 2006) was adapted. After initial 2 min of the baseline context exposure, each three US foot shocks (0.4 mA for 1 s) and three tones (10 kHz tone for 10 s, 80 dB) without the temporal coincidence were delivered. Variable ISIs were used which range from 20 s to 40 s. In *pure context conditioning*, after initial 2 min of baseline context exposure, three un-signaled US foot shocks (0.4 mA for 1 s) without any tone-cues were delivered. In all three paradigms, mice were returned to their home cages 2 min after the last stimulus.
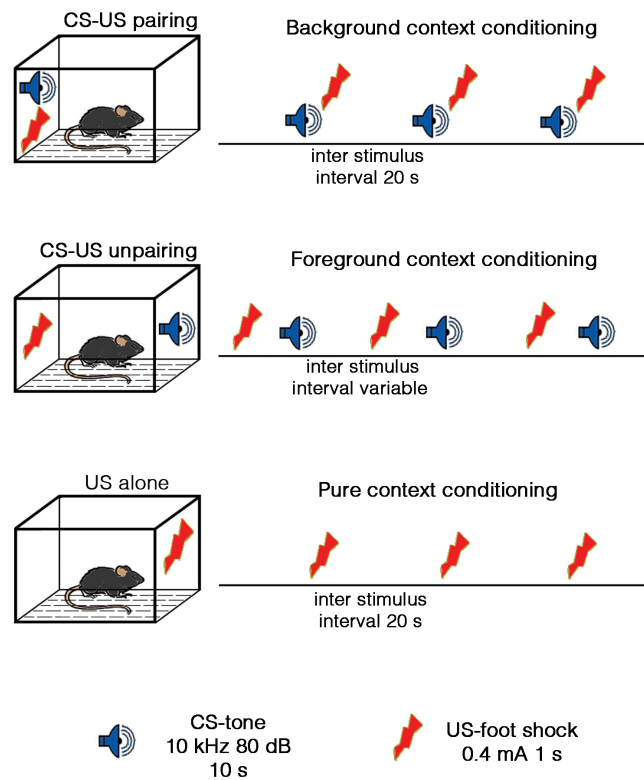

Fig. 2.1: An overview of the training protocols. Three types of training protocols were used in this study that are known to generate different fear responses.

One day (24 h) after the training, contextual fear memory was tested for a total period of 6 min by placing the mice individually in the training context. Fear

memory to the CS was checked 48 h after the training where mice were individually placed in a clean standard cage that contained normal bedding material serving as a neutral context (Fig. 2.2). Here, after initial neutral context exposure of 2 min, a set of 4 CSs (10 s, with each 20 s ISI) were delivered. In one of the control experiment, the order of retrieval was reversed. Here a group of mice were placed, 24 h after training, first in the neutral context with CSs presentation and 48 h after training to the shock context. An online photo beam detection system (TSE System, Bad Homburg, Germany) that detected immobility periods >1 s was used to determine the animals' freezing behavior. This automated detection system is proved to reliably detect immobility in accordance with observer-rated freezing measurement (Laxmi et al., 2003; Albrecht et al., 2010). The freezing score was calculated as a percentage of total time spent freezing during the different phases. Simply, freezing during the last 2 min of the baseline context exploration (habituation), last 2 min immediately after training (post-training), first 2 min of the conditioning context exposure (shock context), first 2 min of the neutral context exploration (neutral context) and during the presentation of CSs, was calculated as a percentage of total time.
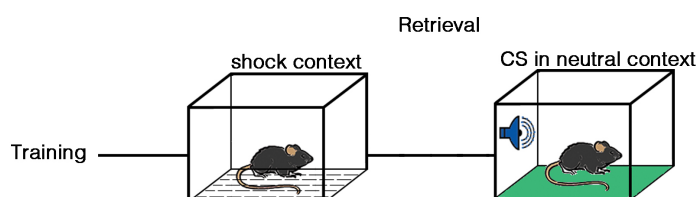
Fig. 2.2. An overview of the memory retrieval protocol. Throughout the study (otherwise stated), 24 h after training mice were first placed in the shock context and 48 h after training memory to the CS was tested in the neutral context.

2.2.2 Anxiety testing

The natural tendency of mice entails them to avoid conditions with heighten exposure to potential predators which may correspond to open and well illuminated spaces, and by contrast to their exploratory nature, mice with increased anxiety-like behavior tend to avoid exploration of potentially harmful environment. In this study, I used open field and elevated plus maze as behavior paradigms to assess anxiety in mice.

2.2.2.1 Open field

In an open field test, mice were placed individually in the center of a square arena (50 × 50 cm) and allowed to explore the field for 20 min in low light conditions (10

lux). The animals' behavior was recorded online via the ANYmaze software with a video tracking system (ANY-maze™ video Tracking System, version 4.50, Stoelting Co., Wood Dale, USA). The total distance covered by the animal during the test session corresponds to the parameter for general activity while the anxiety levels were assessed with the time spent as well as the number of entries to the center field (25 × 25 cm) of the arena.

2.2.2.2 Elevated plus maze

Mice were tested in an elevated plus maze consisting of two open and two closed arms for 5 min at low light conditions (10 lux). Each arm was 35 cm long and 5 cm wide with 15 cm high walls and elevated 110 cm above the floor. The position of the animal, % open arm entries as an anxiety measure and total arm entries as an activity measure was assessed online via the ANYmaze software with a video tracking system (ANY-maze™ video Tracking System, version 4.50, Stoelting Co., Wood Dale, USA).

2.3 Viral vectors

Viral manipulation of a specific area or particular cell population within the brain has been widely used to unravel the complex networks of neural circuits. In this study, to investigate the dorsal DG circuits involved in the formation of fear memory, I used different conditional viral vectors. In general, these viral vectors consisted of two different incompatible loxP pairs and constitute a double-floxed system. LoxP is a specific 34bp sequence that allows the recombination of DNA with a bacteriophage Cre recombinase enzyme (Naggy, 2000). The viral constructs used in this study consisted of LoxP sites in an opposite orientation that flank the target sequence which was placed in an inverted open reading frame. Therefore, Cre recombinase leads to the inversion of both LoxP sites resulting in an irreversible inversion of the target sequence.

2.3.1 Adeno-associated viruses (AAV)

The conditional adeno-associated viruses that carry the mutated muscarinic G protein coupled receptors were obtained from the vector core facility of the University of North Carolina, USA. This virus system is termed as DREADD (designer receptors exclusively activated via designer drug). In this study, I used double-floxed hM4Di (AAV8-DIO-hM4Di-mCherry) and hM3Dq (AAV8-DIO-hM3Dq-mCherry) DREADDs that carry mCherry fluorescent protein as a marker. Viruses containing

only the mCherry tag (AAV8-DIO-mCherry) were used as controls. The hM4Di is a Gi coupled DREADD that is derived from the rat muscarinic receptor M4 sequence with two point mutations (Y148C, A238G) while the hM3Dq is a Gq coupled DREADD that is derived from the human muscarinic receptor M3 sequence with two point mutations (Y149C, A239G) (Fig. 2.3). Upon conditional expression, the mutated receptors are activated via a synthetic drug: clozapine-N-oxide (CNO). hM4Di causes inhibition while hM4Di excites the infected cells. The viral titer used in this study are: hM4Di - 6.1×10^{12}, hM3Dq - 5.9×10^{12} and control - 5.4×10^{12} as obtained from the provider.
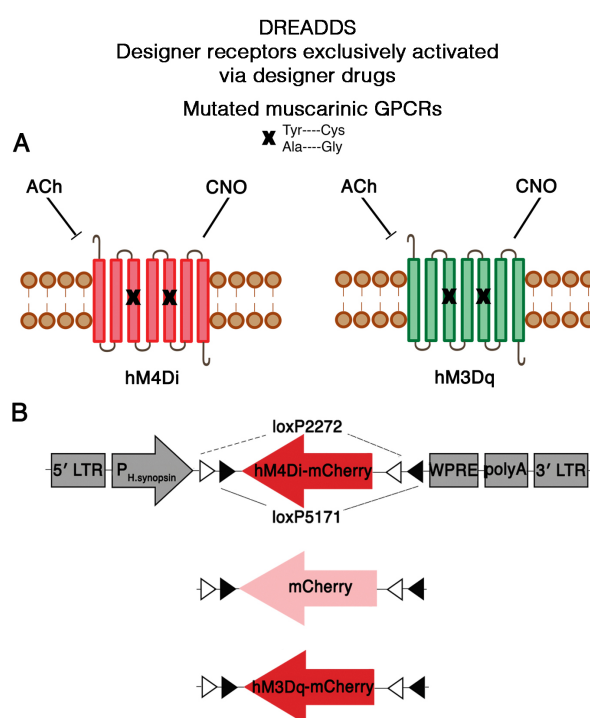
Fig. 2.3: Schematic of the DREADD virus technology. (**A**) These AAV viruses were generated in the University of North Carolina via mutations in the muscarinic receptors rendering them to be activated with the synthetic Clozapine-N-oxide (CNO) but not with their natural acetylcholine (ACh) agonist. (**B**) Schematic of hM4Di that provides inhibition, hM3Dq that provides excitation of infected cells, while virus that only express mCherry is used as a control.

2.3.2 Conditional lentiviral vector

For conditional gene manipulation experiments, Bettina Müller (PhD) generated lentiviral vectors in our lab, which were based on the vector backbone pLL3.7 (Rubinson et al., 2003). Using AgeI and NotI restriction sites, a DsRed cassette was obtained from MSCV-RmFF and used to replace the GFP in the MSCV-FlipFF (Stern et al., 2008), which harbors an empty miR30-FF cassette for the conditional expression of shRNA constructs. Next, a cassette that contained a combination of

DsRed/miR30FF having an upstream loxP5171 site and downstream inverted loxP5171 and loxP2272 sites, was excised with the BamHI and PciI. The restriction enzymes, ApaI and BamHI were used to excise an additional upstream loxP2272 site. With the ApaI and PciI restriction sites of pLL3.7, both fragments were inserted, thus replacing the U6 and conditional CMV_{IE} promoters as well as the GFP cassette of pLL3.7. Finally, pHA-CMV derived CMV promoter using the reconstituted ApaI site was inserted that ultimately yielded pLL-dfRmFF.

2.3.2.1 Dominant-negative CREB

The commercially available vectors, pCMV-CREB and pCMV-CREB[S133A] for the expression of native and dominant negative human CREB were purchased (Clontech, Saint-Germain-en-Laye, France). In the CREB[S133A] form, the phosphorylation site Serine 133 is mutated to Alanine, thus preventing the transcriptional activity of CREB but still allowing its dimerization (Gonzales and Montminy, 1989). Hence, the expression of CREB[S133A] in neuronal cells leads to efficient functional inactivation of the endogenous CREB (Carlezon et al., 1998). To facilitate the exogenous CREB detection, CREB and CREB[S133A] were first amplified from the commercial vectors and with EcoRI and NotI, they were cloned into the pCMV-HA vector (Clontech, Saint-Germain-en-Laye, France). The so derived HA-CREB and HA-CREB[S133A] constructs replaced the mir30 and DsRed elements. The completed vectors were assigned
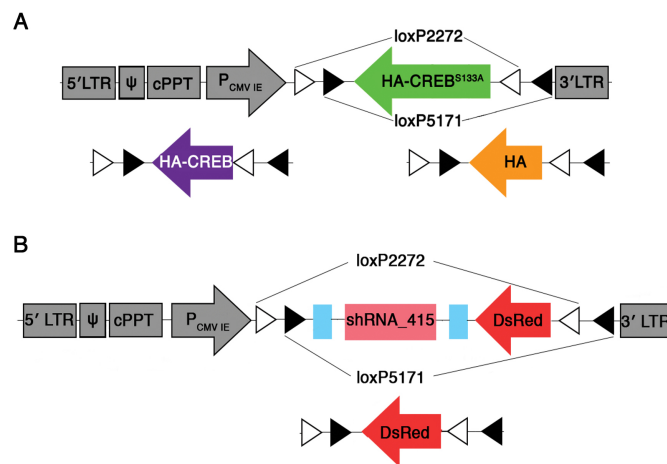
Fig. 2.4: A representative sketch of lentiviral constructs. (**A**) These constructs show lentiviral vectors that are used for the conditional expression of dominant negative CREBS[133A], native CREB and HA that served as a control, under the cytomegalovirus promoter (P_{CMV}). (**B**) Design of a lentiviral vector for conditional shRNA knock down of Chrm1. The vector utilizes a miR30 construct for shRNA expression under the cytomegalovirus promoter (PCMV). DsRed is co-expressed for the visualization of the viral gene.

names as HA-CREB and HA-CREB^{S133A} corresponding to overexpression and dominant negative form, respectively. HA-control vector for the generation of a control lentiviral particle was generated in the same manner, utilizing the HA tag from pCMV-HA (Fig. 2.4). The Chrm1 knockdown viruses were also prepared in our lab by Susann Ludewig (MSc) (Ludewig, 2013).

2.3.2.2 Generation of lentiviral particles

For the generation of lentiviral particles, each 10^6 HEK293T cells were seeded in 10 cm cell culture plates and grown in DMEM with 10% fetal calf serum (FCS) and each 1% streptomycin and penicillin (Life Technologies, Darmstadt, Germany) at 37° C with 5% CO_2. For transfection, fresh DMEM with 25 µM chloroquine was used with further incubation of cells for 2-6 h. The calcium phosphate method was used for transfection after the cells reached 80% confluence, with a final concentration of 0.125 M $CaCl_2$, 5 µg of pRSV-Rev, 3 µg of pMD2. G, 5 µg of pMDLg/pRRE and 10 µg of the respective pLL transfer vector. After overnight incubation, cells were further allowed to grow with fresh DMEM, 10% FCS and each 1% streptomycin and penicillin, after overnight incubation. On the following 2 days supernatant was collected, filtered with a 0.45 µm syringe filter (Corning, Germany) and concentrated by ultracentrifugation for 2 h at 50.000 g (MLA-55, Beckman Coulter). Phosphate buffer saline (PBS) was used to re-suspend the pallets and then stored at -80° C. The QuickTiter™ Lentivirus Titer Kit (Cell Biolabs, USA) was used to determine the viral titer, according to the manufacturer's instructions. Experimental (HA-CREB^{S133A}, HA-CREB, shChrm1) and the control vectors were always prepared in parallel.

2.4 Drugs

For inactivation of NPY type Y1 receptors, the selective NPY-Y1 receptor blocker BIBP3226 (((R)-N2-(diphenylacetyl)-N-[(4-hydroxyphenyl)methyl]-argininamide)) (Tocris Bioscience, UK) was dissolved in 0.9% saline, 1% dimethyl sulfoxide. To block cholinergic signaling in the DG, Scopolamine hydrobromide S1845 (Sigma-Aldrich) was dissolved in 0.9% saline. For Cre recombinase activation in SST-Cre^{ERT2} mice, freshly prepared tamoxifen (Sigma-Aldrich) solution was used. Clozapine-N-oxide (Enzo Life Sciences) was used to activate DREADD receptors.

2.5 Virus application

Mice (10-14 weeks old) were anesthetized with intraperitoneal (i.p.) injection of sodium pentobarbital at a dosage of 50 mg/kg. An individual mouse was then gently placed on a stereotaxic frame (World Precision Instruments, Berlin, Germany). After midline incision on the skin, the skull was cleaned with 0.9% saline and an eye ointment (Bepanthen®) was applied. After craniotomy with a micro drill (World Precision Instruments, Berlin, Germany), 33G injection needle attached to a 10 µl NanoFil microsyringe (World Precision Instruments, Berlin, Germany) was slowly placed into the desired brain area. In this study, I injected conditional viral vectors in both hemispheres aiming at the dorsal DG and dorsal hilus while the medial septum received unilateral injections. The dorsal DG receives injections at the coordinates anterioposterior (AP): -1.94 mm, mediolateral (ML): ±1.3 mm from Bregma and dorsoventral (DV): -1.7 mm from the brain surface. For injections in the dorsal hilus, the coordinates are AP: -1.94 mm, ML: ±1.3 mm from Bregma and DV: -1.7 mm from brain surface. The cholinergic neurons in the medial septum were unilaterally targeted with the coordinates AP: +0.90 mm, ML: -0.6 mm from Bregma and DV: -4.7 mm from the brain surface at an angle of 5°. Viral vectors were injected at a flow rate of 0.1 µl per min via a digital microsyringe pump (World Precision Instruments, Berlin, Germany). Each hemisphere received 1 µl of a virus solution. The injection needle was kept at the injection site for further 5 min to allow proper infusion of a viral solution before being slowly retracted. After viral injections, the skull was cleaned with 0.9% saline and the skin was closed with non-absorbable suture material (5-0/PS3, Perma-Hand® silk suture). For post-operative analgesia, each mouse received subcutaneous injection of 250 mg/kg Novalgin® in 0.9% saline. Each mouse was placed under an infrared lamp until recovery from anesthesia. All mice were allowed to recover from surgery for one week before the onset of subsequent experiments. For efficient viral expression at the hippocampal cholinergic terminals, Chat-Cre mice were left for 8-10 weeks before slice preparation.

2.5.1 Virus activation

Tamoxifen solution was used to induce the Cre recombinase activity in the SST-Cre[ERT2] mice. Each mouse received daily 100 µl i.p. injections containing 2, 4 and 8 mg of tamoxifen for three consecutive days. Since tamoxifen is insoluble in water, thus it was first dissolved in 96% ethanol and then diluted to its final concentration

in corn oil (Sigma-Aldrich, Seelze, Germany). The drug solution was finally sonicated for 3 × 15 min. Always fresh aliquots were prepared for each tamoxifen injection. For efficient activation of the Cre recombinase in HIPP cells, this tamoxifen induction protocol was established in our lab, which proved to be better and with minimal adverse side effects then the original reported tomoxifen induction method (Taniguchi et al., 2011). DREADD receptors were activated 1 h (otherwise stated) before fear memory training via i.p injections of 10 mg/kg CNO in physiological saline (Ray et al., 2011).

2.5.2 Analysis of viral expression

Histological verification of a viral expression was done after completion of the behavioral experiments. Mice were anesthetized with i.p. injections of ketamine-xylazine mixture and transcardially perfused with ca. 50 ml Tyrode buffer followed by ca. 100 ml 4% paraformaldehyde (PFA; for fixation of tissue) in PBS. The brain was carefully removed from the skull and immersed overnight in 4% PFA for post-fixation and then for 48 h in 30% sucrose in PBS for cryo-protection. The brain was then snap frozen in methylbutane cooled with liquid nitrogen and stored at -20° C for further processing. The dorsal hippocampal sections with 30 μm thicknesses were prepared in a cryostat (Leica CM1950, Leica Microsystems). Half of the alternating sections were mounted on the glass slides and covered with Immu-Mount™ (Thermo Scientific) to check under the microscope, and the other half were stored in 24 well plate filled with 0.02% sodium azide in 1x PBS for use in immunofluorescence staining.

Efficiency of viral transduction in this study was confirmed with quantification of the control vectors for AAVs and lentiviral constructs. The expression was determined on six alternating sections with 30 μm thicknesses per animal. To cover more then 60% of the rostro-caudal extension of the dorsal DG, the sections were used from Bregma AP: -1.58 to AP: -2.18 mm. Neurons showing viral tag expression were counted between the medial pole of the hilus and beginning of the area CA4 (N=6 per construct). This quantification data revealed a cell density of 0.683 ± 0.067 cells per 1000 μm^2 for AAV and 0.596 ± 0.021 cells per 1000 μm^2 for lentivirus thus suggesting comparable and efficient transduction of HIPP cell by both viral vectors. For behavioral analysis, only those mice were used that showed accurate bilateral viral expression throughout these regions.

2.6 Pharmacological testing

C57BL/6 wild type mice (10-14 weeks old) were anesthetized with i.p. sodium pentobarbital (Sigma-Aldrich) 50 mg/kg and gently placed on a stereotaxic frame (World Precision Instruments). Each animal underwent bilateral craniotomies using a micro drill and then bilateral 26G guide cannula (C235GS-5-2.0/SPC, Plastic One Inc.) was stably implanted into the dorsal DG under stereotaxic guidance (Begado-Acosta et al., 2014). The guide cannula placement was AP: -1.94 mm and ML: ± 1 mm from Bregma and DV: -1.4 mm below pedestal from the brain surface. After careful implantation, the guide cannula was secured with a dental cement (Hoffmann Dental Manufaktur) and a paladur resin (Heraeus Kulzer). The bilateral guide cannula was closed with a dummy cannula and covered with a dust cap. Mice were given a post-surgery recovery period of 7 days before the drug infusion and behavior testing. For drug injections, mice were anesthetized with 5% isoflurane in O_2/N_2O mixture (Rothacher Medical GmbH., Switzerland) and placed on a stereotactic frame (World Precision Instruments, Berlin, Germany). Anesthesia was maintained throughout the surgery at 1.5%-2.0%. A 33G injection cannula was inserted, extending 0.5 mm beyond the guide cannula (total depth 1.5 mm) and each mouse received intra-hippocampal infusions of 1 µl per hemisphere at a rate of 0.5 µl per min of the antagonist or corresponding vehicle. The NPY-Y1 receptor antagonist BIBP3226 was infused at 1.5 pmol/µl in 0.9% saline, 1% DMSO, 45 min before fear memory training or fear memory retrieval. Scopolamine hydrobromide S1845 (Sigma-Aldrich, Seelze, Germany) was infused at a dose of 5 µg/µl in 0.9% saline, 15 min before testing in the elevated plus maze. Histological validation of the cannula placement was done after the completion of behavioral experiments. To this end, mice were infused with 1 µl methylene blue (10 mg/ml in 0.9% saline with 1% DMSO) as described above. The brain was removed after 30 min and snap frozen in methylbutane cooled with liquid nitrogen. Coronal sections (AP: -1.34 mm to -2.54 mm) of 30 µm thicknesses were prepared on a cryostat microtome (Leica CM1950, Leica Microsystems) and weakly counterstained with 1% cresyl violet acetate solution and embedded with Immu-Mount™ (Thermo Scientific). Only mice with correct bilateral cannula placement were selected for data analysis.

2.7 RNA isolation and quantitative PCR

To measure the expression of target genes after viral expression of the dominant negative CREB[S133A] or native CREB, laser capture micro-dissection (LCM) (P.A.L.M

MicroBeam, Carl Zeiss, Jena, Germany) was employed (Albrecht et al., 2010, 2013). Mice were killed with cervical dislocation and the brains were snap frozen in methylbutane cooled with liquid nitrogen and stored at -80° C. The brains were transferred from -80° C to -20° C for 30 min and then to the cryostat chamber (chamber temperature -16° C and object temperature -16° C) before further processing. Coronal sections with 16 μm thicknesses were prepared on a cryostat microtome (Leica CM1950, Leica Microsystems) at the level of dorsal hippocampus. The sections were thaw-mounted directly on special LCM RNase free glass object slides covered with 1.35 μm thick polyethylene naphthalate membranes (Carl Zeiss, Jena, Germany) that facilitate laser cutting and catapulting of the tissue samples. To increase the adherence of the brain tissues, the slides were coated with poly-L-lysine. During this whole process, the conditions were carefully set to minimize RNase activity. After every mounting, the slides were placed on a warming plate at 40° C, hence minimizing RNase activity by drying the sections. The sections were then stained with standard cresyl violet acetate staining protocol under nuclease-minimized conditions. This allowed proper visualization of the dorsal hippocampus at a level of individual layers. The dorsal hilar tissue from 8 to 10 sections per animal (AP: -1.34 mm to AP: -2.54 mm) was marked bilaterally and micro-dissected individually into the adhesive cap of a 50 μl capture tube (Carl Zeiss, Jena, Germany) (Fig. 2.5).
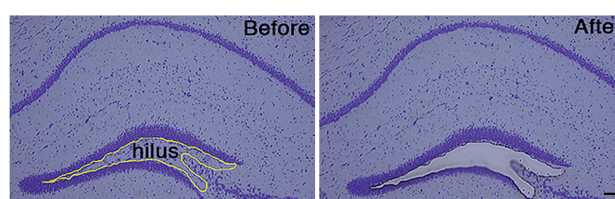
Fig. 2.5: Representative microscopic images of the LCM. The images show hilus of the dorsal hippocampus before and after the tissue capture for quantitative mRNA expression analysis. Scale bar, 100 μm.

Lysis of samples and total RNA isolation was performed via RNeasy® plus micro kit (Qiagen), according to the manufacturer's instructions, including steps for the removal of genomic DNA. First-strand synthesis of cDNA was performed with the Sensiscript Reverse Transcription kit (Qiagen), specifically designed for low amounts of RNA, using a Oligo (dT) 18 and random decamer first strand primers (Life Technologies, Darmstadt, Germany). A 1:5 dilution of cDNA sample was used to measure different genes with real time qPCR via ABI Prism StepOnePlus™ Real-time

PCR system (Life Technologies) using TaqMan® reagents with predesigned FAM-labeled assays for different target genes and VIC-labeled assays for glyceraldehyde 3-phosphate dehydrogenase (GAPDH) as a house keeping gene.

For quantitative PCR, TaqMan® reagents and predesigned FAM-labeled assays for NPY (Mm00445771_m1), SST (Mm00436671_m1), GAD_{67} (Mm00725661_s1), and GAD_{65} (Mm00484623_m1) were used in duplex with VIC-labeled assay for GAPDH serving as an internal control.

2.8 Immunohistochemistry

Immunohistochemistry was performed on the perfused brain sections with 30 µm thicknesses stored in 0.02% sodium azide in 1x PBS. Briefly, the sections were washed 3 times with 1x PBS each for 5 min with gentle tumble on a tabletop shaker. The unspecific binding was blocked with a blocking solution containing 10% normal donkey serum in 1x PBS with 0.5% Triton X (500 µl per well) for 1 h at room temperature. Sections were then incubated overnight at 4° C with primary antibodies, anti HA-tag (Cell Signaling #3724, Frankfurt am Main, Germany) at a dilution of 1:300, anti-NPY (Abcam, Cambridge, UK) at 1:700, anti-SST (Santa Cruz Biotechnology #13099, Heidelberg, Germany) at 1:250 and anti-cFos (Cell Signaling #2250, Frankfurt am Main, Germany) at 1:1000. Sections incubated without primary antibodies were used as negative controls. Slices then underwent three washing steps with 1x PBS, followed by 1 h incubation with Alexa-Fluor488 and Alexa-Fluor555-coupled secondary antibodies at 1:1000 dilution (Life Technologies) in 2% Bovine serum albumin (BSA) and 1x PBS with 0.03% Triton X. For anti-cFos, biotinylated anti-goat (1:200; Vector Laboratories, USA) was used and visualized through conjugation with streptavidin Cy2 at 1:1000 (Jackson ImmunoResearch Labs, UK). After 3 more washing steps with 1x PBS, sections were stained with DAPI (300 nM) to visualize the nuclei. Finally, sections were again washed in 1x PBS and were mounted with Immu-Mount™ and coverslips. Immunostainings in all experiments were examined using a DMI 6000 epifluorescence microscope and a TCS SP2 or a SP8 confocal microscope (all Leica Microsystems, Germany).

For cFos$^+$ and NPY$^+$ cells quantification 30 µm thick coronal sections were obtained from conditioned mice. A total of 6 coronal sections from each animal at intervals of 90 µm starting from the rostral pole of the DG were used for staining and subsequent quantification. cFos$^+$ cells were manually counted in the dorsal DG

granule cell layer and NPY+ cells in the hilus of the dorsal DG. LAS-AF software was used to measure the quantified area and cell densities were expressed as a number of positive cells per mm^2 area. Mean cell densities from corresponding 6 sections from each animal were measured for statistical comparison between groups.

2.9 Field potential recordings

To determine the effect of HIPP cell manipulation on the DG activity in this study, Gürsel Çalışkan (PhD) in our lab, examined the population spikes induced by perforant pathway stimulation.

2.9.1 Slice preparation

Adult male mice (wild type naïve C57BL/6, virus injected SST-Cre[ERT2] and Chat-Cre driver mice) after deep isoflurane anesthesia were decapitated. The brains were carefully and rapidly (~30-60 s) removed and immediately placed in a cold (4-8° C) carbonated (5% CO_2/ 95% O_2) artificial cerebrospinal fluid (aCSF) containing 21 mM $NaHCO_3$, 129 mM NaCl, 1.6 mM $CaCl_2$, 3 mM KCl, 1.25 mM NaH_2PO_4, 1.8 mM $MgSO_4$ and 10 mM glucose. With an angled platform parasagittal slices with 400-μm thicknesses were cut at an angle of about 12° which results in the dorsal hippocampal transverse slices. Most dorsal slices (3-4) were placed in an interface chamber perfused with aCSF at 32 ± 0.5° C with a flow rate: 2.5 ± 0.2 ml per min and a pH 7.4, osmolarity ~300 mosmol/kg. For ~1 h slices were incubated before onset of electrical recordings.

2.9.2 Field recordings

A glass electrode filled with aCSF (~1 MΩ) was used to obtain extracellular field recordings. To investigate electrophysiological parameters in the DG, the recording electrode was placed on the granule cell layer at a depth of 70-100 μm. A bipolar tungsten wire electrode (exposed tips ~20 μm, tip separations ~75 μm and electrode resistance in aCSF ~0.1 MΩ) was used to conduct stimulations of the perforant pathway that presumably activates both of its medial and lateral fibers. An input-output (I/O) curve was obtained after recording the baseline responses (0.033 Hz, pulse duration: 100 μs) for 20-30 min. Seven intensities ranging from 10-150 μA were used to acquire an I/O curve. For baseline excitability measurements, stimulus intensity that resulted in ~70% of the maximum population spike (PS) amplitude was used. Slices obtained from the wild type C57BL/6 mice were used to determine the effects of the selective Y1 receptor antagonist BIBP3226 (1 μM). HIPP cells

silencing was achieved with CNO (10 µM) in slices obtained from the SST-Cre^{ERT2} mice injected with hM4Di vectors. After baseline recordings of 20 min (one stimulus every 2 min) either BIBP3226 (1 µM) or CNO (10 µM) was added to the aCSF. These drugs remained in the solution until the end of the experiments. After 20 min of only BIBP3226 or only CNO bath application, oxotremorine M (oxo, 1 µM) was added to the solution and for another set of 20 min, PS responses were measured. Key findings were confirmed, in a second set of experiments with carbachol (CCh, 10 µM) as general muscarinergic agonist instead of oxotremorine M. Without addition of either BIBP3226 or CNO, control slices were measured in a similar fashion. With a similar protocol, the effects of combined BIBP3226 and CNO vs. only BIBP3226 application in slices from the SST-Cre^{ERT2} mice expressing hM4Di in the dorsal hilus, was determined. Muscarinergic depression of the PS responses was measured with low (0.1 µM) and high (1.0 µM) concentrations of oxo in slices obtained from the SST-Cre^{ERT2} mice that were expressing either the native CREB or CREB^{S133A} viral vectors. With a similar protocol, after 20 min of the baseline recordings (one stimulus every 2 min), BIBP3226 was added to the aCSF that remained in the perfusion solution (until experiment finished), and followed by the application of oxo for 20 min. In a similar fashion, control slices were measured without addition of BIBP3226.

To study the effects of endogenous ACh release on the perforant path stimulation induced PS, parasagittal dorsal hippocampal slices were obtained from the Chat-Cre driver mice expressing hM3Dq in the septo-hippocampal projection neurons. Within dorsal DG, hM3Dq expression in the terminals of the septo-hippocampal projection neurons was confirmed. After 20 min of the baseline recordings (one stimulus every 2 min), to stimulate the cholinergic fibers in the dorsal hippocampus, CNO (10 µM) was added to the aCSF. CNO remained in the perfusion solution until experiment finished. Then after 20 min, BIBP3226 was added in the perfusion solution and responses were recorded for another 20 min. A custom-made amplifier was used for signals pre-amplification and low-pass filtered at 3 kHz. For off-line analysis, signal sampling was done at 10 kHz frequency and stored on a computer hard disc. Data were analyzed offline using self-written MATLAB-based analysis tools (MathWorks, Natick, MA, USA). The area above the curve was integrated to calculate the PS area (ms.mV).

2.10 Statistical analysis

All data are summarized as mean ± s.e.m (standard error of the mean). Shapiro-Wilk's test was used to test the normality of data. One-way analysis of variance (ANOVA) was performed for multiple comparisons followed by Fisher's protected least significant difference test (LSD) for post-hoc comparison. Whenever only two groups were compared either the Student's two-tailed t-test was used or the Mann-Whitney U test. The program g*power v3.1 was used to calculate statistical power and post-hoc analysis confirmed that critical t and F values were reached in each case of reported significance. For field electrophysiology, when appropriate, either one-way repeated ANOVA, paired t-test or Wilcoxon signed rank test were used. To assess the interactions of viral manipulation of the CREB activation and BIBP3226 treatment in field electrophysiology data, two-way ANOVA was used. Differences were considered statistically significant, if $P < 0.05$.

3. Results

3.1 Different conditioning protocols to study fear memory

Rationale

Pavlovian fear conditioning has been extensively used since Ivan Pavlov (1927), to delineate the brain circuits and neuronal mechanisms of fear memory formation. To date, by using Pavlovian fear conditioning, neuroscientists have gained detailed knowledge about neural circuits, thus proving to be one of the best mammalian model system for studying how sensory information is transformed by the nervous system into memories ultimately leading to adaptive behaviors. This form of conditioning has been shown to work throughout the animal phyla and observed in dogs, cats, flies, worms, fish, pigeons, rodents, snails, monkeys and even in humans (LeDoux, 2000). Moreover, it enables the organisms to form a neural representation of their habitat, which ultimately assist them in deciphering the relationship between aversive or traumatic events and the environmental stimuli that predict them. In a simple conditioning paradigm, when an initially neutral stimulus (CS-tone) is paired with a biologically significant event such as a foot-shock in rodents, the CS ultimately acquires affective properties of the US. Onset of CS alone then produces the innate physiological and behavioral responses of the US. The CS-tone is the main significant predictor but the contextual features where the conditioning takes place also carry some predictive value. Thus, if the elemental CS lacks the significant predictive value of the US then the contextual features induce full memory response. By contrast, if the CS is the sole predictor then the presentation of contextual features in its absence induce only a partial response (Rescorla and Wagner, 1972).

In this study, I first adapted and optimized the conditioning protocols that are known to result in different contextual processing using the C57BL/6 wild type mice. These conditioning paradigms - background context conditioning (CS-US paired), foreground context conditioning (CS-US unpaired) and pure context conditioning (US alone) further enabled me to directly assess the relative contribution of the hippocampal circuits (Phillips and LeDoux, 1994; Desmedt et al., 1998, 1999).

3.1.1 Background vs. Foreground vs. Pure contextual conditioning

To evaluate the salience of memory for the context or the cue or for both, naïve wild

type C57BL/6 mice were divided into three groups. One group of mice 'background context group' underwent training with paired presentations of CS-US, a second group 'foreground context group' received explicitly unpaired presentations of CS-US and the third group 'pure context group' was trained with the delivery of US alone. All these groups were trained with identical sensory stimuli (3 × CS: 10 kHz, 85 dB, 9 s and 3 × US: 0.4 mA, 1 s). The readout of memory in rodents is typically a freezing response, which is the complete immobility except breathing, calculated in percentage with respect to time. The contextual memory was tested in the conditioning context and the auditory cued memory was tested in the neutral context upon presentation of CSs (Fig. 3.1)
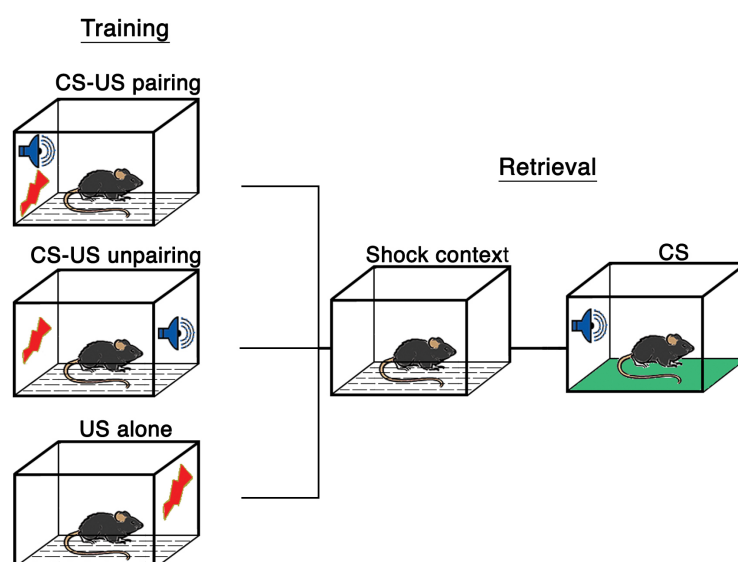
Fig. 3.1. A schematic representation of training protocols and retrieval sessions.

The freezing behavior between the groups remained unchanged during pre-training habituation (One-way ANOVA $F_{(2.21)} = 0.24$, $P = 0.78$) and in the immediate post-training period (One-way ANOVA $F_{(2.21)} = 1.56$, $P = 0.23$). However, a slight increase in freezing was observed in the neutral context after foreground context conditioning then background context conditioning (One-way ANOVA $F_{(2.21)} = 3.82$, $P = 0.03$), but both still remained at or below levels of the pre-training habituation phase (Fig. 3.2). Interestingly, with these training paradigms I was able to generate reduced levels of contextual memory following background context conditioning compared to foreground context condition. Moreover, I showed that foreground context conditioning resulted in a full contextual salience as similar freezing levels were observed with pure context conditioning without an elemental

CS. Thus, these conditioning paradigms produced significantly different levels of freezing behavior during contextual (One-way ANOVA F (2.21) = 10.96, P = 0.001) and auditory cued (F (2.21) = 16.77, P < 0.001) memory retrievals (Fig. 3.2).
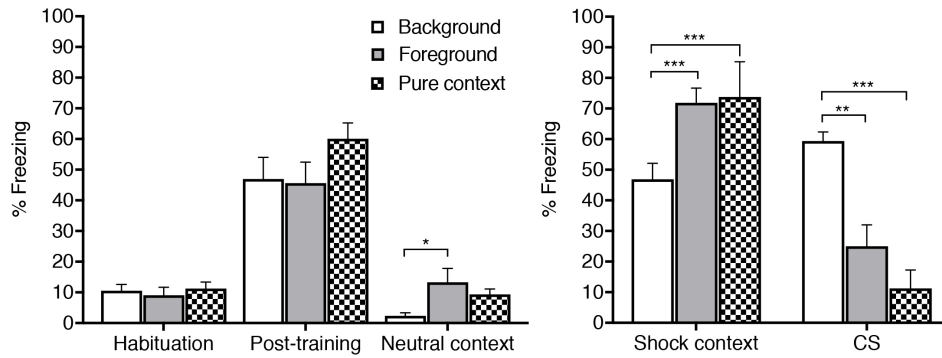
Fig. 3.2: Behavioral comparisons between different training paradigms in C57BL/6 wild type mice. (Left) Wild type C57BL/6 mice display no differences in freezing levels during habituation and immediate post-training phase in conditioning with background context conditioning (n = 8), foreground context conditioning (n = 8) and pure context conditioning (n = 8). A significant increase in the neutral context between the foreground and background context group is seen but both of these groups remain at or below levels of pre-training habituation phase. (Right) Freezing in the shock context is significantly lower in the background context group as compared to both the foreground and pure context group. Moreover, as expected the background context group shows significantly higher freezing response upon presentation of CS-tones compared to both the foreground and pure context group. Data are presented as means + s.e.m. Statistical analysis was performed with Fisher's LSD following one-way ANOVA. *P < 0.05, **P < 0.01 and ***P < 0.001.

In these experiments, during the memory retrieval session mice were first placed in the shock context and then in to the neutral context with onset of CS-tones, thus in order to check the order effect at memory retrieval, one group of naïve wild type C57BL/6 mice was trained in background context conditioning and then 24 h later, first tested in the neutral context with CS-tone presentations and 48 h later, in the shock context. This control experiment with reversed order of retrievals did not produce any difference between groups in the shock context (Student's t-test: t (14) = 0.386, P = 0.70) or during presentation of CSs in the neutral context (Student's t-test: t (14) = 0.31, P = 0.75) . The freezing responses between these groups during habituation (Student's t-test: t (14) = -1.14, P = 0.27), immediate post-training (Student's t-test: t (14) = 1.22, P = 0.24) and in the neutral context (Student's t-test: t (14) = 1.11, P = 0.61) remained unchanged (Fig. 3.3A). In an additional control experiment, to test the effect of possible latent inhibition on fear learning, I used a group of naïve wild type C57BL/6 mice and subjected them to background context conditioning without prior habituation to the conditioning context. The omission of

conditioning context exposure before training did not result in latent inhibition but rather enhanced the representation of contextual features in conditioned mice with pre exposure (Student's *t*-test: t (14) = 4.96, *P* = 0), however the behavior immediately after training (Student's *t*-test: t (14) = 1.93, *P* =0.07) and in the shock context (Student's *t*-test: t (17) = 0.27, *P* =0.79) remained unchanged between groups. The freezing behavior without habituation was increased in the neutral context (Student's *t*-test: t (14) = -3.32, *P* = 0.005) and the group with habituation showed increased memory to the CS-tones (Student's *t*-test: t (14) = 3.12, *P* = 0.007) compared to the group without habituation (Fig. 3.3B).
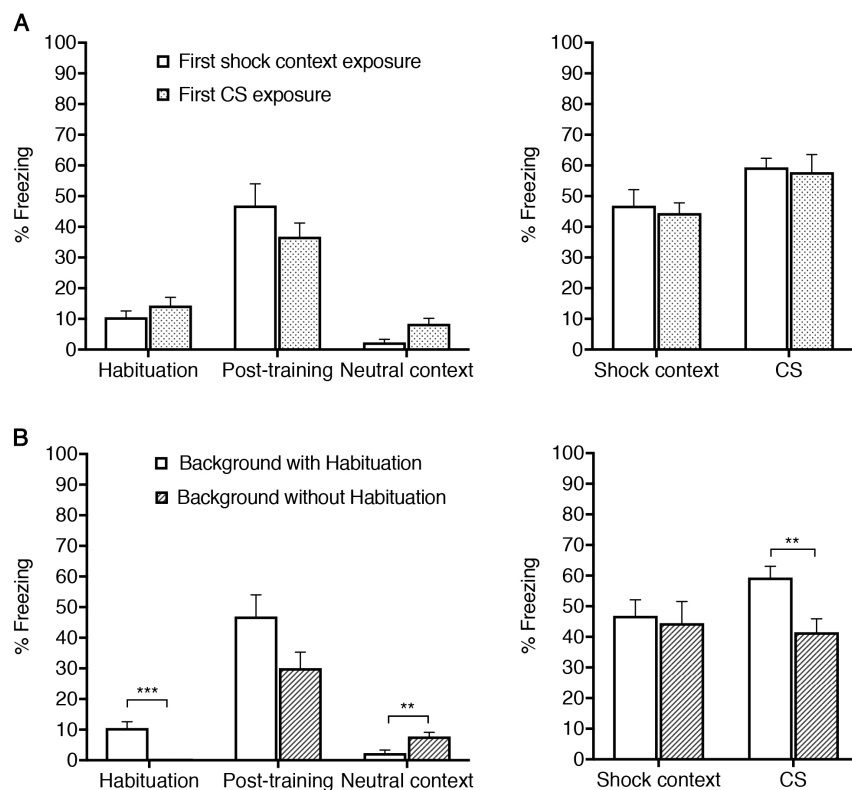
Fig. 3.3: Behavioral control experiments in C57BL/6 wild type mice. (**A**) (Left) Both groups (*n* = 8 each) display no differences in the freezing levels during habituation, in immediate post-training phase and in the neutral context. (Right) Similarly, the freezing levels are not different between the groups during exposure to the shock context and during CSs presentations. (**B**) (Left) Wild type C57BL/6 mice with habituation (*n* = 8) show high freezing levels compared to the group without habituation (*n* = 8) in pre-training habituation phase while no difference is evident in immediate post-training phase between groups. During neutral context exposure, a group without habituation shows higher levels then the other group. (Right) The behavior during exposure to the shock context is not different between groups; however, prior exposure to the conditioning context increases the auditory cued memory compared to the other group. Data are presented as means + s.e.m. Statistical analysis was performed with Student's unpaired *t*-test. **P < 0.01 and ***P < 0.001.

3.2 Dorsal hippocampus circuit is involved in background context conditioning
Rationale

The classical view suggests that memory traces are laid down in cell ensembles across distributed hippocampal-cortical networks and the hippocampus in particular is known to be involved in memory formation, storage and consolidation (Squire et al., 2004), however these specific functions are beginning to be discovered in fine details. While the amygdala is thought to mediate more simple CS-US associations during fear conditioning, the function of the hippocampus in context conditioning is highly specified by the presence or absence of an elemental CS, i.e. by the question whether context is encoded in the foreground or in the background (Phillips and LeDoux 1994; Desmedt et al., 2003). Phillips and LeDoux (1994) showed with lesion studies the differential involvement of the dorsal and ventral hippocampus, where lesions to the dorsal region interferes with background context memory while lesions to the ventral region interferes with foreground context memory. Correspondingly, the DG of hippocampal formation is important for the formation of contextual memory and is critically involved in discriminating similar contexts (McHugh et al., 2007; Lee and Kesner, 2004). Converging evidence suggests that a local DG circuit in the dorsal hippocampus constituted by inhibitory hilar perforant path-associated (HIPP) cells and excitatory granule cells could be involved in background context fear particularly in adjusting its level. During memory encoding, this local inhibitory circuit formed by HIPP cells orchestrates granule cells activity. HIPP cells employ negative feedback and feed-forward circuits to control the firing rate of granule cells and ultimately prevent excessive DG discharge. They also control and check the formation of granule cell memory ensembles during conditioning (Savanathrapadian et al., 2014; Stefanelli et al., 2016).

In this study with pharmacogenetic approach, I first validated a role of the dorsal DG in background context conditioning and then examined the local DG circuitry. I investigated the role of this dorsal DG local circuit formed by HIPP cells in controlling and sharing the strength of memory between the context and cue in background context conditioning.

3.2.1 Dorsal DG controls background context conditioning

To confirm the role of the dorsal DG in background context conditioning, I selectively targeted the excitatory neurons of the DG using the CamK2a-Cre driver

mice. These mice express a Cre recombinase under the control of Ca^{2+}/calmodulin-dependent protein kinase II (*Camk2a*) promoter, thus injection of the adeno-associated virus (AAVs) hSyn-DIO-hM4Di-mCherry in the dorsal DG resulted in the expression of inhibitory DREADD receptors in excitatory neurons. These DREADD receptors allow for transient silencing upon i.p. administration of clozapine-N-oxide (Krashes et al., 2011). The adeno-associated virus hSyn-DIO-mCherry conditionally expressing only the fluorescent marker was used as a control. The complete pharmacogenetic inactivation of the dorsal DG during memory acquisition (Fig. 3.4A) resulted in a profound reduction of background context memory (paired CS-
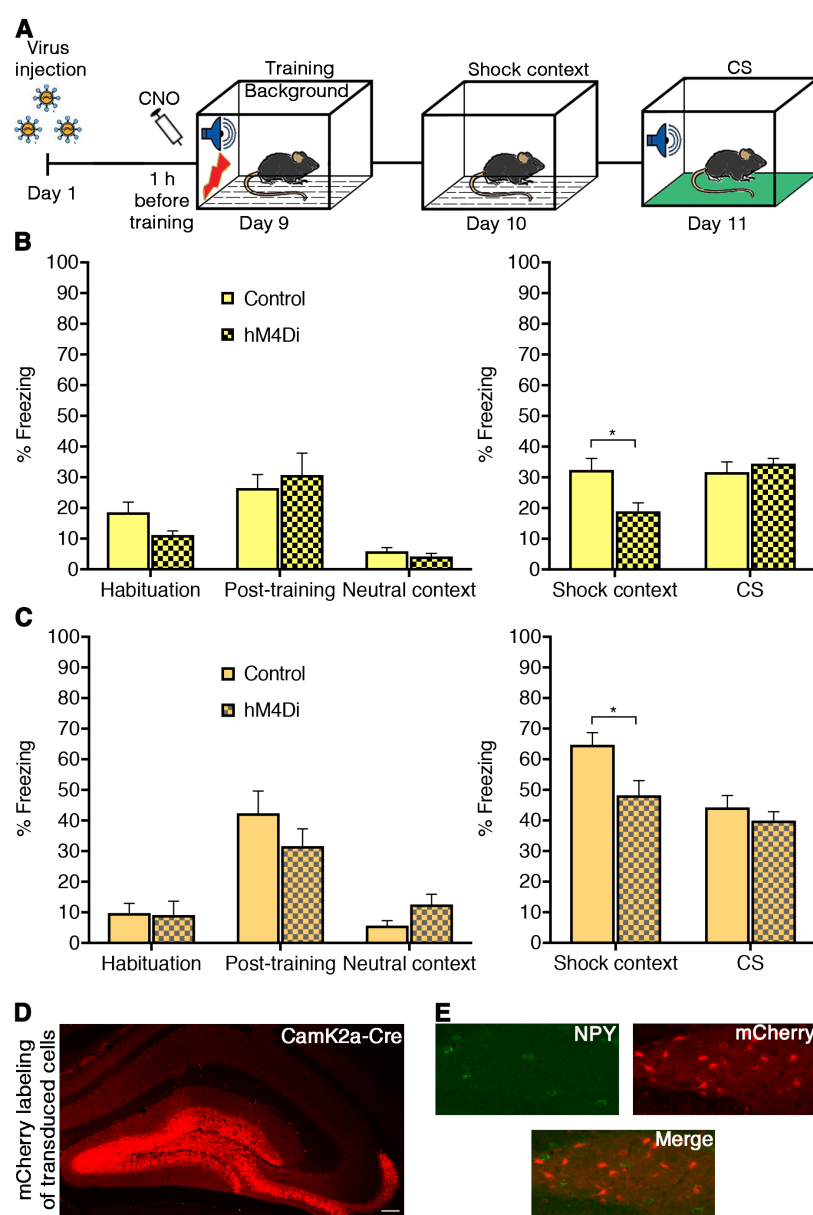

Fig. 3.4: Dorsal DG is important in controlling background context memory. (**A**) The silencing of excitatory granule cells of the dorsal DG in the CamK2a-Cre mice selectively

decreases background context conditioning in the hM4Di injected group (*n* = 9) as compared to the control group (*n* = 10) with mild (0.4 mA) training protocol as well as with (**B**) moderate (0.8 mA) training protocol (hM4Di, *n* = 9; control *n* = 10). (**C**) A schematic of the DG circuit with silencing of complete dorsal DG. (**D**) A representative microscopic image of viral mCherry expression in the DG. Scale bar, 100 μm. (**E**) Effective expression of viral vectors in NPY-negative, but not in NPY+ cells of the hilus in the CamK2a-Cre driver mice. Data are presented as means + sem. Statistical analysis was performed with Student's unpaired *t*-test. *$P < 0.05$.

US presentation) compared to controls, when tested in the conditioning context (shock context). The animals with mild (0.4 mA) training (Student's *t*-test: t (17) = 2.84, *P* =0.01, Fig. 3.4B) as well as with moderate (0.8 mA) training conditions (Student's *t*-test: t (13) = 2.60, *P* = 0.02, Fig. 3.4C) showed significant differences between groups. However, the memory to the conditional stimuli tested in the neutral context in the animals with mild (0.4 mA) training (Student's *t*-test: t (17) = -0.72, *P* = 0.49, Fig. 3.4B) as well as with moderate (0.8 mA) training conditions (Student's *t*-test: t (13) = -1.07, *P* = 0.34, Fig. 3.4C) showed no differences between groups. This pharmacogenetic inhibition of the dorsal DG did not affect freezing behavior with mild training during habituation (Student's *t*-test: t (17) = 1.98, *P* = 0.06), in the neutral context (Student's *t*-test: t (17) = 1.71, *P* = 0.27) and immediate post-training (Student's *t*-test: t (17) = -0.51, *P* = 0.61) (Fig. 3.4B). Similarly, this manipulation did not affect freezing behavior with moderate training during habituation (Student's *t*-test: t (13) = 0.10, *P* = 0.91), in the neutral context (Student's *t*-test: t (13) = -1.78, *P* = 0.09) and immediate post-training (Student's *t*-test: t (13) = 1.17, *P* = 0.26) (Fig. 3.4C). The virus infection appeared to be targeting only the excitatory cell as the immunohistochemical labeling of HIPP cells marker NPY did not show co-labeling with the viral fluorescent tag (Fig. 3.4D).

3.2.2 HIPP cells as salience detector in background context conditioning during acquisition

The involvement of the dorsal DG during acquisition of background context memory intrigued me to test the role of HIPP cells that are known to control the local DG circuit and check the ensemble size of granule cells which correlates with strength of context memory (Stefanelli et al., 2016). Therefore to specifically address the putative role of HIPP cells in the encoding of background context memory, I used SST-Cre[ERT2] mice. These mice express a Cre recombinase under the *SST* promoter upon activation with tamoxifen injections. The behavior of SST-Cre[ERT2] mice under tamoxifen treatment was also tested in pre-experiments (Fig. 3.5A), which showed no change between groups. SST is the marker of HIPP cell in the hilus along with

NPY, where both are expressed in HIPP cells. In this line, by using NPY-GFP and SST-Cre^ERT2 double transgenic mice, I confirmed double labeling of NPY in SST$^+$ cells with conditional DREADD virus that only express fluorescent the marker (Fig. 3.5B).
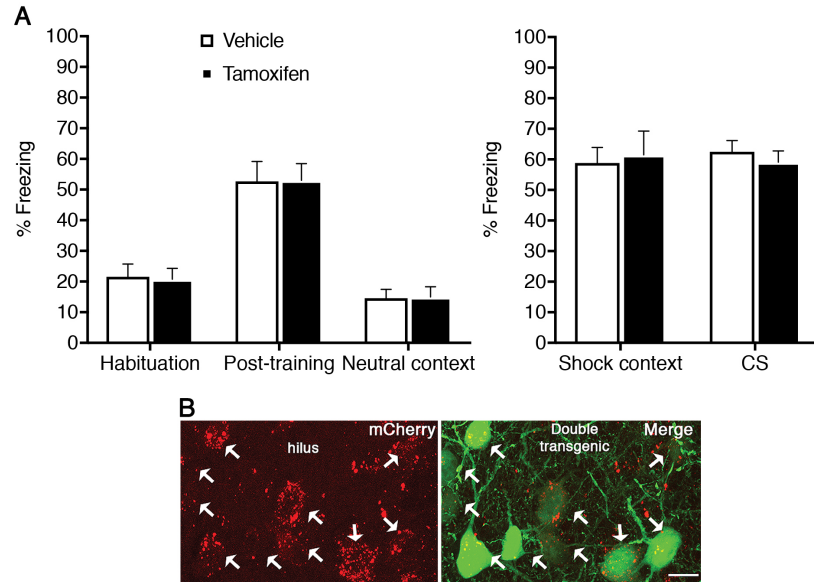
Fig. 3.5: Validation of SST-Cre^ERT2 mouse model to target HIPP cells. (**A**) Tamoxifen treatment (n = 11) did not affect freezing levels measured in habituation (Student's t-test: t (19) = 0.01, P = 0.99), post-training phase (Student's t-test: t (19) = 0.26, P = 0.79), in the neutral context (Student's t-test: t (19) = 0.07, P = 0.94), in the shock context (Student's t-test: t (19) = 0.63, P = 0.53) and during auditory tone presentation (Student's t-test: t (19) = 0.66, P = 0.53) compared to vehicle treated group (n = 11). (**B**) HIPP cells labeled in NPY-GFP x SST-Cre^ERT2 double transgenics upon AAV-mediated expression of mCherry. Green, GFP; red, mCherry. Scale bar, 10 µm. Data are presented as means + sem. Statistical analysis was performed with Student's unpaired t-test.

Since SST-Cre^ERT2 mice can be efficiently used to target HIPP cells, thus I injected them with hM4Di receptors targeting the dorsal hilus. Upon injection of viruses into the hilus and the activation of the Cre recombinase with tamoxifen, HIPP cells were effectively and specifically targeted for pharmacogenetic manipulation. The adeno-associated virus conditionally expressing only the fluorescent marker was used as a control. The HIPP cells were inhibited with i.p. injections of CNO 1 h before training to background context conditioning (Fig 3.6A, C, D). This pharmacogenetic inhibition of HIPP cells during memory acquisition led to a significant increase of contextual memory tested in the shock context (Student's t-test: t (16) = -2.50, P = 0.02, Fig. 3.6B) in background context group, however this manipulation had no effect on auditory cued memory tested in the neutral context (Student's t-test: t (16) = 1.18, P = 0.25, Fig. 3.6B) between groups. The freezing responses of these animals during habituation (Student's t-test: t (16) = -0.73, P = 0.47), immediate post-training

(Student's *t*-test: t (16) = -0.52, *P* = 0.60) and in the neutral context (Student's *t*-test: t (16) = 0.34, *P* = 0.73) remained unchanged (Fig. 3.6B).
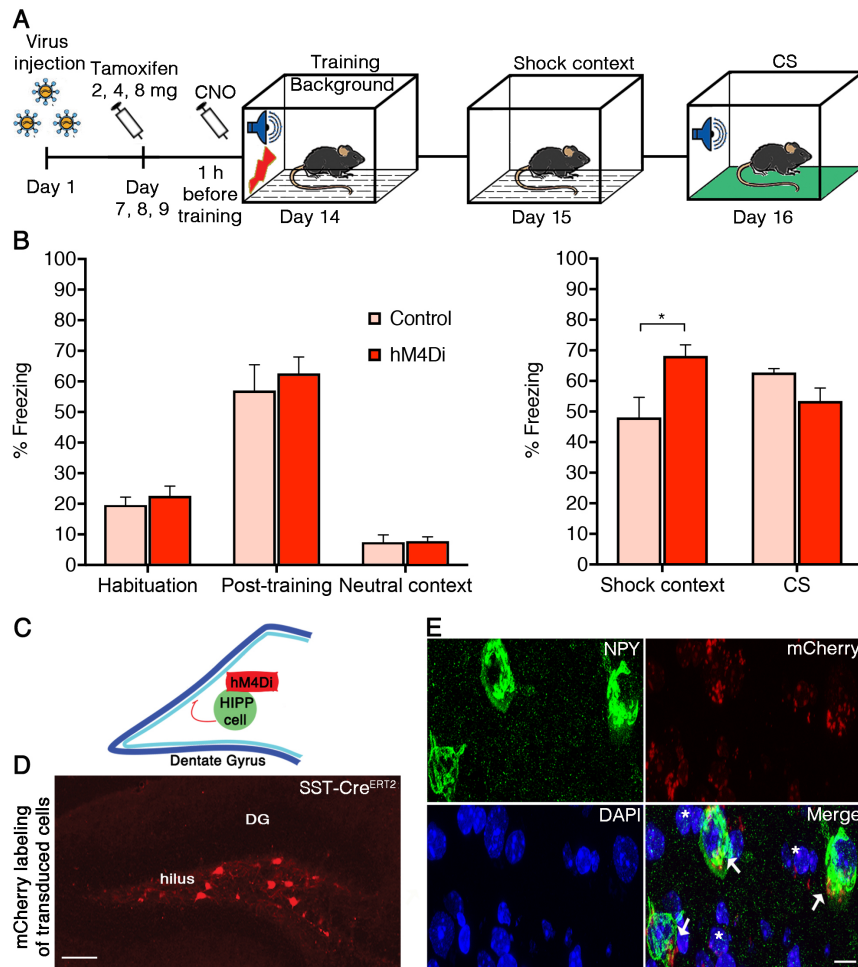
Fig. 3.6: Pharmacogenetic silencing of HIPP cells increases background context conditioning. (**A**) Schematic of background conditioning paradigm and viral transduction. hM4Di viruses were injected into the hilus of SST-Cre^{ERT2} mice and HIPP cells transduction was achieved with the action of Cre recombinase upon increasing doses of tamoxifen injections. Contextual fear memory was tested 24 h after training in the conditioning chamber without CS presentation. Cued fear memory was tested another 24 h later in a neutral context with a set of 4 auditory CSs. (**B**) (Left) The pharmacogenetic inhibition of HIPP cells ((hM4Di, *n* = 8) before training in background context conditioning shows no effect on freezing levels, during habituation, post-training and in the neutral context compared to controls (*n* = 9). (Right) Memory to the background context is increased with silencing of HIPP cells compared to controls. The viral intervention has no effect on the CS response. (**C**) Schematic drawing of the proposed circuitry in the DG with hM4Di selectively blocking HIPP cell during fear memory training. (**D**) A representative image shows viral transduction of HIPP cells with AAVs. Scale bar, 100 μm. (**E**) Representative microscopic images show the mCherry-tagged hM4Di expression and NPY immune staining, where mCherry is observed in NPY$^+$ cells (arrows) and NPY$^-$ cells (asterisks) of the hilus. Scale bar, 10 μm. Data are presented as means + s.e.m. Statistical analysis was performed with Student's unpaired *t*-test. *P < 0.05.

Moreover, the role of HIPP cells with SST-Cre^{ERT2} mice was also tested in background context conditioning with their pharmacogenetic activation with hM3Dq viruses during the acquisition. This activation of HIPP cells did not produce
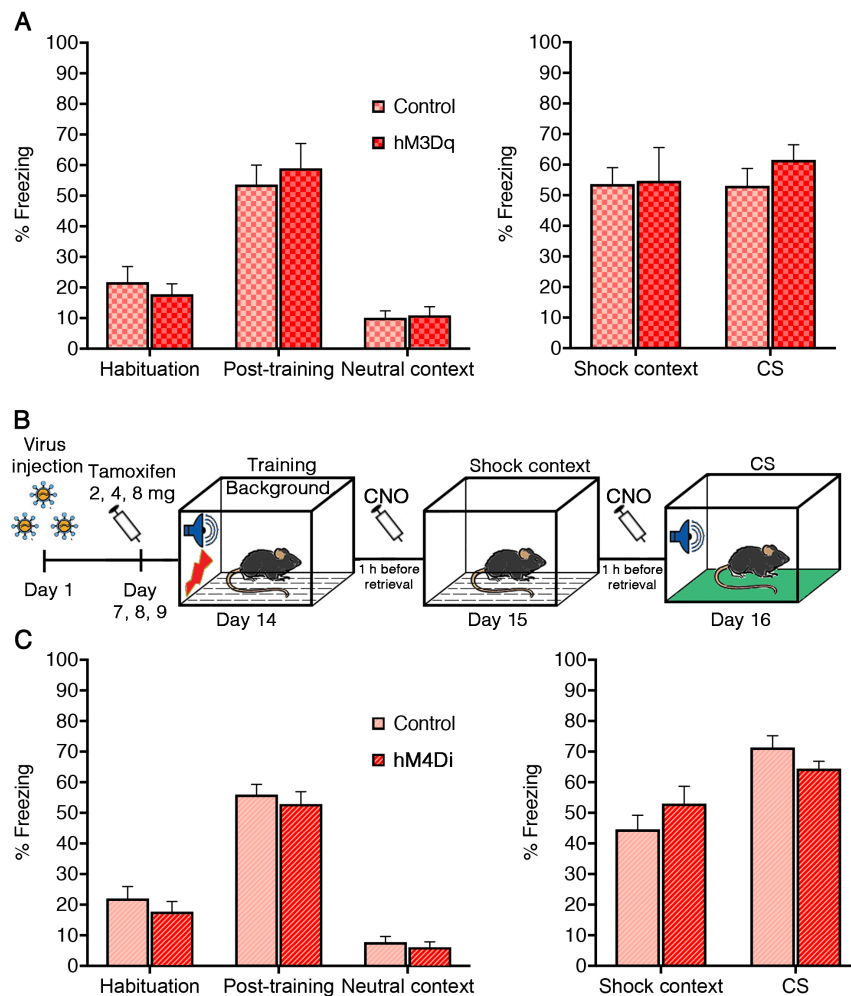
Fig. 3.7: Pharmacogenetic activation of HIPP cells at acquisition and their inhibition at retrieval do not change background context conditioning. (**A**) (Left) The activation of HIPP cells in SST-Cre[ERT2] mice (hM3Dq, *n* = 8) does not induce difference in freezing levels during habituation, post-training, neutral context and (Right) in the shock context as well as during CS presentation compared to vehicle controls (*n* = 8). (**B**) Schematic of background conditioning paradigm and viral transduction. hM4Di viruses were activated with CNO injections 1 h before retrieval sessions. (**C**) (Left) The pharmacogenetic inhibition of HIPP cells ((hM4Di, *n* = 10) before retrieval in background context conditioning shows no effect on freezing levels, during habituation, post-training and in neutral context compared to controls (*n* = 10). (Right) Memory to the background context and CS is not affected with the silencing of HIPP cells at retrieval compared to controls. Data are presented as means + s.e.m. Statistical analysis was performed with Student's *t*-test.

any difference on freezing levels during habituation (Student's *t*-test: t (14) = 0.65, *P* = 0.52), post-training (Student's *t*-test: t (14) = -0.51, *P* = 0.61), in the neutral context (Student's *t*-test: t (14) = -0.23, *P* = 0.82), in the shock context (Student's *t*-test: t (14) = -0.08, *P* = 0.93) and during auditory tone presentations (Student's *t*-test: t (14) = -1.12, *P* = 0.30) (Fig. 3.7A). To further confirm the specificity of HIPP cell function in background context conditioning, another group of SST-Cre[ERT2] mice injected with inhibitory hM4Di viruses were trained and the DREADDs were activated with CNO during retrieval sessions (Fig. 3.7B). This inhibition of HIPP cells

during retrieval did not show any differences between freezing levels in the shock context (Student's *t*- test: t (18) = -1.14, *P* = 0.26) as well as during CSs presentation (Student's *t*-test: t (18) = 1.07, *P* = 0.32) compared to controls (Fig. 3.7C). The freezing behavior during habituation (Student's *t*-test: t (18) = -0.85, *P* = 0.40), in immediate post-training (Student's *t*-test: t (18) = 0.59, *P* = 0.55) and in the neutral context (Student's *t*-test: t (18) = 0.69, *P* = 0.49) also remained unaffected between the groups (Fig. 3.7C).

Since SST-Cre^ERT2 mice with the inhibition of HIPP cells during background context conditioning showed increased freezing to the shock context, thus I tested the role of

Fig. 3.8: Silencing of HIPP cells does not affect foreground and pure context conditioning.
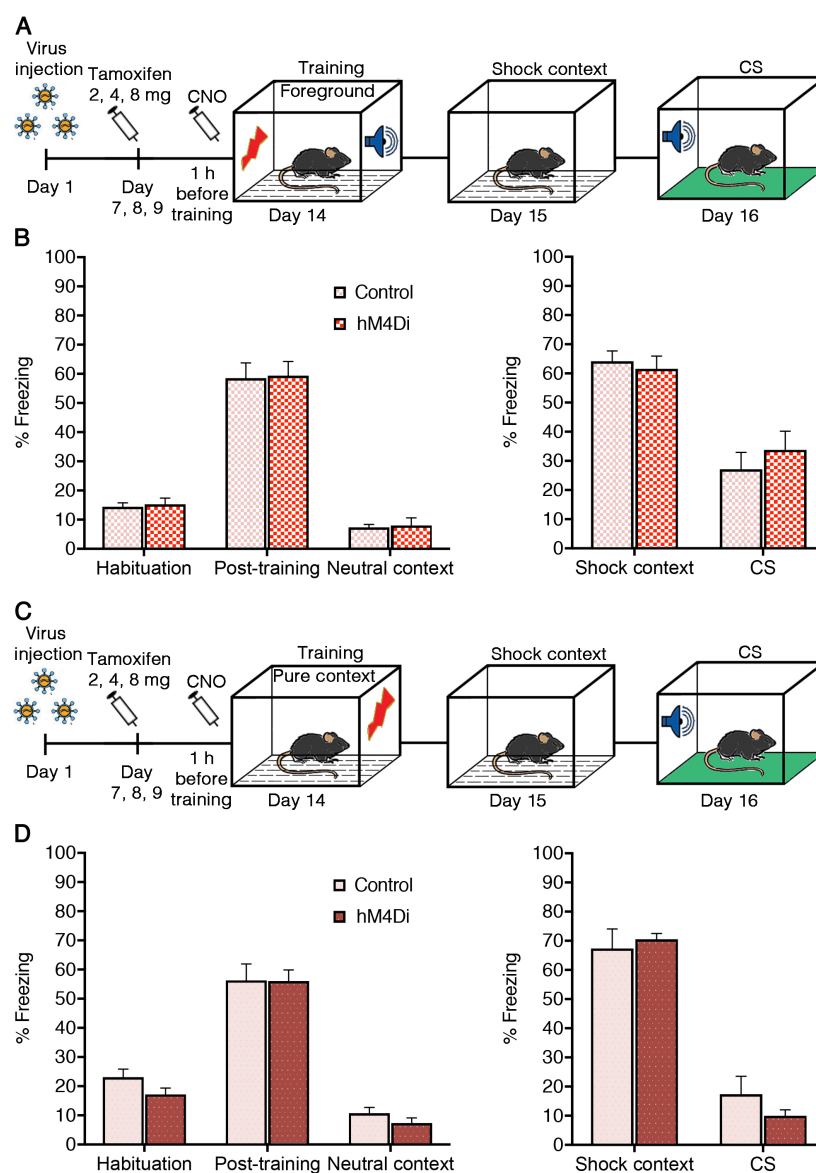(**A**) A schematic of foreground context training paradigm with HIPP cells silencing before

training. (**B**) (Left) No difference is evident between mice with HIPP cell silencing (n = 8) and controls (n = 7) during habituation, post-training and in the neutral context in foreground context conditioning. (Right) No effect of CNO application in freezing responses is observed in the hM4Di group compared to the control group in the contextual and CS responding. (**C**) A schematic of foreground context training paradigm with HIPP cells silencing before training. (**D**) (Left) No difference is seen between mice with HIPP cell silencing (n = 8) and controls (n = 7) during habituation, post-training and in the neutral context in pure context conditioning. (Right) No effect of CNO application in freezing responses is observed in the hM4Di group compared to the control group in the contextual and CS responding. Data are presented as means + s.e.m. Statistical analysis was performed with Student's unpaired t-test.

HIPP cell inhibition with hM4Di receptors in foreground (Fig. 3.8A) and pure context (Fig. 3.8C) conditioning. The adeno-associated virus conditionally expressing only the fluorescent marker was used as a control. The silencing of HIPP cells at acquisition did not produce differences in memory between the groups when tested in the shock context with foreground (Student's t-test: t (13) = 0.45, P = 0.66, Fig. 3.8B) as well as with pure context conditioning (Student's t-test: t (13) = -0.56, P = 0.58, Fig. 3.8D). In foreground context conditioning, the behavior during habituation (Student's t-test: t (13) = -0.35, P = 0.72), immediate post-training (Student's t-test: t (13) = -0.51, P = 0.91), in the neutral context (Student's t-test: t (13) = -0.22, P = 0.82) and during auditory tones (Student's t-test: t (13) = -1.21, P = 0.24) remained unchanged (Fig. 3.8B). And in pure context conditioning, the behavior during habituation (Student's t-test: t (13) = 1.01, P = 0.30), immediate post-training (Student's t-test: t (13) = 0.16, P = 0.87), in the neutral context (Student's t-test: t (13) = 1.13, P = 0.27) and during auditory tones (Student's t-test: t (13) = 1.58, P = 13) also remained unchanged (Fig. 3.8D).

Recently, a study showed increase in context memory with HIPP cells inhibition during pure context conditioning (Stefanelli et al., 2016). However, I did not find any difference with HIPP cells inhibition in pure context conditioning (Fig. 3.8D). To verify these results, I used the St-Cre (Sst[tm2.1(cre)Zjh]/J) driver mice, which were used by Stefanelli et al but I was unable to reproduce these results (Fig. 3.9). The behavior during habituation (Student's t-test: t (12) = 0.74, P = 0.47), immediate post-training (Student's t-test: t (12) = 0.06, P = 0.94), in the neutral context (Student's t-test: t (12) = 0.57, P = 0.57), in the shock context (Student's t-test: t (12) = 0.49, P = 0.62) and during auditory tones (Student's t-test: t (12) = 1.86, P = 0.40) also remained unchanged (Fig. 3.9). In summary, the pharmacogenetic silencing of HIPP cells during training selectively enhances contextual memory only in background context conditioning.
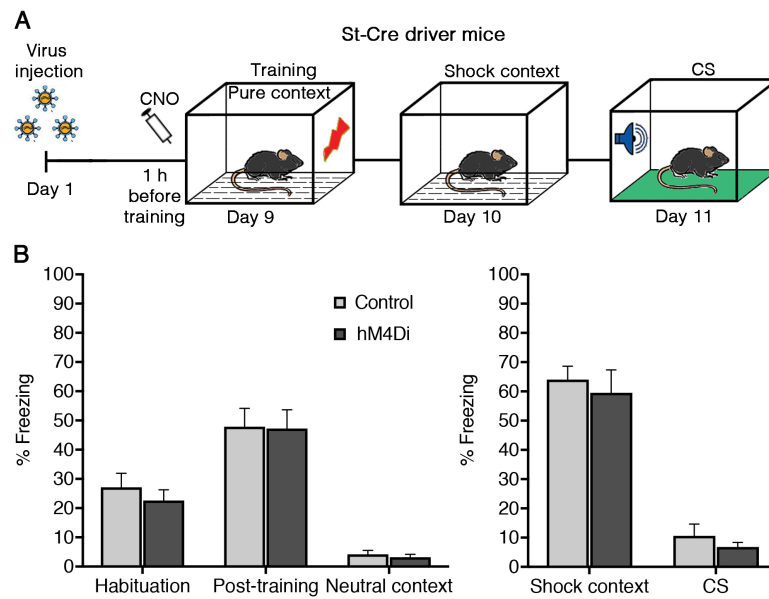
Fig. 3.9: Silencing of HIPP cells in St-Cre mice does not affect pure context conditioning. (**A**) A schematic of pure context training paradigm with HIPP cells silencing before training in St-Cre driver mice. (**B**) (Left) No difference is observed between the groups with HIPP cell silencing ($n = 7$) and controls ($n = 7$) during habituation, post-training and in the neutral context in pure context conditioning. (Right) No effect is observed with HIPP cells silencing compared to control group in contextual and CS responding. Data are presented as means + s.e.m. Statistical analysis was performed with Student's unpaired t-test.

3.2.3 HIPP cells control the DG memory engrams in background context conditioning during acquisition

HIPP cells are known to target the dendrites of granule cells and filter their synaptic output. Thus I set to examine whether HIPP cell activity during the acquisition of background context conditioning also determines neuronal DG ensembles. These ensembles are defined by neuronal activity marker cFos expression in a distinct fraction of granule cells. In this line, I targeted the HIPP cells with hM4Di expressing vectors in SST-Cre^{ERT2} mice. One group of mice received CNO to inhibit the HIPP cells 1 h before training to background context conditioning while the other group received vehicle injections. The brains were removed 1 h after the training to study for cFos expression while the behavior data was also analyzed. Similar to a previous report (Stefanelli et al., 2016), the inhibition of HIPP cells resulted in an increase in the number of cFos$^+$ granule cells in the DG compared to the vehicle-injected group (Fig. 3.10B, C), however the behavior of these animals during habituation (Student's t-test: t (10) = 0.68, P = 0.51) and immediate post-training (Student's t-test: t (10) = -0.96, P = 0.35) remained unchanged (Fig. 3.10A).
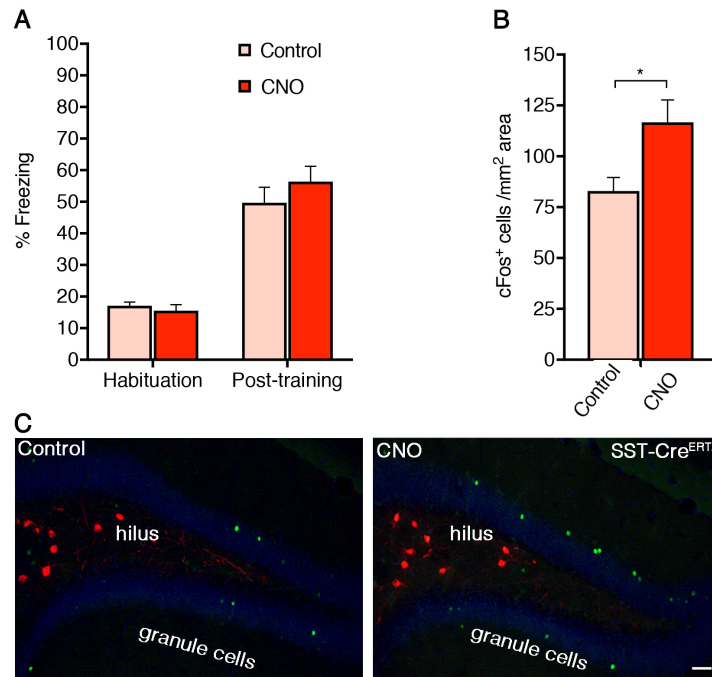
Fig. 3.10: HIPP cells control granule cells expression during background context conditioning. (**A**) HIPP cells silencing with CNO (n = 6) during background context training does not affect habituation and post-training phase compared to controls (n =6). (**B**) However, the silencing of HIPP cells with CNO results in increase number of granule cells seen with activity marker cFos. (**C**) Representative images show the mCherry-tagged hM4Di expression in the hilus and cFos^{+} cells in the granule cell layer of the DG. Scale bar, 50 μm. Data are presented as means + s.e.m. Statistical analysis was done with Student's unpaired t-test. *P < 0.05.

3.2.4 HIPP cells modulate the DG parvalbuminergic cells in background context conditioning

Along with HIPP cells, there is another population of GABAergic cells in the DG that are also known to contact granule cells. These are parvalbumin (PV)-expressing basket cells and they exert powerful control over granule cells by targeting the soma and axon initial segment. They also modulate the action potential output of excitatory granule cells (Freund and Katona, 2007). HIPP cells are also known to target PV^{+} cells and modulate their firing precision in the DG. Thus, HIPP cell inactivation is likely to induce a disinhibition of the DG granule cells as well as PV[+] interneurons (Savanathrapadian *et al.*, 2014). In this line, to mimic a potential disinhibition of PV[+] interneurons through HIPP cell silencing, I targeted them bilaterally with hSyn-DIO-hM3Dq-mCherry in the dorsal DG with using the PV-Cre driver mice. This manipulation resulted in the expression of excitatory DREADD receptors specifically in the PV[+] interneurons. The AAVs, which conditionally express only the fluorescent marker, served as a control. The receptors were activated 1 h before training to background context conditioning with CNO injection

(Fig. 3.11A, C, D). Fascinatingly, this intervention resulted in a reduced background context memory compared to controls (Student's *t*-test: t (14) = 2.25, *P* = 0.04, Fig. 3.11B). However, memory to the auditory cue tested in the neutral context remained unaffected (Student's *t*-test: t (14) = 0.53, *P* = 0.60, Fig. 3.11B) compared to controls.
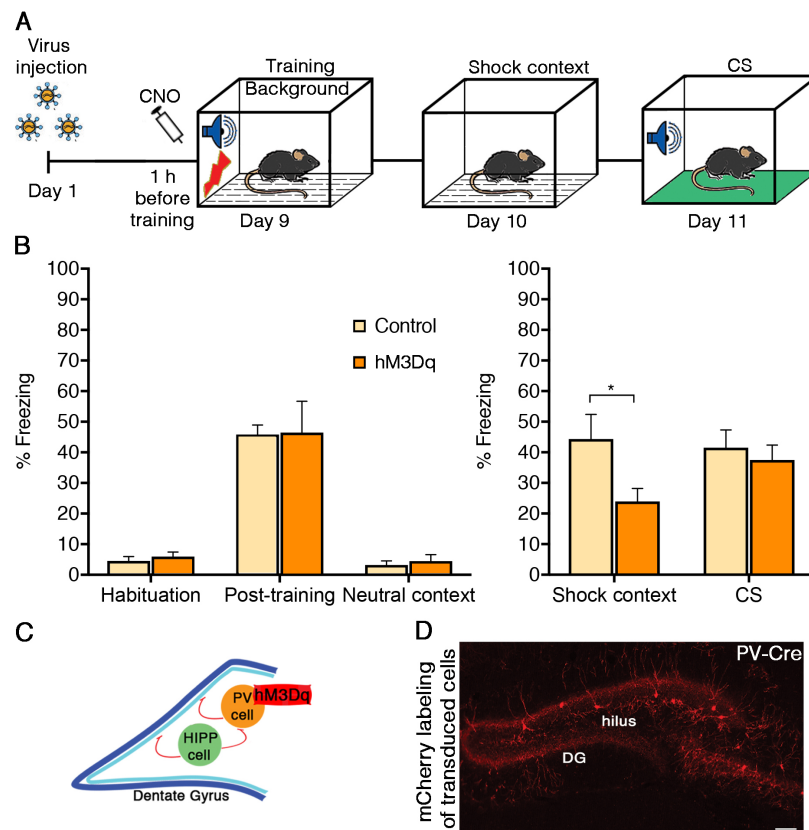
Fig. 3.11: Pharmacogenetic activation of parvalbumin positive cells in the DG results in a reduction in background context memory. (**A**) Schematic of viral injection and background context paradigm. (**B**) Activation of PV+ interneurons of the DG in the PV-Cre driver mice with hM3Dq vector (*n* = 8) decreases background context memory without disturbing auditory cued memory compared to animals with control vector (*n* = 8). Thus, PV+ cells inhibition cannot account for HIPP cells functioning in background context conditioning, however granule cell inhibition in general with the PV+ interneuron activation may attenuate the background context memory formation. (**C**) Schematic of a proposed circuit with PV+ cell manipulation. (**D**) A microscopic image shows mCherry expression in the PV+ basket cells that are mostly present in the granule cell layer of the DG. Scale bar, 100 μm. Data are presented as means + s.e.m. Statistical analysis was performed with Student's unpaired *t*-test. *$P < 0.05$.

This intervention did not affect behavior during habituation (Student's *t*-test: t (14) = -0.66, *P* = 0.51), immediate post-training (Student's *t*-test: t (14) = -0.05, *P* = 0.95) and in the neutral context (Student's *t*-test: t (14) = -0.50, *P* = 0.62) (Fig. 3.11B). Hence, activation of HIPP cells mimicked the inhibition of PV+ cells in this experiment and resulted in a decrease in memory to the shock context in background context conditioning.

3.3 Intracellular signaling in HIPP cells in background context conditioning

Rationale

The pharmacogenetic intervention within the dorsal DG revealed a firm role of HIPP cells in controlling the salience of background context conditioning. This indicates that the activation of GABAergic HIPP cells expressing NPY and SST as co-transmitter (Tasan et al., 2016), is necessary during the acquisition of background context conditioning. Recent studies have conclusively used the expression profile of the immediate early gene *cFos* as a marker to identify activation of neuronal ensembles in the DG (Skórzewska et al., 2006) and gainfully employed this mechanism (Liu et al., 2014) during fear conditioning. Another important protein CREB that belongs to a family of transcription factors is implicated in long-term memory in variety of species especially mice (Bourtchuladze et al., 1994; Reijmers et al., 2007). CREB is activated by phosphorylation of its serine amino acid at a position 133 via different kinases and this phosphorylated CREB (pCREB) acts as a transcription factor (Carlezon et al., 2005). Within the hippocampus, only a strong activation of neurons leads to an increase in pCREB and hence facilitates the acquisition and formation of memory (Silva et al., 1998; Stanciu et al., 2001). Thus considering the important role of CREB in fear memory formation, Anne Albrecht (PhD) in our lab found differential induction of pCREB 1 h after background context conditioning compared to foreground context conditioning particularly in the HIPP cells labeled by NPY-GFP transgenic mice (Albrecht, 2013). One of the targets of CREB transcription factor is the NPY (Pandey, 2003; Hsieh et al., 2008). NPY$^+$ cells of the hilus receive inputs from granule cells via mossy fibers and in return they provide feedback inhibition to these by targeting their dendrites at the outer molecular layer of the DG (Houser, 2007). Thus, this pCREB induction in the hilar NPY$^+$ cells in background but not in foreground conditioning suggested that NPY might be a part of contextual salience determination in background context conditioning. The major postsynaptic receptor of NPY in the DG is the Y1 receptor (Sperk et al., 2007). These Y1 receptors are expressed on the granule cells, which suppress currents on them via voltage-dependent calcium channels upon activation (Parades et al., 2003). These Y1 receptors are also expressed on HIPP cells and play a role in G-protein coupled inwardly rectifying potassium currents. NPY Y1 receptor activity has been shown to play important roles in cued and contextual fear conditioning (Karlsson et al., 2008; Verma et al., 2012; Lach and Lima, 2013).

Based on these observations and apparent relation between CREB activity and NPY expression in HIPP cells, first I tend to further examine the control of NPY via CREB activation and subsequent involvement of HIPP cells on CREB activity in background context conditioning. Secondly, I further tested the role of NPY-Y1 receptors in fear conditioning.

3.3.1 CREB controls background context fear in HIPP cells

Fear memory engrams are regularly identified and manipulated with viral vectors that express CREB (Kim et al., 2014) and viral expression of a dominant negative CREB in the dorsal hippocampus is used to suppress contextual fear memory (Kathirvelu et al., 2013). Therefore, to identify intracellular signaling processes in HIPP cells, Bettina Müller in our lab generated conditional lentiviral vectors to express a dominant negative form of CREB (CREB^{S133A}). This double-floxed vector contains CREB^{S133A} and hemaglutinine (HA) sequences in an inverted open reading frame. HA served as a detection marker for the viral expression. The cell type specific expression of CREB^{S133A} upon the Cre recombinase activation results in a CREB isoform where serine 133 is mutated to alanine, thus phosphorylation deficient isoform dimerizes and inactivates the endogenous wild type CREB leading to its functional disruption. Upon bilateral injection of these viruses into the dorsal hilus of SST-Cre^{ERT2} mice, CREB functions are disrupted in HIPP cells. The viral construct carrying only the HA tag served as a control. The animals were first tested in the open field to check for anxiety-like behavior. Both the CREB^{S133A} and control group showed similar responses that did not depict any anxiety-like state (Student's t-test: distance t (16) = -1.86, P = 0.08, %Center time t (16) = 0.44, P = 0.66, Fig. 3.12B). These mice then underwent standard background context conditioning protocol used in this study (Fig. 3.12A). Similar to the hM4Di-mediated effect, the CREB^{S133A} expression resulted in an increase of background context memory as compared to mice with control viruses (Student's t-test: t (16) = -2.59, P = 0.02, Fig. 3.12C). The freezing response to auditory cued memory tested in the neutral context remained unaffected between the groups (Student's t-test: t (16) = 0.32, P = 0.75, Fig. 3.12C). The freezing behavior during habituation (Student's t-test: t (16) = 1.69, P = 0.10), immediate post-training (Student's t-test: t (16) = -2.09, P = 0.053) and in the neutral context (Student's t-test: t (16) = -0.32, P = 0.74) was not changed between the groups (Fig. 3.12C). Although the expression of CREB^{S133A} is expected to induce a constant commotion of the neuronal function, the effects observed on

behavioral level are quite similar to that found after HIPP cell silencing during the memory acquisition.
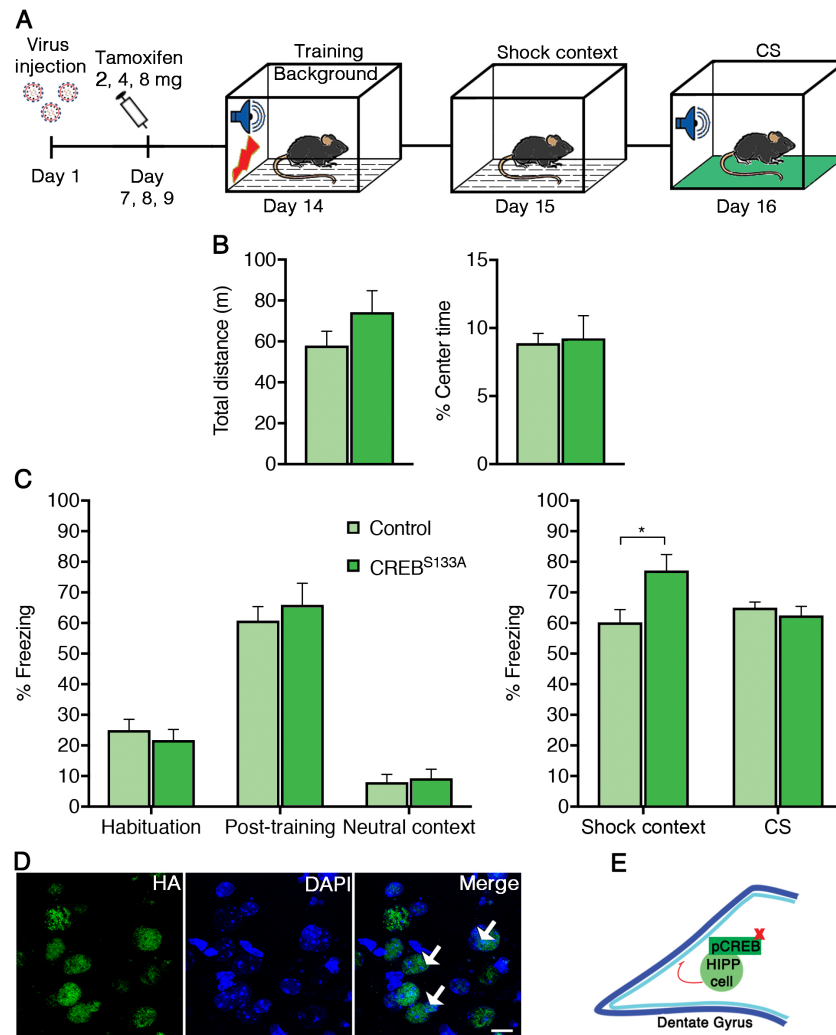
Fig. 3.12: Dominant negative CREB^S133A expression in HIPP cells increases background context conditioning. (**A**) Schematic of the lentiviral delivery and its induced expression with tamoxifen during the background context conditioning paradigm. (**B**) (Right) locomotor activity and (Left) anxiety-like behavior when tested in the open field and (**C,** Left) the behavior during habituation, post-training and neutral context with the dominant negative CREB^S133A (n = 8) compared to controls (n = 10) do not change. (**C,** Right) The expression of the dominant negative CREB^S133A in HIPP cells of the SST-Cre^ERT2 driver mice increases contextual memory of background conditioning compared to the mice with control viruses. Similar to the HIPP cells pharmacogenetic manipulation, the auditory cued response remains unaltered. (**D**) Representative microscopic images of the hilar tissue with immune labeling of HA-tag to visualize viral expression. Green, HA; blue, DAPI; Scale bar, 10 μm. (**E**) Schematic of a proposed local inhibitory circuit in the DG with CREB activation blocked via CREB^S133A in the HIPP cell. Data are presented as means + s.e.m. Statistical analysis was performed with Student's unpaired t-test. *$P < 0.05$.

3.3.2 CREB controls NPY expression

In order to verify the specificity and to confirm the effectiveness of CREB mediated viral expression, I set to measure the expression levels of HIPP-cell markers and

putative CREB targets, SST, NPY and GAD_{67} in the virus injected hilar tissue. To this end, SST-Cre[ERT2] mice were bilaterally injected with viral vectors containing CREB[S133A], or native CREB or HA control. After the viral expression, the animals were sacrificed and the hilar tissue was micro-dissected with the laser dissection. The expression of dominant negative CREB[S133A] in HIPP cells resulted in reduced mRNA levels of NPY in the hilus, whereas enhanced native CREB expression increased the NPY mRNA levels (One-way ANOVA: $F_{(2.16)} = 30.221$; $P = 0.001$). SST mRNA levels were also affected via this viral manipulation (One-way ANOVA: $F_{(2.15)} = 4.507$; $P = 0.03$) along with GAD67 mRNA levels (One-way ANOVA: $F_{(2.16)} = 18.595$; $P = 0.001$), but while both viral vectors increased SST expression only native CREB enhanced GAD_{67} (Fig. 3.13). This data also confirms that SST-Cre[ERT2] mice are a suitable model for targeting the genetic regulatory mechanisms in hilar SST^{+} cells and determining their relevance on memory formation including the regulation of NPY.
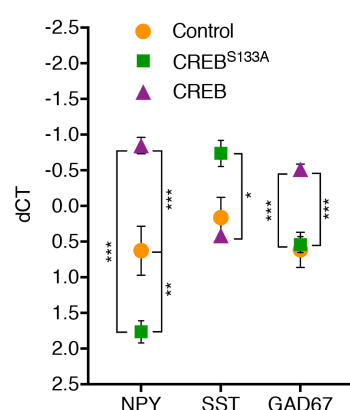
Fig. 3.13: CREB manipulation in the hilus. The expression of dominant negative CREB (CREB[S133A]) in the HIPP cells significantly reduces NPY mRNA levels while native CREB increases NPY as well as GAD_{67} ($n = 6$ each). SST is also expressed independent of CREB phosphorylation as indicated by its increased mRNA levels with CREB[S133A]. Note that higher dCT values indicate lower expression levels; therefore, scaling at the Y-axis is inverted. Data are presented as means ± s.e.m. Statistical analysis was performed with Fisher's LSD following one-way ANOVA. *$P < 0.05$, **$P < 0.01$, ***$P < 0.001$.

3.3.3 NPY controls background context fear via its Y1 receptor in the DG

The major post-synaptic receptor for NPY in the DG is Y1 receptor, which mediates the NPY-induced inhibition of both granule cells and hilar interneurons (Hájos et al., 1998). The NPY-Y1 receptors, compared to Y2 and Y5 that are also widely expressed, are the key players in NPY signaling in the DG (Sperk et al., 2007). To directly test the putative role of NPY on the control of background context salience, NPY signaling was pharmacologically blocked during background context conditioning. In this line, BIBP3226 that acts as a selective NPY-Y1 receptor antagonist has been widely used to study effects of anxiety related behavior in rodents (Kask et al., 1998, 1999; Redrobe et al., 2002; Primeaux et al., 2005; Cohen et al., 2012).

In this experiment, Anne Albrecht (PhD) in our lab found that pre-training BIBP3226 infusion increased contextual memory in background context conditioning compared to the control group while memory to the CS remained unaffected (Albrecht, 2013). Furthermore, in this line I tested the role of NPY signaling in foreground context conditioning. Similarly I implanted bilateral cannulas in C57BL/6 wild type mice and infused the NPY-Y1 antagonist BIBP3226, 45 min
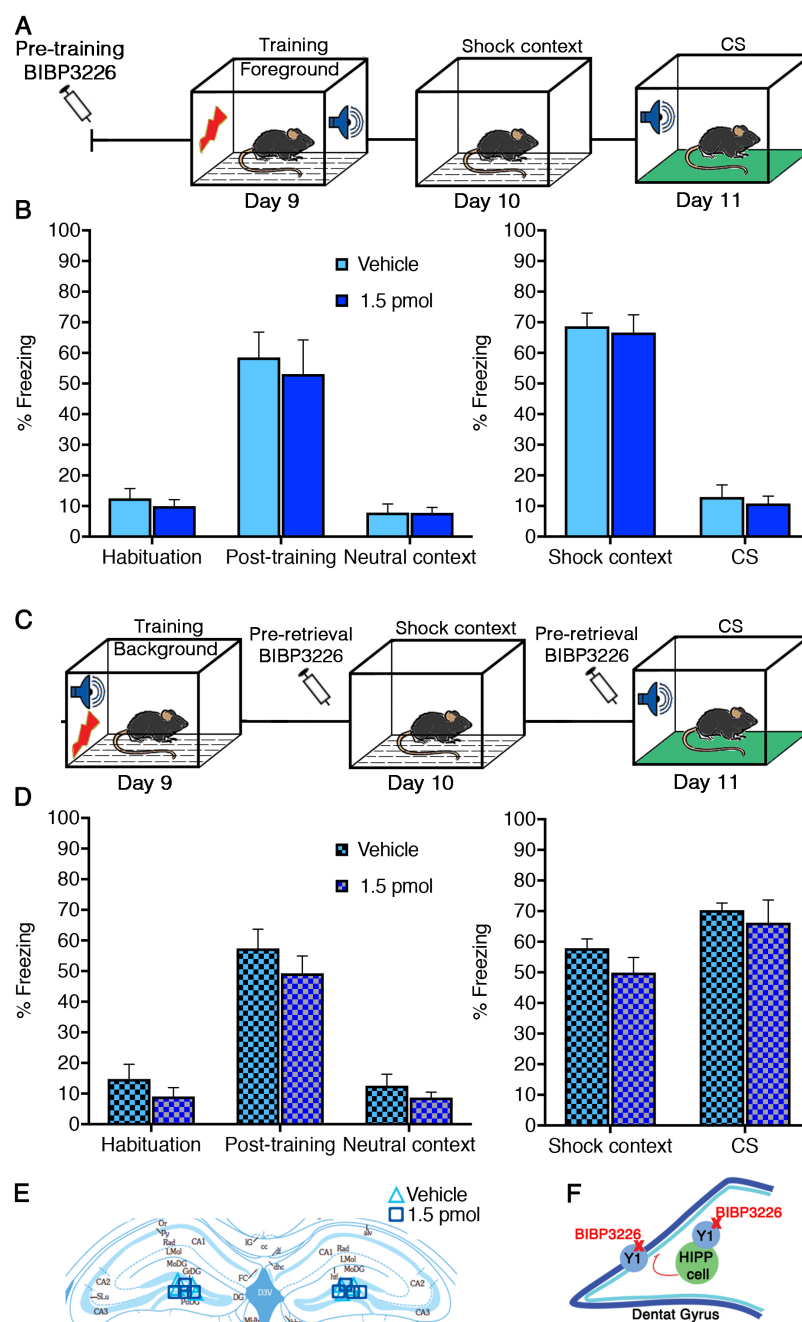
Fig. 3.14: Neuropeptide Y through its Y1 receptor in the DG does not affect foreground context fear memory as well as background fear when applied at retrieval. (**A**) Schematic of pharmacological experiment. The Y1 antagonist BIBP3226 was applied bilaterally to the dorsal

DG 45 min before foreground context conditioning. (**B**) Infusion of NPY-Y1 receptor antagonist BIBP3226 (1.5 pmol / hemisphere) before foreground context conditioning (*n* = 8) does not change the freezing response during (Left) habituation, immediate post-training and in the neutral context and (Right) in the shock context and during the CSs presentation compared to the vehicle treated group (*n* = 7)**.** (**C**) Schematic of behavior paradigm and BIBP3226 infusion before retrieval. (**D**) Blockage of NPY-Y1 signaling with BIBP3226 (*n* = 8) before retrieval does not change the freezing response during (Left) habituation, immediate post-training and in the neutral context and (Right) in the shock context and during the CSs presentation compared to vehicle treated group (*n* = 8). (**E**) Localization of guide cannulas placement in the dorsal DG in different groups, as verified histologically after completion of the behavioral experiments. Only mice with correct cannula placement are included in the data analysis. (**F**) Schematic of a local inhibitory circuit in the DG, highlighting HIPP cells that provide NPY-mediated feedback inhibition to granule cells. Data are presented as means + s.e.m. Statistical analysis was done with Student's unpaired *t*-test.

before unpaired training in foreground conditioning (Fig. 3.14A). By contrast to background context conditioning, no significant differences were observed in foreground context conditioning in the freezing behavior in the shock context (Student's *t*-test: t (13) = -0.27, *P* = 0.78, Fig. 3.14B) as well as during the presentation of auditory tones (Student's *t*-test: t (13) = 1.10, *P* = 0.28, Fig. 3.14B). Also the behavior during habituation (Student's *t*-test: t (13) = 0.67, *P* = 0.51), post-training (Student's *t*-test: t (16) = 0.38, *P* = 0.70) and in the neutral context (Student's *t*-test: t (13) = 0.01, *P* = 0.98) remained unchanged between groups (Fig. 3.14B). To further validate a specific role of NPY signaling through NPY-Y1 receptor in the acquisition of background context conditioning, the additional group of cannulated C57BL/6 wild type mice were infused with BIBP3226, 45 min before retrieval in the shock context as well as before the CS presentations (Fig. 3.14C). BIBP3226 injections before retrieval had no effect on background context memory (Student's *t*-test: t (14) = 1.37, *P* = 0.19, Fig. 3.14D) as well as memory to the CS (Student's *t*-test: t (14) = 0.62, *P* = 0.54, Fig. 3.14D). Again the behavior in the neutral context (Student's *t*-test: t (14) = 0.93, *P* = 0.36), during habituation (Student's *t*-test: t (14) = 1.02, *P* = 0.32) and post-training (Student's *t*-test: t (14) = 0.96, *P* = 0.35) remained unchanged between the groups (Fig. 3.14D).

Earlier experiments in our lab, with intracerebroventricular injections of a higher anxiogenic dose of BIBP3226 showed no such effects in background context conditioning (Albrecht, 2013), thus confirming the functional control of NPY on the salience of background context conditioning which is independent of anxiolytic properties of NPY. Together these findings suggest that NPY signaling via its Y1 receptor is specifically involved in the acquisition and not in the retrieval of

background context conditioning. Furthermore, NPY controls the contextual salience determination in CS-US paired conditioning and not in the unpaired one.

3.4 Cholinergic modulation of HIPP cells

Rationale

The pharmacogenetic intervention within the dorsal DG and the pharmacological blockage revealed a firm role of HIPP cells controlling the contextual salience using NPY transmission in background context conditioning. In general, the molecular mechanisms suggest that these HIPP cells must distinctively be activated during background context conditioning by neurotransmitter systems which in turn mediate the activation of the transcription factor pCREB that ultimately release NPY in the DG. The main neurotransmitters are GABA and glutamate, inhibitory and excitatory, respectively. However, monoaminergic neuromodulator systems are known to embark important roles in shaping and fine tuning the neurotransmission in different brain circuits and are also active during fear conditioning (Izquierdo et al., 2016). To identify the pathways that activate HIPP cells and their NPYergic transmission, Anne Albrecht (PhD) in our lab investigated the mRNA expression levels of various neuromodulator receptor subtypes on NPY-positive HIPP cells. To this end, behaviorally naïve NPY-GFP mice were used to isolate HIPP cells as well as NPY$^+$ cells in other hippocampal layers and the remaining cell population that contained neither HIPP nor NPY$^+$ cells, via laser capture microdissection. Quantitative PCR analysis revealed a cell type specific expression of the M1 subtype of muscarinic acetylcholine receptors (Chrm1) on the HIPP cells (Albrecht, 2013).

These results provided a strong platform to study the role of cholinergic modulation of the hippocampus during fear conditioning particularly in background context conditioning at a local DG circuit level specifically focusing on the circuit formed by the HIPP cells.

3.4.1 M1 acetylcholine receptors control the activity of NPYergic HIPP cells

The cholinergic afferent terminals to the hippocampus arise from the medial septum (Senut et al., 1989) forming a septo-hippocampal pathway and differentially innervate GABAergic interneurons in the DG. Both nicotinic and muscarininc receptors are expressed in the DG and both of these receptors are involved in learning and memory processes (Parfitt et al., 2012). Thus, Nicolai Faber (MD) from the Institute of Anatomy confirmed the previous anatomical findings about septo-

hippocampal pathway. Firstly, by using naïve NPY-GFP transgenic mice, the immunohistochemical approach confirmed the reported rich cholinergic fiber innervation onto the hilar NPY+ cells (Fig. A3.1A). Secondly, the expression of M1 receptors in these GFP+ hilar NPY cell bodies was also demonstrated indicating septal afferences to the DG targeting the NPYergic HIPP cells via M1 receptors (Fig. A3.1B-D). Next, Susanne Meis (PhD) our collaborator from the Institute of Physiology employed the patch clamp technique to study the functional properties of NPYergic HIPP cells and found that application of specific muscarinic agonist oxotremorine M (oxo) resulted in a transient membrane depolarization from resting membrane potential. And these effects were abolished when oxo was added in the presence of the M1-receptor antagonist pirenzepine (Fig. A3.2A, B).

Next, I determined M1 receptor functions with the use of acute slice preparations of the dorsal hippocampus and further investigated the role of NPY in mediating these M1 receptor functions. To this end, Gürsel Çalışkan (PhD) in our lab recorded field potentials from acute slice preparations of the dorsal hippocampus from wild type naïve C57BL/6 mice as well as hM4Di injected SST-Cre^{ERT2} driver mice. We found that the bath application of either 10 μM carbachol (general muscarinic agonist) or 1 μM oxo (specific M1 agonist), both resulted in increased muscarinic activation and led to a significant reduction in the population spike (PS) area in control slices. However, NPY-Y1 blockage with 1 μM BIBP3226 before oxo application strongly counteracted this oxo-mediated inhibition and thus resulted in increased PS area in comparison to the control slices (Student's t-test: oxo vs. BIBP3226 + oxo: t (10) = -3.46, P = 0.006, Fig. 3.15A-left panel). The pharmacogenetic inhibition of HIPP cells with the bath application of 10 μM CNO also mimicked this BIBP3226 effect (Student's t-test: oxo vs. CNO + oxo: t (16) = -2.18, P = 0.04, Fig. 3.15A-right panel). Similar effects were observed in combination with 10 μM carbachol instead of 1 μM oxo (Fig. A3.2C, D). In the absence of oxo application, interestingly, the baseline excitability observed with the PS area was unaltered with either Y1 receptors blockade (Paired t-test: BIBP3226 vs. aCSF: t (15) = 0.99, P = 0.37, Fig. 3.15B-left panel) or HIPP cells silencing (Paired t-test: CNO vs. aCSF: t (15) = 2.03, P = 0.06, Fig. 3.15B- left panel). To identify NPY-independent components that could be present in HIPP cells, we performed an occlusion experiment. Here, application of 1 μM BIBP3226 only or application of 1 μM BIBP3226 + 10 μM CNO on slices expressing hM4Di, no differences were evident in oxo-mediated depression in the PS area

(Paired *t*-test: BIBP3226 vs. BIBP3226 + CNO: t (10) = -0.49, *P* = 0.63, Fig. 3.15B-right panel). These results confirm that NPY signaling, but not the NPY-independent component in HIPP cells, is the main player in conducting these effects.
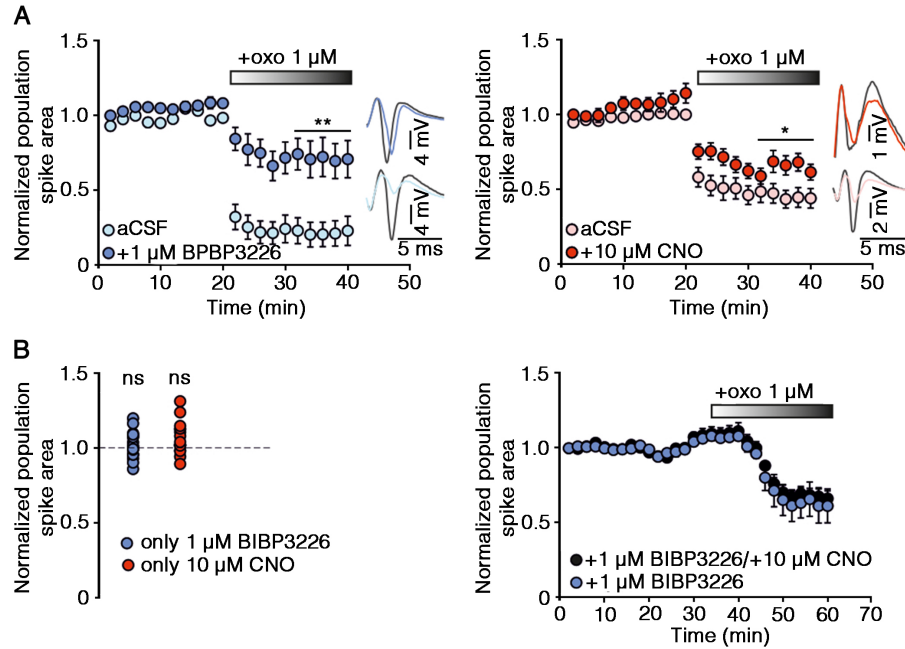
Fig. 3.15: Cholinergic response of NPYergic HIPP cells on a local DG circuit. (**A**) Pharmacological blockage of the NPY-Y1 signaling (Left) (*n* = 6 slices each with and without BIBP3226) and (Right) HIPP cells pharmacogenetic silencing, counteracts the oxotremorine M (oxo) induced depression of PS. Example traces in the graphs indicate differences in the perforant path stimulation responses. (**B**) (Left) In the absence of muscarinic activation, pharmacological blockage of Y1 receptors and pharmacogenetic silencing of HIPP cells in the dorsal DG did not alter the population spike area (1 μM BIBP3226, *n* = 16 slices; CNO, *n* = 16 slices). (Right) Treatment of slices with BIBP3226 (*n* = 6 slices) or combined treatment with BIBP3226 + CNO (*n* = 6 slices) produce no difference in oxo induced depression of the PS responses indicating a main role of NPY signaling in HIPP cell mediated effect. Data are presented as means ± s.e.m. Statistical analysis was performed with student's unpaired *t*-test. *$P < 0.05$, **$P < 0.01$.

Next, to test the involvement of CREB signaling in this circuit function and to link the intracellular pathways of HIPP cells activation, we determined PS in the brain slices from SST-Cre[ERT2] driver mice expressing dominant negative CREB[S133A] in HIPP cells. Two different concentrations of oxo (0.1 μM and 1 μM) were used with or without the application of 1 μM BIBP3226 and potential changes in HIPP cells sensitivity were investigated. With low concentration of oxo an effect of CREB[S133A] expression was observed. Comparison between groups confirmed significant main effects of CREB[S133A] expression (Two-way ANOVA: F (1.25) = 5.013; *P* = 0.034) and BIBP3226 treatment (Two-way ANOVA: F (1.25) = 13.543; *P* = 0.001), as both decreased the oxo-mediated inhibition (Fig. 3.16A). However, a less pronounced CREB[S133A] effect compared to that of BIBP3226 was observed. Further, no interaction was found

between these factors (Two-way ANOVA: F (1.25) = 0.291). Moreover, higher concentration of oxo again resulted in BIBP3226 effect (Two-way ANOVA: F (1.25) = 5.711; P = 0.025), while no effect of CREB^{S133A} (Two-way ANOVA: F (1,25) = 0.016, n.s) and no interactions were observed between these factors (Two-way ANOVA: F (1,25) = 0.006, n.s) (Fig. 3.16B). In summary, it is clearly indicated with these physiological data that the NPY-mediated transmission is a major determinant of HIPP cell-mediated cholinergic inhibition.
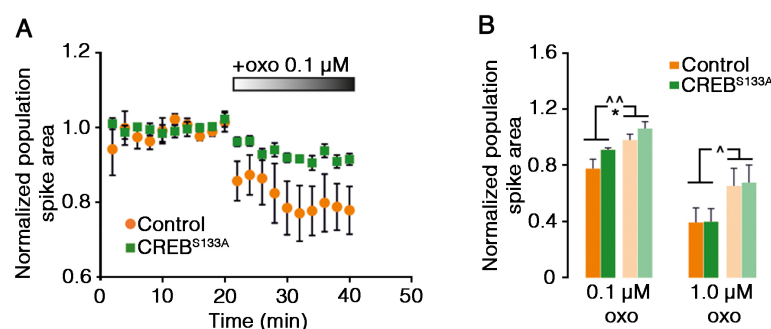
Fig. 3.16: Effects of oxotremorine M depends on CREB signaling. (**A**) Development of population spikes in the DG with bath application of oxo (0.1 µM) in low concentration without BIBP3226 application (n = 8 slices) in slices from SST-Cre^{ERT2} mice expressing CREB^{S133A} compared to controls (n = 8 slices). (**B**) Low concentration of oxo (0.1 µM) results in a decrease depression of population spikes in the DG while high concentration of oxo (1 µM) does not produce this effect. NPY-Y1 receptor blockage with BIBP3226 attenuates oxo effect in both concentrations. Data are presented as means ± s.e.m. Statistical analysis was performed with two-way ANOVA. CREB^{S133A} effect: *P < 0.05; BIBP3226 treatment effect: ^P < 0.05, ^^P < 0.01.

3.4.2 Endogenous ACh release recruits NPY transmission in the DG

To evaluate the effect of endogenous acetylcholine release in the DG, I next utilized the Chat-Cre driver mice. These mice express a Cre recombinase under the promoter/enhancer element of the *Chat* gene in the cholinergic neurons without disrupting the endogenous cholineacetyltransferase expression. Thus, I used these mice to target the septo-hippocampal projection neurons that terminate the dorsal DG. To mimic the endogenous release of acetylcholine in the dorsal DG, these mice
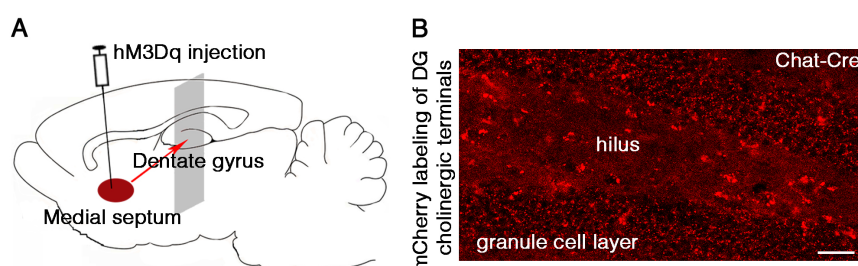
Fig. 3.17. Pharmacogenetic approach of targeting septal cholinergic projections in the hippocampus. (**A**) Schematic representation of AAV-hM3Dq injection into the medial septum.

These conditional viruses in the Chat-Cre driver mice lead to their expression also in the DG. (**B**) A representative microscopic image of the DG from hM3Dq injected mice showing mCherry viral tag in the cholinergic terminals throughout the DG. Scale bar, 25 μm.

were injected with hSyn-DIO-hM3Dq-mCherry in the medial septum. After 6-8 weeks of injections, this experimental manipulation resulted in the expression of excitatory DREADD receptors in the medial septum as well as in their projections to the dorsal DG (Fig. 3.17). By doing so, we investigated the role of endogenous acetylcholine release in the DG on the identified HIPP cell circuit in this study. We
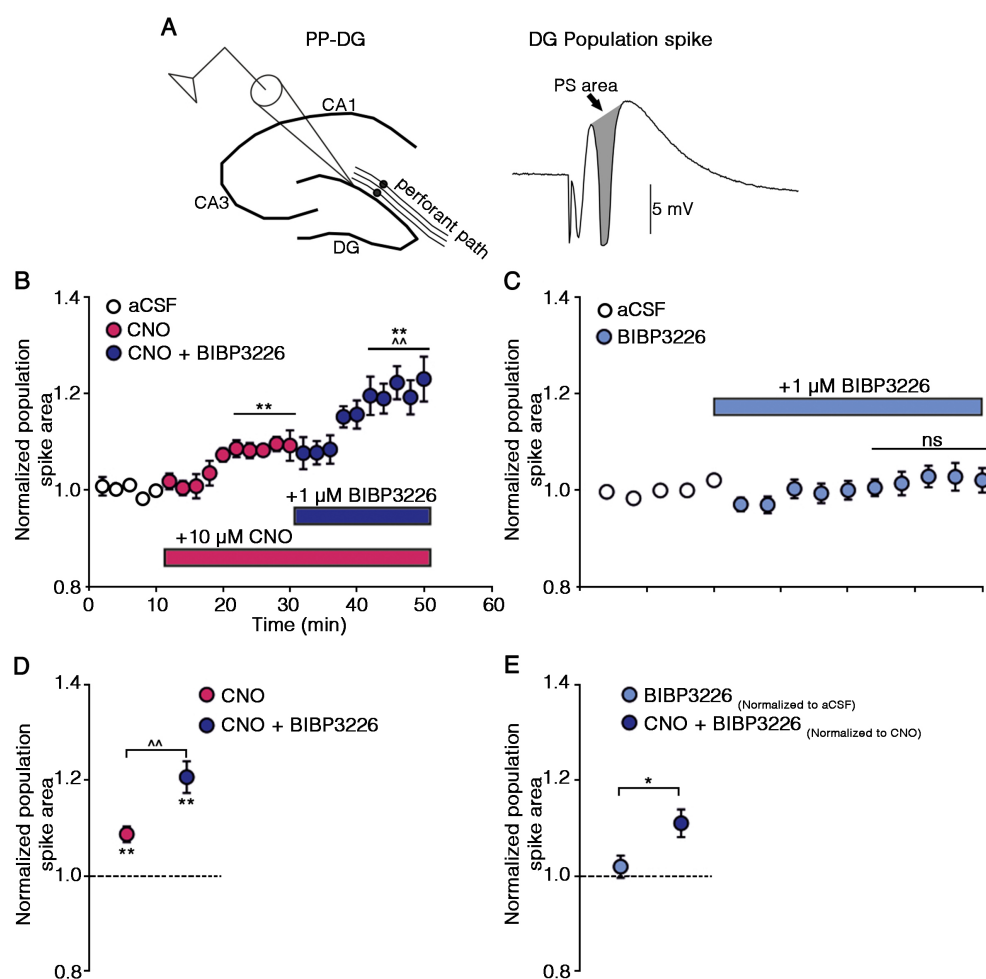
Fig. 3.18. Blockage of NPY-Y1 receptor strengthens the facilitatory effect of endogenous acetylcholine release on the population spikes in the DG. (**A**) Schematic of experimental setup. (**B**) Cholinergic terminals expressing hM3Dq are activated with 10 μM CNO bath application in the hippocampal slices, which results in a slight increase in the DG population spike. This effect is further enhanced with Y1 blockage (BIBP3226, $n = 8$ slices). Data from last 10 min of each condition was used for statistical analysis that provided full availability of drug action. (**C**) Summary graph shows change in the mean PS area with CNO alone and CNO + BIBP3226 combined application relative to aCSF. (**D**) PS area is not affected with BIBP3226 without CNO ($n = 16$ slices). (**E**) In line, comparison of normalized BIBP3226 effect on PS area with or without cholinergic activation shows a significant change only after CNO application. Data are presented as means ± s.e.m. Statistical analysis was performed with Fischer's LSD following one-way repeated measure ANOVA ($^{\wedge\wedge}P < 0.01$, CNO vs. CNO+BIBP3226; $**P < 0.01$

CNO or CNO+BIBP3226 vs. aCSF condition) in **B** and **D**, paired *t*-test in **C** and Student's unpaired *t*-test in **E**, *$P < 0.05$.

selectively activated the cholinergic terminals in our slice preparations of the dorsal hippocampus from these driver mice through the bath application of 10 µM CNO. This cholinergic activation produced a moderate increase in the PS area, which was further supplemented with NPY-Y1 receptor blockage with 1 µM BIBP3226 (One-way repeated measures ANOVA: $F_{(2.14)} = 28.701$, $P < 0.001$, Fig. 3.18B, D). Of note, in the absence of CNO no effect of BIB3226 was observed on the PS responses (Fig. 3.18C). A significant increase was seen under cholinergic activation of the DG with CNO upon comparing the isolated BIBP3226 effect between experiments (Fig. 3.18E).

3.4.3 HIPP cells control the background context salience via Chrm1 receptors

These results imply that M1 receptors present on the HIPP cells are the targets of septal projections carrying acetylcholine to the DG. Finally, I determined the behavioral consequences of M1 receptor manipulation. In fact, Susann Ludewig (MSc) in our lab did pre-experiments with *in vivo* pharmacology, where C57BL/6 wild type mice were implanted with cannulas and the general muscarinic antagonist scopolamine was injected 15 min before training to background context conditioning. This pharmacological blockage of the DG muscarinic receptors suppressed the immediate post-training freezing and the context fear response, in line with findings in other tasks (Babar et al., 2002) while the cued memory was not affected (Ludewig, 2013). I then completed the experiment where the role of scopolamine on C57BL/6 wild type mice during elevated plus maze was tested and found that scopolamine injections 15 min before elevated plus maze testing, dose dependently altered the activity and anxiety like behavior (Fig. A3.3A).

Because scopolamine pharmacology in the DG not only affected muscarinic receptors on the hilar interneurons but also on granule cells, therefore I decided to selectively target M1 receptors on the HIPP cells only. To this end, Bettina Müller (PhD) in our lab produced lentiviral vectors to conditionally knockdown Chrm1. These vectors co-express DsRed that is used as a detection marker. The lentiviral vectors expressing only the DsRed marker was used as a control. I injected them into the dorsal hilus of the SST-CRE[ERT2] driver mice (Fig. 3.19A). Upon tamoxifen injections, the Cre recombinase activated the virus to inhibit Chrm1 specifically in

HIPP cells (Fig. 3.19C, D). Similar to pharmacogenetic inhibition of HIPP cells and NPY-Y1 receptors blockage, Chrm1 knockdown resulted in a significant increase in background context memory (Student's *t*-test: t (13) = -2.26, *P* = 0.04, Fig. 3.19B). No
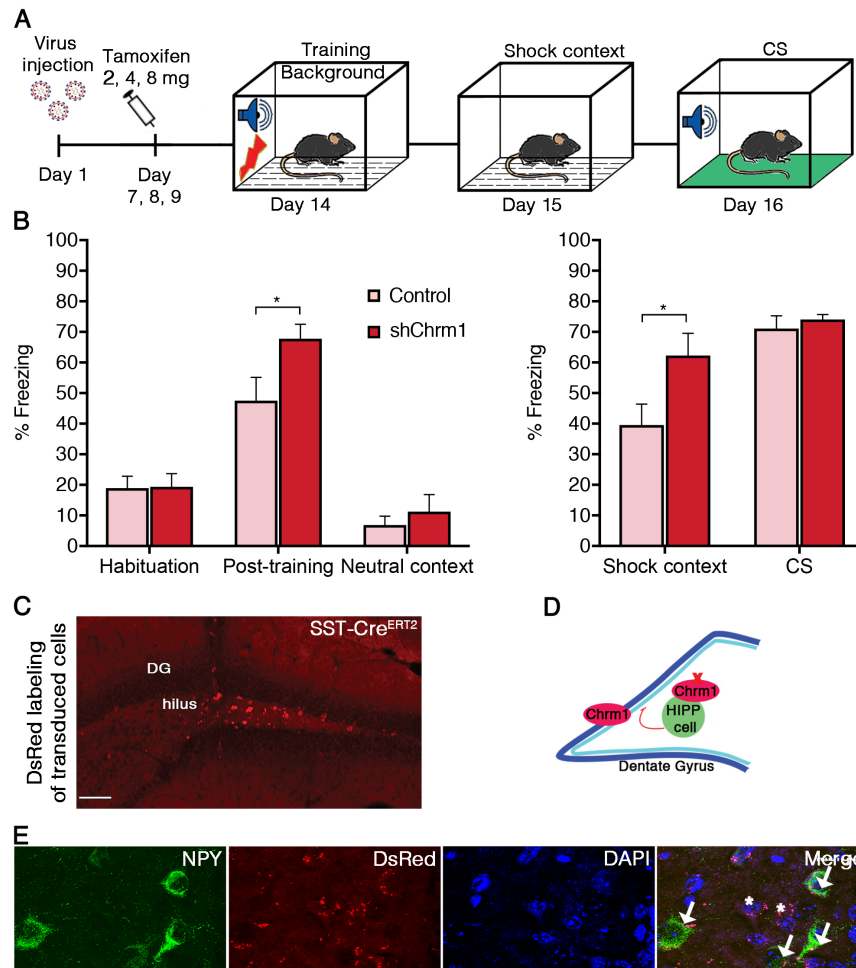
Fig. 3.19: The knockdown of muscarinic M1 receptors in HIPP cells increases background context memory. (**A**) Experimental scheme of Chrm1 knockdown and behavior testing. (**B**) Chrm1 knockdown in the dorsal hilus of the SST-Cre^{ERT2} mice significantly increases the memory to the background context (*n* = 7) compared to mice injected with a control virus (*n* = 8). This Chrm1 knockdown could not affect the auditory cued memory tested in the neutral context. (**C**) Schematic drawing of a proposed local inhibitory circuit in the DG with selective Chrm1 knockdown in HIPP cells. (**D**) A microscopic image of the coronal brain section showing the expression of a lentiviral construct. Scale bar, 100 μm. (**E**) Representative microscopic images of the hilar tissue expressing lentivirus with DsRed labeling and NPY immune staining. Note viral expression in NPY$^+$ (arrows) and NPY$^-$ cells (asterisks) of the hilus. Scale bar, 10 μm. Data are presented as means + s.e.m. Statistical analysis was performed with Student's unpaired *t*-test. *P < 0.05.

change was evident in the response to the CS presentation (Student's *t*-test: t (13) = -0.48, *P* = 0.53, Fig. 3.19B), which clearly suggested the context specificity of HIPP-cell directed Chrm1 knockdown. This knockdown had no effect on the freezing behavior during habituation (Student's *t*-test: t (13) = -0.07, *P* = 0.94) or in the neutral context (Student's *t*-test: t (13) = -0.66, *P* = 0.51), but an enhancement of

immediate post training freezing was observed (Student's *t*-test: t (13) = -2.33, *P* = 0.03) (Fig. 3.19B). Indeed, immunostaining showed that the DsRed marker was found in NPY$^+$ and also in some NPY$^-$ cells of the hilus but not in the granule cell layer (Fig. 3.19E). Thus, the specific knockdown of M1 receptors on the HIPP cells resulted in increased contextual memory in background context conditioning.

4. Discussion

Memories are formed in the brain, where different circuits via dynamic processes encode and store different types of information. Thus the brain in general does not form memories in a unitary fashion, on contrary, different aspects of memory with multiple kinds of learning experiences are conceived by different brain circuits. Evidences of varying circuits representing different memories come from studying patients with focal lesions in different areas of the brain, particularly the hippocampus and amygdala (LaBar et al., 1995; Bechara et al., 1995). In light of these facts, the fundamental mechanisms of memory storage have been clarified over the last years. Moreover, neuroscientists are now deciphering different aspects of learning and memory at global and local brain circuit levels as well as on the cellular level, and the principles of neuronal ensemble formation during learning in these circuits are beginning to unfold. However, most of the ongoing work focuses on principle cells and their modulation with monoamine transmitters, little is known about the involvement of GABAergic local circuits. Furthermore, little is still known about the cellular and molecular processes that control the specificity and stability of memories. To date, the encoding of memory salience along with its precise mechanism at a local circuit level is not understood. In the current study, I describe a local NPYergic circuit formed by HIPP cells in the DG of the dorsal hippocampus that mediates the cholinergic modulation of the background context salience during Pavlovian fear conditioning. This local circuit critically determines the loading of the salience information onto the background context fear memory. By evaluating the episodic aspects of an aversive experience, this circuit may help to specify the strength and specificity of fear memories (Phelps, 2004).

Highly processed information from the entorhinal cortex enters the DG via the perforant path, which is the main gateway to the hippocampus. The DG possesses a set of unique properties by which it first transforms the noisy and dense signals from upstream cortical areas into sparse and specific information and then delivers this information to rest of the hippocampal formation. This is an evolutionary and indispensable role of the DG for efficient storage and later recall of the hippocampus dependent memories. The DG is also known to discriminate similar contexts (Rudy, 2009) and supports the formation of distinct representations through a conjunctive encoding process integrating the multiple sensory inputs to organized contextual representations (Kesner, 2007; Morris et al., 2013). During fear conditioning with an

elemental CS, the predictive value of a training situation loads onto both the context and cue. So it is assumable that during fear memory acquisition, the DG uses this function to compute the predictive strength of full and partial context configurations. Thus at memory retrieval, the DG discriminates the context as a full or a partial predictor. In the current study with optimization of background vs. foreground vs. pure context fear conditioning protocols, training-induced differences in the context salience therefore are reflected. It is thus suggested that the DG differentiates the loading strength of the CS as a main predictor and the context as a partial predictor in background context conditioning. Here, the contextual cues did engage in a cue competition with explicitly paired CSs but were unable to gain associative strength (Shanks, 2010). By contrast, in the absence of explicitly paired CSs, the US promoted the prediction of the context as a salient factor in foreground and pure context conditioning (Fig. 3.2). However, the reversal of retrieval phases could not affect this prediction strategy by the DG, which indicates that this information processing is more of an acquisition phenomenon (Fig. 3.3A). The data obtained in the experiment comparing non-exposure and pre-exposure (habituation) to the conditioning context clearly suggest that the latent inhibition did not show any role in my experiments, which requires extensive exposures (Albrecht et al., 2010). However, it has been suggested that pre-exposure results in the strengthening of associated memory (Rudy and O'Reilly, 1999), which is also observed in my experiments with increased conditioning to the CS in the pre-exposure group (Fig. 3.3B).

Pharmacogenetic experiments with the silencing of complete DG in the CamK2a-Cre driver mice resulted in a decrease in contextual memory during background context conditioning with mild as well as moderate training protocols (Fig. 3.4). The difference in the memory strength with both of these protocols suggested that the CamK2a-Cre driver mice posses less sensitivity to foot shocks and thus require moderate training to display comparable freezing levels to the wild type C57BL/6 mice. Nonetheless, a decrease in contextual memory via the pharmacogenetic silencing of the DG confirmed its role in background context conditioning.

The sparse activity patterns of principle excitatory granule cells of the DG is controlled by a local circuit consisting of GABAergic interneurons (Amaral, 1978; Sik et al., 1997; Ascády and Káli, 2007; Houser, 2007). These interneurons are highly adaptive in response to multiple stimuli particularly to stress (Fa et al., 2014). One

prominent group of interneurons that mediate inhibition in the DG is the SST expressing HIPP cells. HIPP cells are known to inhibit both granule cells mediating feedback (Savanthrapadian et al., 2014) and parvalbuminergic basket cells mediating feed-forward inhibition in the DG (Sik et al., 1997) and control the pattern of granule cell activation (Stefanelli et al., 2016). Furthermore, they formulate a local DG network via homosynaptic connections. Thus, it is assumed that during context encoding in the background with fear training by explicit CS-US pairings, the activation of HIPP cells attenuates the activity of granule cells and ultimately results in salience determination at a precise level. Hence, the data obtained in this study via the pharmacogenetic inhibition of HIPP cells in the SST-Cre[ERT2] driver mice indeed supports this analogy that HIPP cells attenuate the activation of granule cells during background context encoding and inhibition of HIPP cells alters this function and thus reduces the context salience (Fig. 4.1).
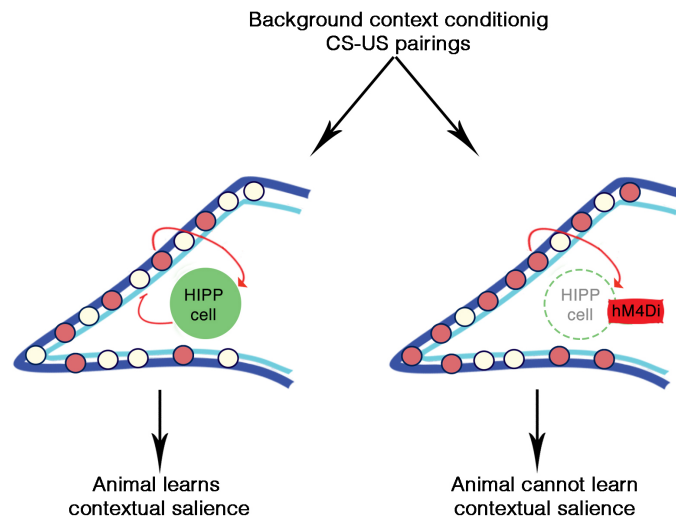
Fig. 4.1: Schematic representation of HIPP cells function. In background context conditioning with CS-US pairings, the DG granule cells via activated HIPP cell are inhibited and the DG granule cell ensemble size is limited. This function of the local DG circuit allows the animal to learn the context as a partial predictor during background context conditioning. hM4Di mediated targeted inhibition of HIPP cells during background context conditioning disrupts this function and the animal cannot properly identify the contextual salience.

One of the dynamic functions of the DG is pattern separation (Leutgeb et al., 2007; Bakker et al., 2008), defined as the ability to transform a set of similar input patterns into a less-similar set of output patterns. In the DG, HIPP cells in conjunction with excitatory mossy cells make a feedback loop and computational modeling suggest that mossy cells and HIPP cells control the capacity of the DG for pattern separation in contrasting ways (Myers and Scharfman, 2009). It is assumable that during fear

memory acquisition, the DG uses this function to compute the predictive strength of full and partial context configurations. Thus during memory retrieval, the DG discriminates the context as a full or a partial predictor. Moreover, HIPP cells in the DG constitute a major population of inhibitory NPY+ interneurons. The majority of HIPP cells co-transmit NPY along with SST that provide inhibition to granule cells via its Y1 receptor (Deller and Leranth, 1990; Sperk et al., 2007). It has recently been proposed that NPY in the DG reduces the stability of CS-US associations in eyeblink conditioning (Madroñal et al., 2016), which is in agreement with a specific role of NPY in the adjustment of memory salience. In this study, with the data from NPY-Y1 blockade before foreground memory encoding as well as before background memory retrieval (Fig. 3.14), I was able to confirm the specific role of NPY in controlling the background context salience during memory encoding. Further, I provide evidence showing that the transcription factor CREB, which is known to be a regulator of NPY expression in neuronal cells (Hsieh et al., 2008) controls the mRNA expression levels of NPY over a considerable range. Furthermore, it is also in line with the activity-dependent regulation of NPY in the hilus, e.g. in response to stress and stressful situations (Conrad and McEwen, 2000; Cohen et al., 2012). Here, after background context conditioning, the enhanced induction of phospho-CREB[S133] proves its activity-dependent regulation in HIPP cells and further suggested its role in the replenishment of NPY stores. Moreover, additional roles are attributed to the CREB in HIPP cells, whereby it controls HIPP cells excitability and/or molecular processes during the memory consolidation phase (Viosca et al., 2009). In fact, present data show that GAD_{67} mRNA levels are also elevated by the viral expression of CREB in a S133 phosphorylation dependent manner in HIPP cells. On the other side, here the observed increase of SST mRNA levels after viral transduction of dominant negative CREB[S133A] (similar to native CREB) could probably suggest constitutive, phosphorylation independent regulation of the SST expression possibly via the Q2 domain of CREB (Asahara et al., 2001).

The expression of cued fear memory remained thoroughly unaffected in all experiments with manipulations of the context representation in HIPP cell circuitry of the dorsal DG. It has been shown that the elemental strategies remain intact under hippocampal damage (Iordanova et al., 2009). In one study, inactivation of the medial septum with lidocaine that provides cholinergic afferents to the hippocampus increases the background context memory while sparing the auditory

cued memory (Calandreau et al., 2007). Thus, it suggests the involvement of cholinergic control of background context conditioning and evaluation of its stimulus salience, however, the adjustment of background context salience via cholinergic modulation of HIPP cells appear to be secondary to this function.

The septal complex forms a loop where cholinergic input to the hippocampal formation arises from the medial septum and the glutamatergic fibers from the hippocampus innervate the lateral septum via the fornix pathway (Jakab and Leranth 1995; Schwegler et al., 1996; Swanson and Risold, 2000). It has been shown that this cholinergic input to the hippocampus is triggered through the amygdala during conditioning with elemental stimuli. The brain circuits that mediate foreground or background context representations in the hippocampus are interrelated with the activation of projections from the medial septum and towards the lateral septum (Calandreau et al., 2007; 2010). The cholinergic system is tightly connected with the glutamatergic as well as the GABAergic systems and the cholinergic innervation to the hippocampus frequently targets the GABAergic cells demonstrating the exclusive cholinergic-GABAergic neuronal connectivity (Khakpai et al., 2013). Data obtained in the present study suggest that background context fear is controlled indirectly by the cholinergic circuit via the M1 receptor-mediated activation of HIPP cells, which in turn control granule cells excitability and their respective memory ensemble size. In addition, HIPP-independent activation of the basket cells also reduced background context fear (Fig. 3.11). Further, granule cells also express M1 receptors and muscarinic signaling in the DG directly modulates their excitability and plasticity (Foster and Deadwyler, 1992; Levey et al., 1995; Van der Zee and Luiten, 1999; Martinello et al., 2015). Moreover, blockade of muscarinic signaling in the hippocampus impairs contextual fear (Gale et al., 2001; Wallenstein and Vogo, 2001). This function mainly depends on the M1 receptors (Soares et al., 2006) as M2 knockout mice showed no differences in fear memory (Bainbridge et al., 2008) and M3 deficient mice showed lower contextual memory (Poulin et al., 2010). These studies suggest that cholinergic stimulation of principle cells in the hippocampus are essential for the formation of the context memory *per se*, the involvement of HIPP cells with muscarinic activation leads to devaluation of the background context information during elemental conditioning. Indeed, in the absence of muscarinic stimulation in hippocampal slices, perforant path-induced granule cell activity remained unchanged upon NPY-Y1 receptor blockage (Fig.

3.15B-left panel). By contrast, oxotremorine M induced inhibition is decreased with NPY-Y1 receptor blockage. Similar effects were seen with the pharmacogenetic inhibition of HIPP cells, thus, suggesting that release of NPY via HIPP cells mediate the cholinergic inhibition of granule cells (Fig. 3.15A). In addition to their direct activation via M1 receptors, HIPP cells may also be activated indirectly, e.g., via acetylcholine induced glutamate release from hilar astrocytes (Pabst et al., 2016).

The majority of HIPP cells are NPY[+] but NPY^{-} HIPP cells also exist as seen with NPY immune labeling of virally transduced HIPP cells. In this study, it is likely that the changes in GABAergic and/or somatostatinergic transmission occurs in NPY[+] as well as in NPY^{-} HIPP cells and are potentially involved in the behavioral effects of CREB- or its activity-manipulation. Interestingly, the more general interference with HIPP cell functions through the hM4Di timed inhibition or CREB[S133A] expression could not affect immediate post-training memory. By contrast, only the more specific intervention with the NPYergic and muscarinergic transmission leads to an enhancement of immediate post-training memory in my experiments. The interaction of HIPP cells with other interneuron populations within the DG may account for these changes (Savanthrapadian et al., 2014) or these differences may be related to additional cellular effects of these manipulations. Similarly, the involvement of NPY[+] and also NPY[-] subpopulations of HIPP cells may relate to this increase in immediate context memory. Nevertheless, the physiological data of this study clearly indicate that HIPP cell-mediated cholinergic inhibition is mainly based on NPY transmission. The pharmacogenetic inhibition of HIPP cells showed similar response to the NPY receptor blockage in the DG. Further, the simultaneous pharmacogenetic inhibition of HIPP cells and NPY-Y1 receptor blockage did not show a larger effect on oxotremorine M induced inhibition than NPY-Y1 receptor blockage alone (Fig. 3.15B-right panel). Of note, in the absence of cholinergic stimulation, blockage of NPY-Y1 signaling had no effect on the DG population spikes, which is in line with a recent report (Lee et al., 2016). By contrast, NPY-Y1 blockage enhanced the excitatory effect of acetylcholine released from the medial septum terminals in the DG. Thus, it is notable to assume that HIPP cells regulate the balance between excitatory and inhibitory effects of acetylcholine in the DG (Martinello et al., 2015).

Recently it has been shown that the pharmacogenetic blockage of HIPP cell activity increases the pure context memory (Stefanelli et al., 2016). However, I was unable to

reproduce these results in our experimental settings (Fig. 3.9). By contrast, my data suggest that local inhibitory circuit formed by HIPP cells control the background context salience and have no role in the acquisition of pure contextual memory. There are certain clear differences between the housing and training conditions, animals' activity phase as well as mouse phenotypes between the present study and the experiments by Stefanelli et al. Between-lab variability in mouse phenotypes is frequently observed and may be attributed to minor differences in housing or training conditions (Crabbe et al., 1999; Richter et al., 2009). One possible reason could also involve the time of training and testing. Stefanelli et al., performed their experiments during the light phase and I conducted all my experiments during the dark phase that corresponds to animals' active phase. Evidence suggests that the activation of CREB is also under circadian effect and under the control of clock genes (Albrecht and Stork, 2017). Furthermore, the involvement of NPY is also dependent on the circadian rhythm. Increased endogenous NPY during light phase checks the exogenous NPY administration and could result in variable results (Yannielli and Harrington, 2001). It is plausible that local circuit formed by HIPP cells may be more generally involved in the adjustment of context memory salience by acetylcholine from the medial septum. This could be caused by the role of HIPP cells in controlling the size of granule cell ensembles, thereby mediating the competition and lateral inhibition between training-activated and training-silent granule cells (Stefanelli et al., 2016).

The cholinergic mechanisms targeting background context memories are also shown in other hippocampal sub-regions. In the CA3 area, increased cholinergic signaling enhances the CS-US encoding (Rogers and Kesner, 2004), contributes to the salience of contextual processing (McHugh and Tonegawa, 2009) and regulates long-term potentiation in the CA3 pyramidal cell synapses (Zheng et al., 2012). Cholinergic projections from the medial septum during context conditioning activate dendrite-targeting SST$^+$ interneurons in the CA1 area, which shape the US-related information on pyramidal cells (Lovett-Barron et al., 2014). The data obtained in the current study suggest that cholinergic input to the DG from the medial septum stimulates the DG functions to control pattern separation and context discrimination. Thus, information processing in the CA1 and CA3 areas may, in conjunction with the DG, further contribute to the adjustment of contextual salience in fear memory formation and successfully contribute with generally enhancing the

context memory salience. Thus dendrite-targeting local circuit neurons together with NPY adjust the relative weight of converging direct as well as indirect entorhinal cortex pathways to the hippocampal formation and thereby control synaptic plasticity in the CA1 area (Madroñal et al., 2016). Notably, the level of acetylcholine release within the hippocampus is shown to be dependent on the type of conditioning protocol. Simple CS-US association leads to a less pronounced release of acetylcholine while upon context-US association it is enhanced (Calandreau et al., 2006). This integration process could also depend on previous experiences and also involve adaptive changes within the local DG circuit along with neuropeptide expression. In this study, it is indicated by the dominant negative CREB^{S133A} expression in the HIPP cells and associated neuropeptide regulation. Indeed dominant negative CREB^{S133A} expression reduced the oxotremorine M responsiveness albeit less efficiently than the complete blockage of Y1 receptor with BIBP3226 (Fig. 3.16). The hippocampal cholinergic signaling also contributes to the adjustment of the hippocampal-amygdalar network (Calendreau et al., 2006) and this circuit is ultimately under influence of the lateral amygdala and is required to restrict background context fear conditioning in the presence of a predictive elemental stimulus (Calendreau et al., 2005).
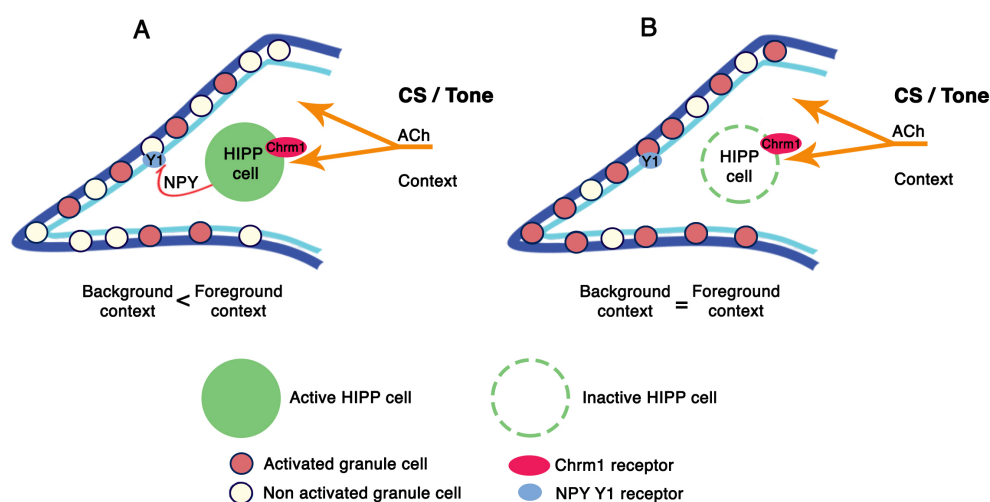
Fig. 4.2: Schematic of a local DG circuit that mediates the cholinergic modulation of the background context salience. (**A**) HIPP cells control context memory strength during background context learning in the septo-hippocampal pathway. HIPP cells are activated along with the DG granule cells by cholinergic afferences projecting through the medial septum, which triggers the release of Chrm1 dependent NPY from HIPP cells. Granule cells are then controlled via the Y1 receptor signaling of HIPP cells. During elemental conditioning (context in background), this functioning of HIPP cells is effective in controlling the granule cell memory ensembles, thus reducing the contextual salience. (**B**) However, the pharmacogenetic inhibition of HIPP cells and pharmacological blockage of NPY signaling disrupts the cue-induced

devaluation of background context conditioning via increased recruiting of granule cell memory ensembles.

Altogether the data obtained in this study with different experiments strongly propose that NPYergic HIPP cells act as a relay stations in the septo-hippocampal pathway and form a local circuit that adjust the context memory strength. This local circuit formed by HIPP cells helps the DG specifically and exclusively to discriminate full and partial recapitulation of the learned configuration during retrieval of memory (Fig. 4.2). The behavioral effects found in this study with either pharmacogenetic disruption of HIPP cells function or Y1 receptors blockage are analogous to other studies in terms of their magnitude to the difference in freezing levels induced by foreground or background context conditioning (Calendreau et al., 2007; 2010). There are other factors that contribute to the enhancement of background context fear memory as has also been shown in rodents with intensive auditory cued fear conditioning (Laxmi et al., 2003; Albrecht et al., 2010) and the juvenile stress exposure prior to conditioning (Müller et al., 2014). Similarly, acute stress also leads to changes in the NPY expression levels in the DG (Conrad and McEwen, 2000). Hence, these changes could provide a neurochemical correlate for the adaptive and maladaptive adjustment of the salience in background context. This maladaptation that leads to difficulty in predicting the contextual salience could play a critical role in the development of PTSD (Acheson et al., 2012). A possible mechanism could be that with HIPP cells inhibition, the hippocampal function is lowered and results in using individual contextual cues along with elemental cues. Thus, allowing the context to produce heightened fear response. The involvement of the DG in relation to PTSD is also evident with a study that shows volume reduction on the CA3/DG subfield in PTSD patients (Wang et al., 2010). In animal models of PTSD, decreased levels of NPY expression are observed in the DG of rats sensitive to stress-induced behavioral pathology thus suggesting that NPY actively contributes to stress resilience (Cohen et al., 2012). This is in line with disturbed contextual memory observed in this study with the CREB and NPY-Y1 manipulations. Therefore it is plausible that the HIPP cell circuit described in this study contributes to a pathology development in PTSD. One prominent feature of PTSD is the occurrence of intrusive memories, which are known to result from inappropriate understanding of the context. Thus the increase of background context fear could result from vivid reconstruction of the fearful context during encoding and implicated in the

formation of intrusive memories (Pearson et al., 2012). It is possible to assume that escalation of background context fear attenuates fear extinction (Vervliet et al., 2013) and constitutes one of the characteristic features of PTSD.

5. Conclusion

This study evaluates the novel aspect of a local DG circuit in the hippocampal formation during background context conditioning. Although, the hippocampal cholinergic modulation of background context conditioning has been shown previously, in this study I highlighted the involvement of HIPP cells in mediating the cholinergic modulation of the background context salience. Here I showed with pharmacogenetic experiments that HIPP cells are indispensible in controlling the contextual salience during the acquisition of background context conditioning likely via restricting the granule cell ensemble size. By contrast, this HIPP cells function is not observed with foreground or pure foreground conditioning as well as during retrieval of fear memory. I showed that the phosphorylation of CREB selectively activates HIPP cells during background context conditioning. Inhibiting this process by the expression of dominant negative CREB^{S133A} in HIPP cells resulted in increased fear memory to the background context. CREB induces the expression of NPY in HIPP cells, thereby controlling DG excitability. I proved with control experiments that indeed the pharmacological blockage of NPY-Y1 receptors resulted in a similar increase in only background context fear and not in foreground or pure context fear. Further I showed that muscarinic signaling from the medial septum also activates HIPP cells via their M1 receptors and the knockdown of this receptor, selectively in HIPP cells, enhanced the background context.

Collectively, the data furnish novel evidence for an adaptive local peptidergic circuit in the DG that mediates the cholinergic encoding of the background context salience via NPY during the acquisition of fear memory. The hippocampal dysfunction and its relationship of fear responding that might occur via the disturbance in the identified circuit could direct towards novel treatment strategies for PTSD.

6. Future perspectives

Understanding neuronal circuits that are involved in the formation of fear memory has gained prime importance in the field of learning and memory. Of particular relevance, even a minor maladjustment at a minute level in these circuits could lead to the formation of psychiatric conditions. Thus learning the functioning and connectivity of this phenomenon paves the way for better understanding the fear-related disorders as well as their ultimate treatment. The identified circuit in this study is fairly important because it not only describes the mechanism of salience

determination but also the underlying molecular correlates. In addition, the use of this circuit in other experimental conditions could also solve further questions.

The animal models of juvenile stress are repeatedly used to replicate PTSD in the laboratory conditions, where contextual discrepancies are commonly seen (Albrecht et al., 2017). Thus the involvement of this local DG circuit could be tested with an established juvenile stress paradigm (Müller et al., 2014) with the pharmacogenetic activation or inhibition of HIPP cells during background context conditioning. Abnormal extinction of contextual memories is seen with patients of panic disorders and PTSD (Michael et al., 2007; Milad et al., 2009) and the pharmacogenetic inhibition of whole of the DG impairs fear extinction (Bernier et al., 2017). Thus the involvement of HIPP cells in the extinction of contextual memories or their spontaneous recoveries could also be tested with a similar pharmacogenetic approach. Evidence suggests that the GABAergic cells are also prone to epigenetic modification of the GAD_{67} gene in schizopherenia (Costa et al., 2003), however the specific GABAergic subtype is not known. During juvenile age, if a lasting epigenetic mark is placed on these cells then ultimately this could lead to an inability in discriminating neutral vs. fearful context configurations. One could test this hypothesis with a juvenile stress paradigm and identify the molecular epigenetic marks on the HIPP cells. The identified factors could then later be manipulated.

Finally, this circuit is also implicated in the remote memory paradigms where the DG granule cells memory ensembles loose their strength over time and other cortical areas take control (Kitamura et al., 2017). This phenomenon could lead to the generalization of contextual memories over time because of a loss of memory strength. Here I show that HIPP cells control the ensemble size, thus, it is plausible to assume that the precise activity of HIPP cells could control the information flow to the cortical areas and help in retaining the memory strength for longer durations in time. This hypothesis could be tested in this identified circuit with the CREB and DREADD viruses.

I expect that answering these questions will provide novel molecular and behavioral insights into the mechanisms of learning and memory at this local circuit level.

7. References

1. Acheson, D. T., Gresack, J. E., & Risbrough, V. B. (2012). Hippocampal dysfunction effects on context memory: possible etiology for posttraumatic stress disorder. *Neuropharmacology*, *62*(2), 674-685.

2. Acsády, L., & Káli, S. (2007). Models, structure, function: the transformation of cortical signals in the dentate gyrus. *Progress in brain research*, *163*, 577-599.

3. Alberini, C. M. (2009). Transcription factors in long-term memory and synaptic plasticity. *Physiological reviews*, *89*(1), 121-145.

4. Albrecht, A. (2013). Mechanisms of contextual fear memory generalization (Doctoral dissertation). Magdeburg, Univ., Fak. Für Naturwiss., XVII, 214 Bl.

5. Albrecht, A., & Stork, O. (2017). Circadian Rhythms in Fear Conditioning: An Overview of Behavioral, Brain System, and Molecular Interactions. *Neural Plasticity*, *2017*.

6. Albrecht, A., Bergado-Acosta, J. R., Pape, H. C., & Stork, O. (2010). Role of the neural cell adhesion molecule (NCAM) in amygdalo-hippocampal interactions and salience determination of contextual fear memory. *International Journal of Neuropsychopharmacology*, *13*(5), 661-674.

7. Albrecht, A., Çalışkan, G., Oitzl, M. S., Heinemann, U., & Stork, O. (2013). Long-lasting increase of corticosterone after fear memory reactivation: anxiolytic effects and network activity modulation in the ventral hippocampus. *Neuropsychopharmacology*, *38*(3), 386-394.

8. Albrecht, A., Müller, I., Ardi, Z., Çalışkan, G., Gruber, D., Ivens, S., ... & Richter-Levin, G. (2017). Neurobiological consequences of juvenile stress: A GABAergic perspective on risk and resilience. *Neuroscience & Biobehavioral Reviews*.

9. Amaral, D. G. (1978). A Golgi study of cell types in the hilar region of the hippocampus in the rat. *Journal of Comparative Neurology*, *182*(5), 851-914.

10. Amaral, D. G., Scharfman, H. E., & Lavenex, P. (2007). The dentate gyrus: fundamental neuroanatomical organization (dentate gyrus for dummies). *Progress in brain research*, *163*, 3-790.

11. Andersen, P., Bliss, T. V., & Skrede, K. K. (1971). Lamellar organization of hippocampal excitatory pathways. *Experimental brain research*, *13*(2), 222-238.

12. Arruda-Carvalho, M., & Clem, R. L. (2014). Pathway-selective adjustment of prefrontal-amygdala transmission during fear encoding. *Journal of Neuroscience*, *34*(47), 15601-15609.

13. Asahara, H., Santoso, B., Guzman, E., Du, K., Cole, P. A., Davidson, I., & Montminy, M. (2001). Chromatin-dependent cooperativity between constitutive and inducible activation domains in CREB. *Molecular and cellular biology*, *21*(23), 7892-7900.

14. Babar, E., Melik, E., Özgünen, T., & Polat, S. (2002). Effects of excitotoxic median raphe lesion on working memory deficits produced by the dorsal hippocampal muscarinic receptor blockade in the inhibitory avoidance in rats. *Brain research bulletin*, *57*(5), 683-688.

15. Bainbridge, N. K., Koselke, L. R., Jeon, J., Bailey, K. R., Wess, J., Crawley, J. N., & Wrenn, C. C. (2008). Learning and memory impairments in a congenic C57BL/6 strain of mice that lacks the M 2 muscarinic acetylcholine receptor subtype. *Behavioural brain research*, *190*(1), 50-58.

16. Bakker, A., Kirwan, C. B., Miller, M., & Stark, C. E. (2008). Pattern separation in the human hippocampal CA3 and dentate gyrus. *Science*, *319*(5870), 1640-1642.

17. Bannerman, D. M., Rawlins, J. N. P., McHugh, S. B., Deacon, R. M. J., Yee, B. K., Bast, T., ... & Feldon, J. (2004). Regional dissociations within the hippocampus—memory and anxiety. *Neuroscience & Biobehavioral Reviews*, *28*(3), 273-283.

18. Bargmann, C. I., & Marder, E. (2013). From the connectome to brain function. *Nature methods*, *10*(6), 483-490.

19. Bechara, A., Tranel, D., Damasio, H., & Adolphs, R. (1995). Double dissociation of conditioning and declarative knowledge relative to the amygdala and hippocampus in humans. *Science*, *269*(5227), 1115.

20. Bergado-Acosta, J. R., Müller, I., Richter-Levin, G., & Stork, O. (2014). The GABA-synthetic enzyme GAD65 controls circadian activation of conditioned fear pathways. *Behavioural brain research*, *260*, 92-100.

21. Bergado-Acosta, J. R., Sangha, S., Narayanan, R. T., Obata, K., Pape, H. C., & Stork, O. (2008). Critical role of the 65-kDa isoform of glutamic acid decarboxylase in consolidation and generalization of Pavlovian fear memory. *Learning & memory*, *15*(3), 163-171.

22. Bernier, B. E., Lacagnina, A. F., Ayoub, A., Shue, F., Zemelman, B. V., Krasne, F. B., & Drew, M. R. (2017). Dentate gyrus contributes to retrieval as well as encoding: Evidence from context fear conditioning, recall, and extinction. *Journal of Neuroscience*, *37*(26), 6359-6371.

23. Blanchard, D. C., & Blanchard, R. J. (1972). Innate and conditioned reactions to threat in rats with amygdaloid lesions. *Journal of comparative and physiological psychology*, *81*(2), 281.

24. Bliss, T. V., & Lømo, T. (1973). Long-lasting potentiation of synaptic transmission in the dentate area of the anaesthetized rabbit following stimulation of the perforant path. *The Journal of physiology*, *232*(2), 331-356.

25. Bourtchuladze, R., Frenguelli, B., Blendy, J., Cioffi, D., Schutz, G., & Silva, A. J. (1994). Deficient long-term memory in mice with a targeted mutation of the cAMP-responsive element-binding protein. *Cell*, *79*(1), 59-68.

26. Bouton, M. E., Westbrook, R. F., Corcoran, K. A., & Maren, S. (2006). Contextual and temporal modulation of extinction: behavioral and biological mechanisms. *Biological psychiatry*, *60*(4), 352-360.

27. Brambilla, P., Perez, J., Barale, F., Schettini, G., & Soares, J. C. (2003). GABAergic dysfunction in mood disorders. *Molecular psychiatry*, *8*(8), 721-737.

28. Bremner, J. D., Elzinga, B., Schmahl, C., & Vermetten, E. (2007). Structural and functional plasticity of the human brain in posttraumatic stress disorder. *Progress in brain research*, *167*, 171-186.

29. Bremner, J. D., Vythilingam, M., Vermetten, E., Southwick, S. M., McGlashan, T., Staib, L. H., ... & Charney, D. S. (2003). Neural correlates of declarative memory for emotionally valenced words in women with posttraumatic stress disorder related to early childhood sexual abuse. *Biological psychiatry*, *53*(10), 879-889.

30. Bucci, D. J., Phillips, R. G., & Burwell, R. D. (2000). Contributions of postrhinal and perirhinal cortex to contextual information processing. *Behavioral neuroscience*, *114*(5), 882-893.

31. Buzsáki, G. (2002). Theta oscillations in the hippocampus. *Neuron*, *33*(3), 325-340.

32. Cabrele, C., & Beck-Sickinger, A. G. (2000). Molecular characterization of the ligand–receptor interaction of the neuropeptide Y family. *Journal of peptide science*, *6*(3), 97-122.

33. Cahill, L., & McGaugh, J. L. (1998). Mechanisms of emotional arousal and lasting declarative memory. *Trends in neurosciences*, *21*(7), 294-299.

34. Calandreau, L., Desgranges, B., Jaffard, R., & Desmedt, A. (2010). Switching from contextual to tone fear conditioning and vice versa: the key role of the glutamatergic hippocampal-lateral septal neurotransmission. *Learning & memory*, *17*(9), 440-443.

35. Calandreau, L., Desmedt, A., Decorte, L., & Jaffard, R. (2005). A different recruitment of the lateral and basolateral amygdala promotes contextual or elemental conditioned association in Pavlovian fear conditioning. *Learning & Memory*, *12*(4), 383-388.

36. Calandreau, L., Jaffard, R., & Desmedt, A. (2007). Dissociated roles for the lateral and medial septum in elemental and contextual fear conditioning. *Learning & Memory*, *14*(6), 422-429.

37. Calandreau, L., Trifilieff, P., Mons, N., Costes, L., Marien, M., Marighetto, A., ... & Desmedt, A. (2006). Extracellular hippocampal acetylcholine level controls amygdala function and promotes adaptive conditioned emotional response. *Journal of Neuroscience*, *26*(52), 13556-13566.

38. Carlezon, W. A., Duman, R. S., & Nestler, E. J. (2005). The many faces of CREB. *Trends in neurosciences*, *28*(8), 436-445.

39. Carlezon, W. A., Thome, J., Olson, V. G., Lane-Ladd, S. B., Brodkin, E. S., Hiroi, N., ... & Nestler, E. J. (1998). Regulation of cocaine reward by CREB. *Science*, *282*(5397), 2272-2275.

40. Caroni, P. (2015). Inhibitory microcircuit modules in hippocampal learning. *Current opinion in neurobiology*, *35*, 66-73.

41. Cho, J. H., Deisseroth, K., & Bolshakov, V. Y. (2013). Synaptic encoding of fear extinction in mPFC-amygdala circuits. *Neuron*, *80*(6), 1491-1507.

42. Cohen, H., Liu, T., Kozlovsky, N., Kaplan, Z., Zohar, J., & Mathé, A. A. (2012). The neuropeptide Y (NPY)-ergic system is associated with behavioral resilience to stress exposure in an animal model of post-traumatic stress disorder. *Neuropsychopharmacology*, *37*(2), 350-363.

43. Cohen, S. M., Tsien, R. W., Goff, D. C., & Halassa, M. M. (2015). The impact of NMDA receptor hypofunction on GABAergic neurons in the pathophysiology of schizophrenia. *Schizophrenia research*, *167*(1), 98-107.

44. Conrad, C. D., & McEwen, B. S. (2000). Acute stress increases neuropeptide Y mRNA within the arcuate nucleus and hilus of the dentate gyrus. *Molecular brain research*, *79*(1), 102-109.

45. Costa, E., Grayson, D. R., & Guidotti, A. (2003). Epigenetic downregulation of GABAergic function in schizophrenia: potential for pharmacological intervention?. *Molecular interventions*, *3*(4), 220.

46. Costanzi, M., Cannas, S., Saraulli, D., Rossi-Arnaud, C., & Cestari, V. (2011). Extinction after retrieval: effects on the associative and nonassociative components of remote contextual fear memory. *Learning & Memory*, *18*(8), 508-518.

47. Cowansage, K. K., Shuman, T., Dillingham, B. C., Chang, A., Golshani, P., & Mayford, M. (2014). Direct reactivation of a coherent neocortical memory of context. *Neuron*, *84*(2), 432-441.

48. Crabbe, J. C., Wahlsten, D., & Dudek, B. C. (1999). Genetics of mouse behavior: interactions with laboratory environment. *Science*, *284*(5420), 1670-1672.

49. DeFelipe, J., López-Cruz, P. L., Benavides-Piccione, R., Bielza, C., Larrañaga, P., Anderson, S., ... & Fishell, G. (2013). New insights into the classification and nomenclature of cortical GABAergic interneurons. *Nature Reviews Neuroscience*, *14*(3), 202-216.

50. Deller, T., & Leranth, C. (1990). Synaptic connections of neuropeptide Y (NPY) immunoreactive neurons in the hilar area of the rat hippocampus. *Journal of comparative neurology*, *300*(3), 433-447.

51. Denny, C. A., Kheirbek, M. A., Alba, E. L., Tanaka, K. F., Brachman, R. A., Laughman, K. B., ... & Hen, R. (2014). Hippocampal memory traces are differentially modulated by experience, time, and adult neurogenesis. *Neuron*, *83*(1), 189-201.

52. Desmedt, A., Garcia, R., & Jaffard, R. (1998). Differential modulation of changes in hippocampal–septal synaptic excitability by the amygdala as a function of either elemental or contextual fear conditioning in mice. *Journal of Neuroscience*, *18*(1), 480-487.

53. Desmedt, A., Garcia, R., & Jaffard, R. (1999). Vasopressin in the lateral septum promotes elemental conditioning to the detriment of contextual fear conditioning in mice. *European Journal of Neuroscience*, *11*(11), 3913-3921.

54. Desmedt, A., Marighetto, A., Garcia, R., & Jaffard, R. (2003). The effects of ibotenic hippocampal lesions on discriminative fear conditioning to context in mice: impairment or facilitation depending on the associative value of a phasic explicit cue. *European Journal of Neuroscience*, *17*(9), 1953-1963.

55. Dougherty, K. D., & Milner, T. A. (1999). Cholinergic septal afferent terminals preferentially contact neuropeptide Y-containing interneurons compared to parvalbumin-containing interneurons in the rat dentate gyrus. *Journal of Neuroscience*, *19*(22), 10140-10152.

56. Dudai, Y. (2004). The neurobiology of consolidations, or, how stable is the engram?. *Annu. Rev. Psychol.*, *55*, 51-86.

57. Ehrlich, I., Humeau, Y., Grenier, F., Ciocchi, S., Herry, C., & Lüthi, A. (2009). Amygdala inhibitory circuits and the control of fear memory. *Neuron*, *62*(6), 757-771.

58. Everitt, B. J., & Robbins, T. W. (1997). Central cholinergic systems and cognition. *Annual review of psychology*, *48*(1), 649-684.

59. Fa, M., Xia, L., Anunu, R., Kehat, O., Kriebel, M., Volkmer, H., & Richter-Levin, G. (2014). Stress modulation of hippocampal activity–Spotlight on the dentate gyrus. *Neurobiology of learning and memory*, *112*, 53-60.

60. Fanselow, M. S. (1980). Signaled shock-free periods and preference for signaled shock. *Journal of Experimental Psychology: Animal Behavior Processes*, *6*(1), 65.

61. Fanselow, M. S. (1989). The adaptive function of conditioned defensive behavior: An ecological approach to Pavlovian stimulus-substitution theory.

62. Fanselow, M. S. (2010). From contextual fear to a dynamic view of memory systems. *Trends in cognitive sciences*, *14*(1), 7-15.

63. Foster, T. C., & Deadwyler, S. A. (1992). Acetylcholine modulates averaged sensory evoked responses and perforant path evoked field potentials in the rat dentate gyrus. *Brain research*, *587*(1), 95-101.

64. Freund, T. F., & Katona, I. (2007). Perisomatic inhibition. *Neuron*, *56*(1), 33-42.

65. Freund, T. F., Gulyas, A. I., Acsady, L., Görcs, T., & Toth, K. (1990). Serotonergic control of the hippocampus via local inhibitory interneurons. *Proceedings of the National Academy of Sciences*, *87*(21), 8501-8505.

66. Gale, G. D., Anagnostaras, S. G., & Fanselow, M. S. (2001). Cholinergic modulation of pavlovian fear conditioning: effects of intrahippocampal scopolamine infusion. *Hippocampus*, *11*(4), 371-376.

67. Gale, G. D., Anagnostaras, S. G., Godsil, B. P., Mitchell, S., Nozawa, T., Sage, J. R., ... & Fanselow, M. S. (2004). Role of the basolateral amygdala in the storage of fear memories across the adult lifetime of rats. *Journal of Neuroscience*, *24*(15), 3810-3815.

68. Gonzalez, G. A., & Montminy, M. R. (1989). Cyclic AMP stimulates somatostatin gene transcription by phosphorylation of CREB at serine 133. *Cell*, *59*(4), 675-680.

69. Gøtzsche, C. R., & Woldbye, D. P. D. (2016). The role of NPY in learning and memory. *Neuropeptides*, *55*, 79-89.

70. Graham, B. M., & Milad, M. R. (2011). The study of fear extinction: implications for anxiety disorders. *American Journal of Psychiatry*, *168*(12), 1255-1265.

71. Gulyás, A. I., Toth, K., Danos, P., & Freund, T. F. (1991). Subpopulations of GABAergic neurons containing parvalbumin, calbindin D28k, and cholecystokinin in the rat hippocampus. *Journal of Comparative Neurology*, *312*(3), 371-378.

72. Hajos, N., Papp, E. C., Acsady, L., Levey, A. I., & Freund, T. F. (1997). Distinct interneuron types express m2 muscarinic receptor immunoreactivity on their dendrites or axon terminals in the hippocampus. *Neuroscience*, *82*(2), 355-376.

73. Han, J. H., Kushner, S. A., Yiu, A. P., Hsiang, H. L. L., Buch, T., Waisman, A., ... & Josselyn, S. A. (2009). Selective erasure of a fear memory. *Science*, *323*(5920), 1492-1496.

74. Han, Z. S., Buhl, E. H., Lörinczi, Z., & Somogyi, P. (1993). A High Degree of Spatial Selectivity in the Axonal and Dendritic Domains of Physiologically Identified Local-circuit Neurons in the Dentate Gyms of the Rat Hippocampus. *European Journal of Neuroscience*, *5*(5), 395-410.

75. Harrison, P. J. (2015). GABA circuitry, cells and molecular regulation in schizophrenia: life in the graveyard. *Schizophrenia research*, *167*(1), 108-110.

76. Heimer, L., & Van Hoesen, G. W. (2006). The limbic lobe and its output channels: implications for emotional functions and adaptive behavior. *Neuroscience & Biobehavioral Reviews*, *30*(2), 126-147.

77. Holtmaat, A., & Caroni, P. (2016). Functional and structural underpinnings of neuronal assembly formation in learning. *Nature neuroscience*.

78. Hosp, J. A., Strüber, M., Yanagawa, Y., Obata, K., Vida, I., Jonas, P., & Bartos, M. (2014). Morpho-physiological criteria divide dentate gyrus interneurons into classes. *Hippocampus*, *24*(2), 189-203.

79. Houser, C. R. (2007). Interneurons of the dentate gyrus: an overview of cell types, terminal fields and neurochemical identity. *Progress in brain research*, *163*, 217-811.

80. Hsieh, Y. S., Yang, S. F., Chu, S. C., Ho, Y. J., Kuo, C. S., & Kuo, D. Y. (2008). Transcriptional interruption of cAMP response element binding protein modulates superoxide dismutase and neuropeptide Y-mediated feeding behavior in freely moving rats. *Journal of neurochemistry*, *105*(4), 1438-1449.

81. Iordanova, M. D., Burnett, D. J., Aggleton, J. P., Good, M., & Honey, R. C. (2009). The role of the hippocampus in mnemonic integration and retrieval: complementary evidence from lesion and inactivation studies. *European Journal of Neuroscience*, *30*(11), 2177-2189.

82. Izquierdo, I., Furini, C. R., & Myskiw, J. C. (2016). Fear memory. *Physiological reviews*, *96*(2), 695-750.

83. Izquierdo, I., Medina, J. H., Vianna, M. R., Izquierdo, L. A., & Barros, D. M. (1999). Separate mechanisms for short-and long-term memory. *Behavioural brain research*, *103*(1), 1-11.

84. Jacobson-Pick, S., & Richter-Levin, G. (2010). Differential impact of juvenile stress and corticosterone in juvenility and in adulthood, in male and female rats. *Behavioural brain research*

85. Jacobson, L., & Sapolsky, R. (1991). The role of the hippocampus in feedback regulation of the hypothalamic-pituitary-adrenocortical axis. *Endocrine reviews*, *12*(2), 118-134.

86. Jakab, R. L., & Leranth, C. (1995). Septum. In The rat nervous system. (ed. G. Paxinos), pp. 405–442. Academic Press, New York

87. Jinno, S., & Kosaka, T. (2006). Cellular architecture of the mouse hippocampus: a quantitative aspect of chemically defined GABAergic neurons with stereology. *Neuroscience research*, *56*(3), 229-245.

88. Johansen, J. P., Cain, C. K., Ostroff, L. E., & LeDoux, J. E. (2011). Molecular mechanisms of fear learning and memory. *Cell*, *147*(3), 509-524.

89. Jovasevic, V., Corcoran, K. A., Leaderbrand, K., Yamawaki, N., Guedea, A. L., Chen, H. J., ... & Radulovic, J. (2015). GABAergic mechanisms regulated by miR-33 encode state-dependent fear. *Nature neuroscience*, *18*(9), 1265-1271.

90. Kandel, E. R., Dudai, Y., & Mayford, M. R. (2014). The molecular and systems biology of memory. *Cell*, *157*(1), 163-186.

91. Karlsson, R. M., Choe, J. S., Cameron, H. A., Thorsell, A., Crawley, J. N., Holmes, A., & Heilig, M. (2008). The neuropeptide Y Y1 receptor subtype is necessary for the anxiolytic-like effects of neuropeptide Y, but not the antidepressant-like effects of fluoxetine, in mice. *Psychopharmacology*, *195*(4), 547-557.

92. Kash, S. F., Tecott, L. H., Hodge, C., & Baekkeskov, S. (1999). Increased anxiety and altered responses to anxiolytics in mice deficient in the 65-kDa isoform of glutamic acid decarboxylase. *Proceedings of the National Academy of Sciences*, *96*(4), 1698-1703.

93. Kask, A., Kivastik, T., Rägo, L., & Harro, J. (1999). Neuropeptide YY 1 receptor antagonist BIBP3226 produces conditioned place aversion in

rats. *Progress in Neuro-Psychopharmacology and Biological Psychiatry*, *23*(4), 705-711.

94. Kask, A., Rägo, L., & Harro, J. (1998). Anxiogenic-like effect of the NPY Y 1 receptor antagonist BIBP3226 administered into the dorsal periaqueductal gray matter in rats. *Regulatory peptides*, *75*, 255-262.

95. Kathirvelu, B., East, B. S., Hill, A. R., Smith, C. A., & Colombo, P. J. (2013). Lentivirus-mediated chronic expression of dominant-negative CREB in the dorsal hippocampus impairs memory for place learning and contextual fear conditioning. *Neurobiology of learning and memory*, *99*, 10-16.

96. Kesner, R. P. (2007). A behavioral analysis of dentate gyrus function. *Progress in brain research*, *163*, 567-576.

97. Kessler, R. C., Berglund, P., Demler, O., Jin, R., Merikangas, K. R., & Walters, E. E. (2005). Lifetime prevalence and age-of-onset distributions of DSM-IV disorders in the National Comorbidity Survey Replication. *Archives of general psychiatry*, *62*(6), 593-602.

98. Khakpai, F., Nasehi, M., Haeri-Rohani, A., Eidi, A., & Zarrindast, M. R. (2013). Septo-hippocampo-septal loop and memory formation. *Basic and clinical neuroscience*, *4*(1), 5.

99. Kheirbek, M. A., Drew, L. J., Burghardt, N. S., Costantini, D. O., Tannenholz, L., Ahmari, S. E., ... & Hen, R. (2013). Differential control of learning and anxiety along the dorsoventral axis of the dentate gyrus. *Neuron*, *77*(5), 955-968.

100. Kheirbek, M. A., Klemenhagen, K. C., Sahay, A., & Hen, R. (2012). Neurogenesis and generalization: a new approach to stratify and treat anxiety disorders. *Nature neuroscience*, *15*(12), 1613-1620.

101. Kim, J., Kwon, J. T., Kim, H. S., Josselyn, S. A., & Han, J. H. (2014). Memory recall and modifications by activating neurons with elevated CREB. *Nature neuroscience*, *17*(1), 65-72.

102. Kitamura, T., Ogawa, S. K., Roy, D. S., Okuyama, T., Morrissey, M. D., Smith, L. M., ... & Tonegawa, S. (2017). Engrams and circuits crucial for systems consolidation of a memory. *Science*, *356*(6333), 73-78.

103. Kitamura, T., Sun, C., Martin, J., Kitch, L. J., Schnitzer, M. J., & Tonegawa, S. (2015). Entorhinal cortical ocean cells encode specific contexts and drive context-specific fear memory. *Neuron*, *87*(6), 1317-1331.

104. Knierim, J. J. (2015). The hippocampus. *Current Biology*, 25, R1107–R1125.

105. Knox, D. (2016). The role of basal forebrain cholinergic neurons in fear and extinction memory. *Neurobiology of learning and memory*, *133*, 39-52.

106. Krashes, M. J., Koda, S., Ye, C., Rogan, S. C., Adams, A. C., Cusher, D. S., ... & Lowell, B. B. (2011). Rapid, reversible activation of AgRP neurons drives feeding behavior in mice. *The Journal of clinical investigation*, *121*(4), 1424.

107. LaBar, K. S., LeDoux, J. E., Spencer, D. D., & Phelps, E. A. (1995). Impaired fear conditioning following unilateral temporal lobectomy in humans. *Journal of Neuroscience*, *15*(10), 6846-6855.

108. Lach, G., & de Lima, T. C. M. (2013). Role of NPY Y1 receptor on acquisition, consolidation and extinction on contextual fear conditioning: dissociation between anxiety, locomotion and non-emotional memory behavior. *Neurobiology of learning and memory*, *103*, 26-33.

109. Laxmi, T. R., Stork, O., & Pape, H. C. (2003). Generalisation of conditioned fear and its behavioural expression in mice. *Behavioural brain research*, *145*(1), 89-98.

110. LeDoux, J. E. (2000). Emotion circuits in the brain. *Annual review of neuroscience*, *23*(1), 155-184.

111. LeDoux, J. E. (2007). Emotional memory. *Scholarpedia*, *2*(7), 1806.

112. LeDoux, J. E. (2014). Coming to terms with fear. *Proceedings of the National Academy of Sciences*, *111*(8), 2871-2878.

113. Lee, C. T., Kao, M. H., Hou, W. H., Wei, Y. T., Chen, C. L., & Lien, C. C. (2016). Causal Evidence for the Role of Specific GABAergic Interneuron Types in Entorhinal Recruitment of Dentate Granule Cells. *Scientific reports*, *6*.

114. Lee, I., & Kesner, R. P. (2004). Differential contributions of dorsal hippocampal subregions to memory acquisition and retrieval in contextual fear-conditioning. *Hippocampus*, *14*(3), 301-310.

115. Lee, J. L., Everitt, B. J., & Thomas, K. L. (2004). Independent cellular processes for hippocampal memory consolidation and reconsolidation. *Science*, *304*(5672), 839-843.

116. Leutgeb, J. K., Leutgeb, S., Moser, M. B., & Moser, E. I. (2007). Pattern separation in the dentate gyrus and CA3 of the hippocampus. *science*, *315*(5814), 961-966.

117. Levey, A. I., Edmunds, S. M., Koliatsos, V., Wiley, R. G., & Heilman, C. J. (1995). Expression of m1-m4 muscarinic acetylcholine receptor proteins in rat hippocampus and regulation by cholinergic innervation. *Journal of Neuroscience*, *15*(5), 4077-4092.

118. Li, Y., Stam, F. J., Aimone, J. B., Goulding, M., Callaway, E. M., & Gage, F. H. (2013). Molecular layer perforant path-associated cells contribute to feed-forward inhibition in the adult dentate gyrus. *Proceedings of the National Academy of Sciences*, *110*(22), 9106-9111.

119. Lin, H. C., Mao, S. C., Su, C. L., & Gean, P. W. (2010). Alterations of excitatory transmission in the lateral amygdala during expression and extinction of fear memory. *International Journal of Neuropsychopharmacology*, *13*(3), 335-345.

120. Liu, X., Ramirez, S., Pang, P. T., Puryear, C. B., Govindarajan, A., Deisseroth, K., & Tonegawa, S. (2012). Optogenetic stimulation of a hippocampal engram activates fear memory recall. *Nature*, *484*(7394), 381-385.

121. Lockard, J. S. (1963). Choice of a warning signal or no warning signal in an unavoidable shock situation. *Journal of Comparative and Physiological Psychology*, *56*(3), 526

122. Lovett-Barron, M., Kaifosh, P., Kheirbek, M. A., Danielson, N., Zaremba, J. D., Reardon, T. R., ... & Losonczy, A. (2014). Dendritic inhibition in the hippocampus supports fear learning. *Science*, *343*(6173), 857-863.

123. Ludewig, S. (2013). Interneuronen-spezifische Faktoren in der kontextuellen Furchtkonditionierung. (Master Thesis). Magdeburg, Univ., Fak. Für Naturwiss.

124. Madroñal, N., Delgado-García, J. M., Fernández-Guizán, A., Chatterjee, J., Köhn, M., Mattucci, C., ... & Gross, C. T. (2016). Rapid erasure of hippocampal memory following inhibition of dentate gyrus granule cells. *Nature communications*, *7*.

125. Maggio, N., & Segal, M. (2007). Striking variations in corticosteroid modulation of long-term potentiation along the septotemporal axis of the hippocampus. *Journal of Neuroscience*, *27*(21), 5757-5765.

126. Majchrzak, M., Ferry, B., Marchand, A. R., Herbeaux, K., Seillier, A., & Barbelivien, A. (2006). Entorhinal cortex lesions disrupt fear conditioning

to background context but spare fear conditioning to a tone in the rat. *Hippocampus*, *16*(2), 114-124.

127. Maren, S. (2001). Neurobiology of Pavlovian fear conditioning. *Annual review of neuroscience*, *24*(1), 897-931.

128. Maren, S., Phan, K. L., & Liberzon, I. (2013). The contextual brain: implications for fear conditioning, extinction and psychopathology. *Nature Reviews Neuroscience*, *14*(6), 417-428.

129. Martinello, K., Huang, Z., Lujan, R., Tran, B., Watanabe, M., Cooper, E. C., ... & Shah, M. M. (2015). Cholinergic afferent stimulation induces axonal function plasticity in adult hippocampal granule cells. *Neuron*, *85*(2), 346-363.

130. McGaugh, J. L. (2013). Making lasting memories: Remembering the significant. *Proceedings of the National Academy of Sciences*, *110*(Supplement 2), 10402-10407.

131. McHugh, T. J., & Tonegawa, S. (2009). CA3 NMDA receptors are required for the rapid formation of a salient contextual representation. *Hippocampus*, *19*(12), 1153-1158.

132. McHugh, T. J., Jones, M. W., Quinn, J. J., Balthasar, N., Coppari, R., Elmquist, J. K., ... & Tonegawa, S. (2007). Dentate gyrus NMDA receptors mediate rapid pattern separation in the hippocampal network. *Science*, *317*(5834), 94-99.

133. Michael, T., Blechert, J., Vriends, N., Margraf, J., & Wilhelm, F. H. (2007). Fear conditioning in panic disorder: Enhanced resistance to extinction. *Journal of abnormal psychology*, *116*(3), 612.

134. Milad, M. R., Pitman, R. K., Ellis, C. B., Gold, A. L., Shin, L. M., Lasko, N. B., ... & Rauch, S. L. (2009). Neurobiological basis of failure to recall extinction memory in posttraumatic stress disorder. *Biological psychiatry*, *66*(12), 1075-1082.

135. Möhler, H. (2007). Molecular regulation of cognitive functions and developmental plasticity: impact of GABAA receptors. *Journal of neurochemistry*, *102*(1), 1-12.

136. Möhler, H. (2012). The GABA system in anxiety and depression and its therapeutic potential. *Neuropharmacology*, *62*(1), 42-53.

137. Morris, A. M., Weeden, C. S., Churchwell, J. C., & Kesner, R. P. (2013). The role of the dentate gyrus in the formation of contextual representations. *Hippocampus*, *23*(2), 162-168.

138. Moser, M. B., & Moser, E. I. (1998). Functional differentiation in the hippocampus. *Hippocampus*, *8*(6), 608-619.

139. Müller, I., Obata, K., Richter-Levin, G., & Stork, O. (2014). GAD65 haplodeficiency conveys resilience in animal models of stress-induced psychopathology. *Frontiers in behavioral neuroscience*, *8*.

140. Myers, C. E., & Scharfman, H. E. (2009). A role for hilar cells in pattern separation in the dentate gyrus: a computational approach. *Hippocampus*, *19*(4), 321-337.

141. Nagy, A. (2000). Cre recombinase: the universal reagent for genome tailoring. *genesis*, *26*(2), 99.

142. Nakajima, T., Uchida, C., Anderson, S. F., Parvin, J. D., & Montminy, M. (1997). Analysis of a cAMP-responsive activator reveals a two-component mechanism for transcriptional induction via signal-dependent factors. *Genes & Development*, *11*(6), 738-747.

143. Nitz, D., & McNaughton, B. (2004). Differential modulation of CA1 and dentate gyrus interneurons during exploration of novel environments. *Journal of neurophysiology*, *91*(2), 863-872.

144. O'reilly, R. C., & McClelland, J. L. (1994). Hippocampal conjunctive encoding, storage, and recall: avoiding a trade-off. *Hippocampus*, *4*(6), 661-682.

145. Pabst, M., Braganza, O., Dannenberg, H., Hu, W., Pothmann, L., Rosen, J., ... & Schoch, S. (2016). Astrocyte intermediaries of septal cholinergic modulation in the hippocampus. *Neuron*, *90*(4), 853-865.

146. Pandey, S. C. (2003). Anxiety and alcohol abuse disorders: a common role for CREB and its target, the neuropeptide Y gene. *Trends in Pharmacological Sciences*, *24*(9), 456-460.

147. Paredes, M. F., Greenwood, J., & Baraban, S. C. (2003). Neuropeptide Y modulates a G protein-coupled inwardly rectifying potassium current in the mouse hippocampus. *Neuroscience letters*, *340*(1), 9-12.

148. Parfitt, G. M., Campos, R. C., Barbosa, Â. K., Koth, A. P., & Barros, D. M. (2012). Participation of hippocampal cholinergic system in memory

persistence for inhibitory avoidance in rats. *Neurobiology of learning and memory*, *97*(2), 183-188.

149. Park, S., Kramer, E. E., Mercaldo, V., Rashid, A. J., Insel, N., Frankland, P. W., & Josselyn, S. A. (2016). Neuronal allocation to a hippocampal engram. *Neuropsychopharmacology*.

150. Pavlov, P. I. (2010). Conditioned reflexes: an investigation of the physiological activity of the cerebral cortex. *Annals of neurosciences*, *17*(3), 136.

151. Pearson, D. G., Ross, F. D., & Webster, V. L. (2012). The importance of context: evidence that contextual representations increase intrusive memories. *Journal of behavior therapy and experimental psychiatry*, *43*(1), 573-580.

152. Phelps, E. A. (2004). Human emotion and memory: interactions of the amygdala and hippocampal complex. *Current opinion in neurobiology*, *14*(2), 198-202.

153. Phelps, E. A., & LeDoux, J. E. (2005). Contributions of the amygdala to emotion processing: from animal models to human behavior. *Neuron*, *48*(2), 175-

154. Phillips, R. G., & LeDoux, J. E. (1994). Lesions of the dorsal hippocampal formation interfere with background but not foreground contextual fear conditioning. *Learning & Memory*, *1*(1), 34-44.

155. Phillips, R. G., & LeDoux, J. E. (1992). Differential contribution of amygdala and hippocampus to cued and contextual fear conditioning. *Behavioral neuroscience*, *106*(2), 274.

156. Poulin, B., Butcher, A., McWilliams, P., Bourgognon, J. M., Pawlak, R., Kong, K. C., ... & Charlton, S. J. (2010). The M3-muscarinic receptor regulates learning and memory in a receptor phosphorylation/arrestin-dependent manner. *Proceedings of the National Academy of Sciences*, *107*(20), 9440-9445.

157. Poulter, M. O., Du, L., Zhurov, V., Merali, Z., & Anisman, H. (2010). Plasticity of the GABA A receptor subunit cassette in response to stressors in reactive versus resilient mice. *Neuroscience*, *165*(4), 1039-1051.

158. Primeaux, S. D., Wilson, S. P., Cusick, M. C., York, D. A., & Wilson, M. A. (2005). Effects of altered amygdalar neuropeptide Y expression on anxiety-related behaviors. *Neuropsychopharmacology*, *30*(9), 1589-1597.

159. Ramirez, S., Liu, X., Lin, P. A., Suh, J., Pignatelli, M., Redondo, R. L., ... & Tonegawa, S. (2013). Creating a false memory in the hippocampus. *Science*, *341*(6144), 387-391.

160. Ray, R. S., Corcoran, A. E., Brust, R. D., Kim, J. C., Richerson, G. B., Nattie, E., & Dymecki, S. M. (2011). Impaired respiratory and body temperature control upon acute serotonergic neuron inhibition. *Science*, *333*(6042), 637-642.

161. Redrobe, J. P., Dumont, Y., Fournier, A., & Quirion, R. (2002). The neuropeptide Y (NPY) Y1 receptor subtype mediates NPY-induced antidepressant-like activity in the mouse forced swimming test.

162. Reijmers, L. G., Perkins, B. L., Matsuo, N., & Mayford, M. (2007). Localization of a stable neural correlate of associative memory. *Science*, *317*(5842), 1230-1233.

163. Rescorla, R. A., & Wagner, A. R. (1972) A theory of Pavlovian conditioning: Variations in the effectiveness of reinforcement and non reinforcement. Classical Conditioning II, A.H. Black & W.F. Prokasy, Eds., pp. 64–99. Appleton-Century-Crofts.

164. Richter, S. H., Garner, J. P., & Würbel, H. (2009). Environmental standardization: cure or cause of poor reproducibility in animal experiments?. *Nature methods*, *6*(4), 257-261.

165. Rogers, J. L., & Kesner, R. P. (2004). Cholinergic modulation of the hippocampus during encoding and retrieval of tone/shock-induced fear conditioning. *Learning & Memory*, *11*(1), 102-107.

166. Rozeske, R. R., Valerio, S., Chaudun, F., & Herry, C. (2015). Prefrontal neuronal circuits of contextual fear conditioning. *Genes, Brain and Behavior*, *14*(1), 22-36.

167. Rubinson, D. A., Dillon, C. P., Kwiatkowski, A. V., Sievers, C., Yang, L., Kopinja, J., ... & Gertler, F. B. (2003). A lentivirus-based system to functionally silence genes in primary mammalian cells, stem cells and transgenic mice by RNA interference. *Nature genetics*, *33*(3), 401-406.

168. Rudy, J. W. (2009). Context representations, context functions, and the parahippocampal–hippocampal system. *Learning & memory*, *16*(10), 573-585.

169. Rudy, J. W., & O'Reilly, R. C. (2001). Conjunctive representations, the hippocampus, and contextual fear conditioning. *Cognitive, Affective, & Behavioral Neuroscience*, *1*(1), 66-82.

170. Savanthrapadian, S., Meyer, T., Elgueta, C., Booker, S. A., Vida, I., & Bartos, M. (2014). Synaptic properties of SOM-and CCK-expressing cells in dentate gyrus interneuron networks. *Journal of Neuroscience*, *34*(24), 8197-8209.

171. Scharfman, H. E. (1995). Electrophysiological diversity of pyramidal-shaped neurons at the granule cell layer/hilus border of the rat dentate gyrus recorded in vitro. *Hippocampus*, *5*(4), 287-305.

172. Schmidt, B., Marrone, D. F., & Markus, E. J. (2012). Disambiguating the similar: the dentate gyrus and pattern separation. *Behavioural brain research*, *226*(1), 56-65.

173. Schwegler, H., Boldyreva, M., Pyrlik-Göhlmann, M., Linke, R., Wu, J., & Zilles, K. (1996). Genetic variation in the morphology of the septo-hippocampal cholinergic and GABAergic system in mice. I. Cholinergic and GABAergic markers. *Hippocampus*, *6*(2), 136-148.

174. Senut, M. C., Menetrey, D., & Lamour, Y. (1989). Cholinergic and peptidergic projections from the medial septum and the nucleus of the diagonal band of Broca to dorsal hippocampus, cingulate cortex and olfactory bulb: a combined wheatgerm agglutinin-apohorseradish peroxidase-gold immunohistochemical study. *Neuroscience*, *30*(2), 385-403.

175. Shanks, D. R. (2010). Learning: From association to cognition. *Annual review of psychology*, *61*, 273-301.

176. Shimizu, E., Tang, Y. P., Rampon, C., & Tsien, J. Z. (2000). NMDA receptor-dependent synaptic reinforcement as a crucial process for memory consolidation. *Science*, *290*(5494), 1170-1174.

177. Sik, A., Penttonen, M., & Buzsáki, G. (1997). Interneurons in the hippocampal dentate gyrus: an in vivo intracellular study. *European Journal of Neuroscience*, *9*(3), 573-588.

178. Silva, A. J., Kogan, J. H., Frankland, P. W., & Kida, S. (1998). CREB and memory. *Annual review of neuroscience*, *21*(1), 127-148.

179. Skórzewska, A., Bidziński, A., Lehner, M., Turzyńska, D., Wisłowska-Stanek, A., Sobolewska, A., ... & Płaźnik, A. (2006). The effects of acute and chronic administration of corticosterone on rat behavior in two models of fear responses, plasma corticosterone concentration, and c-Fos expression in the brain structures. *Pharmacology Biochemistry and Behavior*, *85*(3), 522-534.

180. Sloviter, R. S., & Nilaver, G. (1987). Immunocytochemical localization of GABA-, cholecystokinin-, vasoactive intestinal polypeptide-, and somatostatin-like immunoreactivity in the area dentata and hippocampus of the rat. *Journal of Comparative Neurology*, *256*(1), 42-60.

181. Soares, J. C. K., Fornari, R. V., & Oliveira, M. G. M. (2006). Role of muscarinic M1 receptors in inhibitory avoidance and contextual fear conditioning. *Neurobiology of learning and memory*, *86*(2), 188-196.

182. Soghomonian, J. J., & Martin, D. L. (1998). Two isoforms of glutamate decarboxylase: why?. *Trends in pharmacological sciences*, *19*(12), 500-505.

183. Somogyi, P., Hodgson, A. J., Smith, A. D., Nunzi, M. G., Gorio, A., & Wu, J. Y. (1984). Different populations of GABAergic neurons in the visual cortex and hippocampus of cat contain somatostatin-or cholecystokinin-immunoreactive material. *Journal of Neuroscience*, *4*(10), 2590-2603.

184. Sperk, G., Hamilton, T., & Colmers, W. F. (2007). Neuropeptide Y in the dentate gyrus. *Progress in brain research*, *163*, 285-297.

185. Squire, L. R. (1984). Human memory and amnesia. *Neurobiology of learning and memory*, 3-64.

186. Squire, L. R. (2004). Memory systems of the brain: a brief history and current perspective. *Neurobiology of learning and memory*, *82*(3), 171-177.

187. Stanciu, M., Radulovic, J., & Spiess, J. (2001). Phosphorylated cAMP response element binding protein in the mouse brain after fear conditioning: relationship to Fos production. *Molecular brain research*, *94*(1), 15-24.

188. Stefanelli, T., Bertollini, C., Lüscher, C., Muller, D., & Mendez, P. (2016). Hippocampal somatostatin interneurons control the size of neuronal memory ensembles. *Neuron*, *89*(5), 1074-1085.

189. Stegmeier, F., Hu, G., Rickles, R. J., Hannon, G. J., & Elledge, S. J. (2005). A lentiviral microRNA-based system for single-copy polymerase II-regulated

RNA interference in mammalian cells. *Proceedings of the National Academy of Sciences of the United States of America*, *102*(37), 13212-13217.

190. Stern, P., Astrof, S., Erkeland, S. J., Schustak, J., Sharp, P. A., & Hynes, R. O. (2008). A system for Cre-regulated RNA interference in vivo. *Proceedings of the National Academy of Sciences*, *105*(37), 13895-13900.

191. Stork, O., Ji, F. Y., & Obata, K. (2002). Reduction of extracellular GABA in the mouse amygdala during and following confrontation with a conditioned fear stimulus. *Neuroscience letters*, *327*(2), 138-142.

192. Swanson, L. W. (2003). The amygdala and its place in the cerebral hemisphere. *Annals of the New York Academy of Sciences*, *985*(1), 174-184.

193. Swanson, L. W., & Risold, P. Y. (2000). On the basic architecture of the septal region. In *The behavioral neuroscience of the septal region* (pp. 1-14). Springer New York.

194. Sweatt, J. D. (2009). *Mechanisms of memory*. Academic Press.

195. Taniguchi, H., He, M., Wu, P., Kim, S., Paik, R., Sugino, K., ... & Miyoshi, G. (2011). A resource of Cre driver lines for genetic targeting of GABAergic neurons in cerebral cortex. *Neuron*, *71*(6), 995-1013.

196. Tasan, R. O., Verma, D., Wood, J., Lach, G., Hörmer, B., de Lima, T. C. M., ... & Sperk, G. (2016). The role of Neuropeptide Y in fear conditioning and extinction. *Neuropeptides*, *55*, 111-126.

197. Tatemoto, K., Carlquist, M., & Mutt, V. (1982). Neuropeptide Y—a novel brain peptide with structural similarities to peptide YY and pancreatic polypeptide. *Nature*, *296*(5858), 659-660.

198. Thorndike, E. L. (1898). *Animal Intelligence, an Experimental Study of the Associative Processes in Animals, by Edward L. Thorndike,...* Macmillan.

199. Tomioka, R., Okamoto, K., Furuta, T., Fujiyama, F., Iwasato, T., Yanagawa, Y., ... & Tamamaki, N. (2005). Demonstration of long-range GABAergic connections distributed throughout the mouse neocortex. *European Journal of Neuroscience*, *21*(6), 1587-1600.

200. Trifilieff, P., Calandreau, L., Herry, C., Mons, N., & Micheau, J. (2007). Biphasic ERK1/2 activation in both the hippocampus and amygdala may reveal a system consolidation of contextual fear memory. *Neurobiology of learning and memory*, *88*(4), 424-434.

201. Van der Zee, E. A., & Luiten, P. G. M. (1999). Muscarinic acetylcholine receptors in the hippocampus, neocortex and amygdala: a review of immunocytochemical localization in relation to learning and memory. *Progress in neurobiology*, *58*(5), 409-471.

202. Verma, D., Tasan, R. O., Herzog, H., & Sperk, G. (2012). NPY controls fear conditioning and fear extinction by combined action on Y1 and Y2 receptors. *British journal of pharmacology*, *166*(4), 1461-1473.

203. Vervliet, B., Baeyens, F., Van den Bergh, O., & Hermans, D. (2013). Extinction, generalization, and return of fear: a critical review of renewal research in humans. *Biological psychology*, *92*(1), 51-58.

204. Viosca, J., de Armentia, M. L., Jancic, D., & Barco, A. (2009). Enhanced CREB-dependent gene expression increases the excitability of neurons in the basal amygdala and primes the consolidation of contextual and cued fear memory. *Learning & Memory*, *16*(3), 193-197.

205. Wallenstein, G. V., & Vago, D. R. (2001). Intrahippocampal scopolamine impairs both acquisition and consolidation of contextual fear conditioning. *Neurobiology of learning and memory*, *75*(3), 245-252.

206. Wang, Z., Neylan, T. C., Mueller, S. G., Lenoci, M., Truran, D., Marmar, C. R., ... & Schuff, N. (2010). Magnetic resonance imaging of hippocampal subfields in posttraumatic stress disorder. *Archives of general psychiatry*, *67*(3), 296-303.

207. Watson, C., Paxinos, G., & Puelles, L. (Eds.). (2012). *The mouse nervous system*. Academic Press.

208. Wilensky, A. E., Schafe, G. E., & LeDoux, J. E. (1999). Functional inactivation of the amygdala before but not after auditory fear conditioning prevents memory formation. *Journal of Neuroscience*, *19*(24), RC48-RC48.

209. Wolff, S. B., Gründemann, J., Tovote, P., Krabbe, S., Jacobson, G. A., Müller, C., ... & Lüthi, A. (2014).

210. Xu, W., & Südhof, T. C. (2013). A neural circuit for memory specificity and generalization. *Science*, *339*(6125), 1290-1295.

211. Yannielli, P. C., & Harrington, M. E. (2001). Neuropeptide Y in the mammalian circadian system: effects on light-induced circadian responses. *Peptides*, *22*(3), 547-556.

212. Zelikowsky, M., Bissiere, S., Hast, T. A., Bennett, R. Z., Abdipranoto, A., Vissel, B., & Fanselow, M. S. (2013). Prefrontal microcircuit underlies contextual learning after hippocampal loss. *Proceedings of the National Academy of Sciences*, *110*(24), 9938-9943.

213. Zheng, F., Wess, J., & Alzheimer, C. (2012). M 2 muscarinic acetylcholine receptors regulate long-term potentiation at hippocampal CA3 pyramidal cell synapses in an input-specific fashion. *Journal of neurophysiology*, *108*(1), 91-100.

214. Zhou, Y., Won, J., Karlsson, M. G., Zhou, M., Rogerson, T., Balaji, J., ... & Silva, A. J. (2009). CREB regulates excitability and the allocation of memory to subsets of neurons in the amygdala. *Nature neuroscience*, *12*(11), 1438-1443.

Appendix

A1 Methods

A1.1 Chrm1 knockdown

Chrm1 coding sequence in its full length was amplified from pYX-Chrm1 (ImaGenes) with the help of primers 5′-TAGGAACACCTCAGTGCCCCCTGC-3′ and 5′-TATTAGCATTGCTCGAGGCGGGAGGGGGTGC-3′ and inserted in a frame to vector pCMV-HA (Clontech) through the EcoRI and XhoI restricition sites. The efficiency to knock down the co-expressed HA-Chrm1 mRNA was tested in a cell culture with five plasmids that contain shChrm1 knockdown constructs in a vector pLKO.1 (Sigma-Aldrich, Seelze, Germany).

Authenticated NIH3T3 and HEK293T cells were obtained from the German Collection of Microorganisms and Cell Cultures and were regularly tested in our lab for mycoplasma contamination. Dulbeccos Modified Eagles Medium (DMEM) supplemented with 10% fetal bovine serum (FBS, both Life Technologies, Darmstadt, Germany) to 80% confluence was used to culture NIH3T3 cells. HA-Chrm1 and shLuc or shChrm1 plasmids were used for co-transfection of cells using Lipofectamine 2000 (Life Technologies, Darmstadt, Germany), following instructions from manufacturer's protocol. The lysis of transfected cells was carried out in 1% dodecyl maltoside, 0.5% DOC, 1% NP-40, 50 mM Tris (pH 7.5), 1 mM AEBSF, 150 mM NaCl, 1 μM Pepstatin and PIC tablet (Life Technologies, Darmstadt, Germany). The lysate was separated by the SDS-PAGE and transferred to PVDF membranes (Merck Millipore, Darmstadt, Germany), which were probed with primary antibodies against anti-HA (Merck Millipore, Darmstadt, Germany) and anti-tubulin (Sigma-Aldrich, Seelze, Germany) and fluorescence-labeled secondary antibodies (LI-COR, Germany). Protein bands were visualized with Odyssey® imaging system (LI-COR, Germany) and quantified in ImageJ software. Normalization of HA-Chrm1 amounts was done against tubulin levels (Appendix, A 3.7C). Yunus Emre Demiray (MSc) and Susann Ludewig (MSc) efficiently carried out this work in our lab.

An shRNA construct harboring the sequence 5′-CCGG<u>CATGAACCTCTATACCACATAC</u>TGGAGTATGTGGTATAGAGGTTCATGTTTTT-3′ was selected, on the basis of its knockdown efficiency, for *in vivo* experiments. This sequence targets bp758–bp779 of Chrm1 transcript variant 2 (NM_007698.3) and

bp850–bp871 of Chrm1 transcript variant 1 (NM_001112697.1). The website from Cold Spring Harbour Laboratories (katahdin.cshl.org) was used to design a suitable 97-mer oligonucleotide for expression via miR30 (Stegmeier et al, 2005). Amplification of oligomers (Invitrogen, Karlsruhe, Germany) was carried out with using the primers, miR30 5′-GATGGCTGCTGGAGAAGGTATATTGCTGTTGACAGTGAGCG-3′ and miR30rev 5′-GTCTAGAGGAATTCCGAGGCAGTAGGCA-3′ to add restriction sites for XhoI and EcoRI restriction enzymes These restriction sites were then used for subsequent cloning into pLL-dfRmFF. For the generation of control viral particles, pLL-dfRmFF without insertion was used.

A1.2 Immunohistochemistry

To visualize cholinergic fibers and cholinergic muscarinic M1 receptors, Nicolai Faber (MD) performed staining protocols. Briefly, animals were transcardially perfused with 0.9% saline followed by a immunofixative containing 4% PFA and 15% saturated picric acid in 0.1 M PB. After perfusion, brains were removed from the skull, post-fixed for 6 h in the same fixative followed by 24 h storage in 20% sucrose at 8° C and later stored at –80° C until further processing. Brains were cut into 40 μm thick frozen sections, washed 3 times with 0.1 M PB and incubated with a solution containing 10% normal goat serum and bovine serum albumin in 0.1 M PB for 30 min to block unspecific bindings. Incubation with primary antibody (antiChAT, 1:100, Novus biological; antiChrm1, 1:250, Sigma Aldrich) was done for 3 nights at 4° C according to defined protocols (Panther et. al 2012). As secondary antibody, biotinylated anti-goat (1:200, BA-1000 and BA-5000, Vector Laboratories) was used with 2 h incubation. Visualisation was done by conjugation with streptavidin Cy2 or Cy3 (both at 1:1000; #016-160-084, Jackson ImmunoResearch Labs, UK). After three more wash steps with 0.1 M PB, sections were embedded with a solution containing 2% DABCO®, glycerol and Vectashield™. Immunostainings in all experiments were examined using a DMI 6000 epifluorescence microscope and a TCS SP2 or a SP8 confocal microscope (all Leica Microsystems, Germany).

A1.3 Patch clamp recordings

To examine HIPP cells activity modulation through M1 receptors, Susanne Meis (PhD), determine the spiking properties of these cells.

A1.3.1 Slice preparation

Deeply anesthetized NPY-GFP transgenic mice with isoflurane were decapitated. Brain tissue that contained a block of the hippocampus was quickly removed and placed in ice-cold oxygenated physiological saline containing 2.4 mM KCl, 10 mM $MgSO_4$, 0.5 mM $CaCl_2$, 24 mM $NaHCO_3$, 1.25 mM NaH_2PO_4, 10 mM glucose, 195 mM sucrose and bubbled with 95% O_2/5% CO_2. Transverse slices with 300-µm thicknesses were cut with Microslicer™ (Ted Pella, USA) and incubated in a solution containing 125 mM NaCl, 2.5 mM KCl, 1.25 mM NaH_2PO_4, 24 mM $NaHCO_3$, 3.8 mM $MgSO_4$, 0.2 mM $CaCl_2$, 10 mM glucose and bubbled with 95% O_2/5% CO_2 to a final pH of 7.3. Slices were allowed to recover at 34° C for 20 min and maintained for up to 5 h at 20° C.

A1.3.2 Recording technique

Individual slices were transferred to a submersion chamber and continuously perfused at a rate of approx. 2 ml per min at 30° C ± 1° C with aCSF containing 1.25 mM NaCl, 2.5 mM KCl, 1.25 mM NaH_2PO_4, 2 mM $MgSO_4$, 2 mM $CaCl_2$, 22 mM $NaHCO_3$, 10 mM glucose and bubbled with 95%O_2/5% CO_2. 10 µM pirenzipine (Sigma-Aldrich, Seelze, Germany), 10 µM 6,7-dinitroquinoxaline-2,3-dione (DNQX), 50 µM DL-2-amino-5-phosphono-pentanoic-acid (AP5) and 10 µM bicuculline methiodide (all Tocris Bioscience, Ellisville, Missouri, USA) were added to the perfusion solution to constantly block synaptic transmission. 10 µM Oxotremorine M (Tocris Bioscience, Ellisville, Missouri, USA) was applied only once for 3-4 min to each slice.

A patch-clamp amplifier (EPC-9, Heka Elektronik, USA) under visual control of differential interference contrast infrared video microscopy (S/W-camera CF8/1, Kappa, Germany) was used to perform whole cell patch-clamp recordings. A monochromator (Polychrome II, Till Photonics) connected to an epifluorescence system and a 40^x/0.80 water immersion lens was used to identify GFP^+ interneurons. Patch pipettes were pulled from borosilicate glass (GC150T-10, Clark Electromedical Instruments) to resistances around 3 MΩ and were filled with 95 mM K gluconate, 20 mM K_3 citrate, 10 mM NaCl, 10 mM HEPES, 1 mM $MgCl_2$, 0.1 mM $CaCl_2$, 5 mM EGTA, 3 mM MgATP, 0.5 mM NaGTP (pH 7.25 with KOH). A liquid junction potential of 10 mV was corrected. Hyperpolarizing current pulses had an intensity of -30 pA and duration of 500 ms. Depolarizing current pulses were adjusted to elicit 1 to 4 spikes (+100 to +250 pA, 500 ms).

A2 Genotyping of different mouse lines

DNA isolation from tail tissue

For genomic DNA isolation, a minor tissue (< 0.3 cm) is removed from the tails of mice shortly after their weaning. The animals are given earmarks for the identification. The tail tissue is subjected to an overnight digestion with protein kinase K (10 mg/ml, Carl Roth GmbH, Karlsruhe, Germany) and PCR direct lysis buffer (Peqlab, Erlangen, Germany) at 55° C. The lysis reaction is inactivated with water bath at 85° C for 45 min, after 24 h. The samples were then subjected to allele specific PCR for identification of respective genotypes or stored at -20° C. After completion of the PCR reaction, the PCR products are then subjected to ethidium bromide containing agarose gel electrophoresis. This method help visualization of DNA bands under UV light and their size is then confirmed with the standard DNA ladder.

PCR primers and protocol

SST-CreERT2

Primers

P1 Mutant forward	5'-ATA GTT TGC GCA CGT CCA TTT TCC TGT-3'
P2 Common	5'-GCA TGT CAG CAC TGA GTG AAG GTA-3'
P3 Mutant reverse	5'-GGG ACT TTC CAC ACC CTA ACT-3'

Master mix 1x *(11 μl + 1 μl DNA)*

10x CL Buffer	1.25 μl
MgCl$_2$ (25 mM)	0.75 μl
dNTP (2.5 mM)	1.0 μl
Q Solution	2.5 μl
dH$_2$O	3.9 μl
P1	1.25 μl
P2	1.25 μl
P3	1.25 μl
Taq Polymerase	0.1 μl

PCR conditions

Phase	Duration	Temperature	Nr. of cycles
Initial denaturation	5 min	94° C	
Denaturation	15 min	94° C	

Annealing	30 min	60° C	40x
Extension	60 min	72° C	
Final extension	7 min	72° C	
Storage	∞	4° C	

NPY-GFP

Primers

P1 Mutant reverse	*5'-GGT GCG GTT GCC GTA CTG GA-3'*
P2 Common	*5'-TAT GTG GAC GGG GCA GAA GAT CCA GG-3'*
P3 Wild type reverse	*5'-CCC AGC TCA CAT ATT TAT CTA GAG-3'*

Master mix 1x *(9 µl + 1 µl DNA)*

10x Dream Taq green Buffer	1.5 µl
dNTP (2.5 mM)	0.5 µl
Q Solution	2.5 µl
dH₂O	4.4 µl
P1	0.5 µl
P2	0.75 µl
P3	1.25 µl
DreamTaqPolymerase	0.1 µl

PCR conditions

Phase	Duration	Temperature	Nr. of cycles
Initial denaturation	30 s	94° C	
Denaturation	30 s	94° C	
Annealing	1 min	65° C	35x
Extension	1 min	72° C	
Final extension	1 min	72° C	
Storage	∞	4° C	

PV-Cre

Primers

P1 Mutant forward	*5'-GCG GTC TGG CAG TAA AAA CTA TC-3'*
P2 Mutant reverse	*5'-GTG AAA CAG CAT TGC TGT CAC TT-3'*
P3 Wild type forward	*5'-CAG AGC AGG CAT GGT GAC TA-3'*
P4 Wild type reverse	*5'-AGT ACC AAG CAG GCA GGA GA -3'*

Master mix 1x *(9 µl + 1 µl DNA)*

10x CL Buffer	1.0 µl

dNTP (2.5 mM)	0.5 μl
dH$_2$O	5.45 μl
P1	0.5 μl
P2	0.5 μl
P3	0.5 μl
P4	0.5 μl
Taq Polymerase	0.05 μl

PCR conditions

Phase	Duration	Temperature	Nr. of cycles
Initial denaturation	3 min	94° C	
Denaturation	30 s	94° C	
Annealing	30 s	62° C	35x
Extension	45 s	72° C	
Final extension	7 min	72° C	
Storage	∞	4° C	

CamK2a-Cre mice

Primers

P1 Cre-tot 1	*5′-ACG ACC AAG TGA CAG CAA TG-3′*
P2 Cre-tot 2	*5′-CTC GAC CAG TTT AGT TAC CC-3′*
P3 TR1B	*5′-GGC ACA GCT CTC CCT TCT GTT TGC-3′*
P4 TR3	*5′-GCT CTC CTT TCG CGT TCC GAC AG-3′*

Master mix 1x *(9 μl + 1 μl DNA)*

10x Dream Taq green Buffer	1.0 μl
dNTP (2.5 mM)	0.8 μl
dH$_2$O	5.5 μl
P1	0.5 μl
P2	0.5 μl
P3	0.3 μl
P4	0.3
DreamTaqPolymerase	0.05 μl

PCR conditions

Phase	Duration	Temperature	Nr. of cycles
Initial denaturation	5 min	94° C	

Denaturation	30 s	94° C	
Annealing	30 s	60° C	30x
Extension	30 min	72° C	
Final extension	7 min	72° C	
Storage	∞	4° C	

Chat-Cre

Primers

P1 Wild type forward	5'-GCA AAG AGA CCT CAT CTG TGG A-3'
P2 Common	5'-CAG GGT TAG TAG GGG CTG AC-3'
P3 Mutant forward	5'-CAA AAG CGC TCT GAA GTT CCT-3'

Master mix 1x *(9 µl + 1 µl DNA)*

10x Dream Taq green Buffer	1.0 µl
dNTP (2.5 mM)	1.0 µl
dH$_2$O	6.45 µl
P1	0.5 µl
P2	0.5 µl
P3	0.5 µl
DreamTaqPolymerase	0.05 µl

PCR conditions

Phase	Duration	Temperature	Nr. of cycles
Initial denaturation	3 min	94° C	
Denaturation	15 s	94° C	
Annealing	15 s	64° C	35x
Extension	30 min	72° C	
Final extension	7 min	72° C	
Storage	∞	4° C	
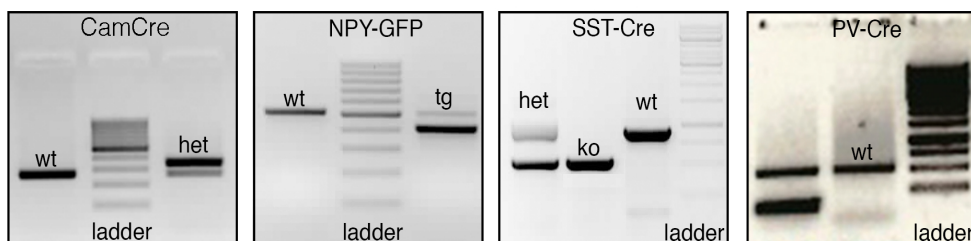
A3 Data corresponding to results section (3.0)

A3.1 M1 acetylcholine receptors confirmation on NPYergic HIPP cells
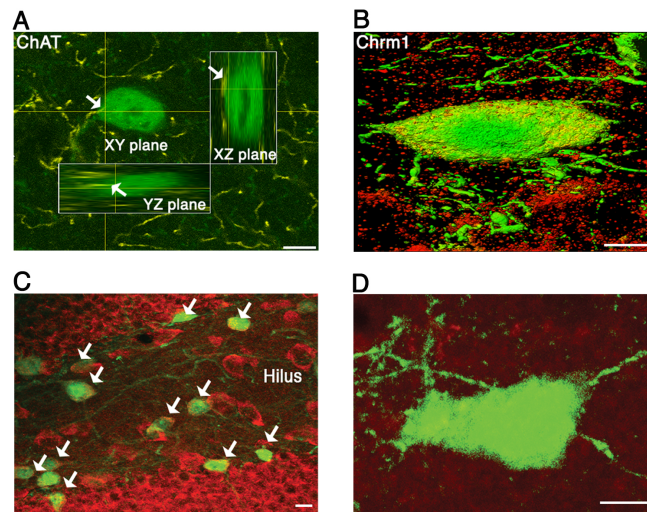
Fig. A 3.1: (**A**) A 3D reconstruction of a confocal image (X, Y, Z spatial planes) of the NPY-GFP neuron that shows cholinergic fibers (arrows) on its soma. Scale bar, 10 μm. (**B**) Somatic immunolabeling for Chrm1 receptors on NPY$^+$ HIPP cell. Green, NPY-GFP cells; red, Chrm1 receptors. Scale bar, 5 μm. (**C**) Immunostaining for Chrm1 in the dorsal DG of an NPY-GFP mouse. Green, NPY-GFP cells; red, Chrm1 receptors. White arrows indicate co-labeling of Chrm1 with the NPY cells. Scale bar, 10 μm. (**D**) A negative control for M1 immune staining. Scale bar 5 μm.

A3.2 Electrophysiological characterization of the muscarinic response of HIPP cell

Fig. A 3.2: (**A**) Representative current-clamp recording of a single NPY$^+$ HIPP cell during action of the muscarinic agonist oxotremorine M, in the absence (upper) and presence (lower) of the M1

antagonist pirenzepine, respectively. Examples illustrate responses to depolarizing and hyperpolarizing test pulses at a faster time scale before, during maximal action and after wash 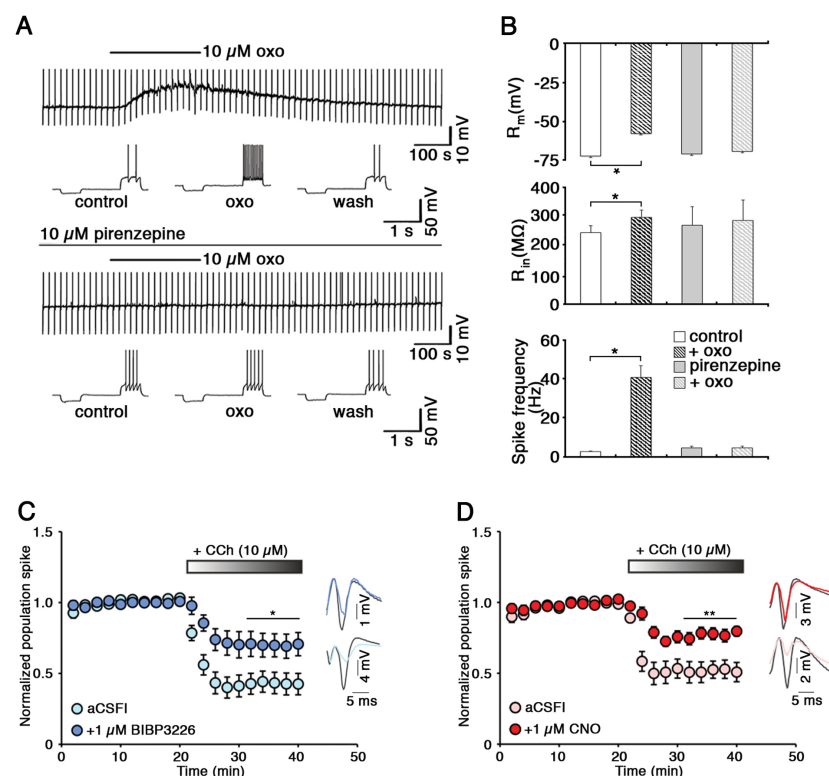out of oxo. Application of oxo induces a transient depolarization associated with an increase in apparent input resistance under control conditions. Note the increase in spike activity during the drug action. The effect of oxo is abolished when applied during continuous presence of pirenzepine. (**B**) Muscarinergic agonist oxo (10 μM) produced a transient membrane depolarization in all 7-recorded neurons from resting membrane potential. These effects are also reflected by a significant increase in a mean spike frequency as well as input membrane resistance provoked by the injections of positive current. In the presence of the M1 receptor antagonist pirenzepine (10 μM; *n* = 5) oxo could not produce such effects. (**C**) (Left) Y1 receptor blockage does not affect baseline excitability of the DG, but counteracts the carbachol-induced inhibition (10 μM CCh (light blue) *n* = 8 slices, 1 μM BIBP3226 + 10 μM CCh (blue) *n* = 10). Example traces to the right of the graph illustrate the difference in response to the perforant path stimulation. (Right) Pharmacogenetic inhibition of HIPP cells (with 10 μM CNO) mimics the effect of BIBP3226. Data are presented as means + s.e.m. Statistical analysis was performed with Wilcoxon signed rank test (**A**) and with Student's unpaired *t*-test. *$P < 0.05$, **$P < 0.01$.

A3.3 Anxiety testing with Chrm1 receptors blockage and Chrm1 receptors knockdown
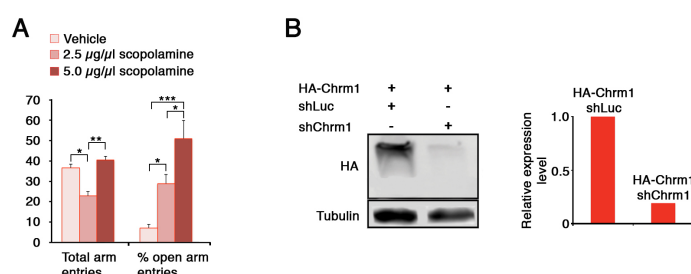
Fig. A3.3: (**A**) Increased entries to open arm in elevated plus maze is seen with scopolamine infusion (2.5 μg/μl scopolamine, *n* = 7; 5 μg/μl scopolamine, *n* = 10) compared to vehicle group (*n* = 9). This indicates anxiolytic like effect of scopolamine. (**B**) (Left) Western blot of NIH3T3 cells expressing HA-tagged Chrm1 receptors that are transfected with either shLuc or shChrm1. (Right) Quantification of the blot shows a drastic decrease of HA-Chrm1 protein in shChrm1-transfected cells compared to the control shLuc. Data are presented as means + s.e.m. Statistical analysis was performed with one-way ANOVA followed by Fischer's LSD . *$P < 0.051$, **$P < 0.01$, ***$P < 0.001$.

A4 Chemicals

Agarose	Peqlab, Erlangen, Germany
BIBP 3226	Tocris, Ellisville, Missouri, USA
Bovine serum albumine (BSA)	Carl Roth, Karlsruhe, Germany
CaCl2	Sigma-Aldrich, Seelze, Germany
Corn oil	Sigma Aldrich, Seelze, Germany
Cresyl violet acetate	Sigma-Aldrich, Seelze, Germany
Clozapine N Oxide	Enzo life sciences, Germany
Dental	cement Hoffmann Dental Manufaktur, Berlin, Germany
di-Nucleotide-Tri-Phosphate (dNTPs)	Fermentas, St. Leon-Rot, Germany
Dimethyl dicarbonat (DMDC)	Sigma-Aldrich, Seelze, Germany
Dimethylsulfoxid (DMSO)	Finnzymes, Vantaa, Finland
DirectPCR-Tail lysis reagent	Peqlab, Erlangen, Germany
Donkey serum	Vector laboratories, Burlingame, USA
Ethanol 96 %	Carl Roth, Karlsruhe, Germany
Ethidium bromid	Carl Roth, Karlsruhe, Germany
Eye ointment	Bepanthen, Germany
Immu-Mount™	Thermo Scientific, Germany
Isoflurane	Nicholas Piramal limited, UK
KCl	Carl Roth, Karlsruhe, Germany
Ketamine/ Xylazine	Sigma-Aldrich, Seelze, Germany
KH_2PO_4	Sigma-Aldrich, Seelze, Germany
Methylbutane	Carl Roth, Karlsruhe, Germany
Na_2HPO_4	Sigma-Aldrich, Seelze, Germany
Na_2HPO_4 x $2H_2O$	Carl Roth, Karlsruhe, Germany
NaCl	Carl Roth, Karlsruhe, Germany
NaHCO3	Carl Roth, Karlsruhe, Germany
NaOH	Carl Roth, Karlsruhe, Germany
Novalgin inj.	Sanofi Aventis
Oligonucleotide (dT)18 primer	Ambion/ Life Technologies, Darmstadt,
Paladur resin	Heraeus Kulzer GmbH, Wehrheim, Germany
Paraformaldehyde	Carl Roth, Karlsruhe, Germany
Pentobarbital	Sigma-Aldrich, Seelze, Germany
Poly-L-Lysine 1 %	Sigma-Aldrich, Seelze, Germany
Primer for genotyping PCRs	Life Technologies, Darmstadt, Germany
Proteinase K	Carl Roth, Karlsruhe, Germany
Random decamer primer	Ambion/ Life Technologies, Darmstadt,
RNAse Zap	Life Technologies, Darmstadt, Germany

Sodium Thiosulfate	Sigma-Aldrich, Seelze, Germany
Sucrose	Sigma-Aldrich, Seelze, Germany
SuperaseIN	Ambion/ Life Technologies, Darmstadt,
Tamoxifen	Sigma-Aldrich, Seelze, Germany
TissueTek	Leica, Nussloch, GermanyNetherlands
TRIS hydrochloride	Carl Roth, Karlsruhe, Germany
Triton X	Sigma-Aldrich, Seelze, Germany
β-Mercaptoethanol	Serva, Heidelberg, Germany
4', 6-diamidino-2-phenylindole dihydrochloride (DAPI)	Life Technologies, Darmstadt, Germany

A5 Solutions and buffers

1 % Cresyl violet solution

- 1 g Cresyl violet acetate
- 50 ml 96 % ethanol
- fill with double-destilled water to 100 ml
- stir for 7 h at room temperature, protected from light
- filter
- store protected from light

DMDC water treatment

- 0.1 % Dimethyldicarbonate in double-destilled water
- Stir for 3 h
- Autoclave

10x Phosphate buffered

- saline (PBS)
- solve 11.5 g Na2HPO x H2O
- 2.0 g KH2PO4
- 80.0 g NaCl
- 2.0 g KCl
- in ca. 900 ml double-destilled water
- adjust pH to 7.4
- fill up to 1 l final volume with double-destilled water

4 % Paraformaldehyde (PFA)

- solve 40 g PFA in ca. 700 ml double-destilled water,
- stir on heating plate at 70 ÅãC until solution is clear
- add 500 μl NaOH (5 M) for better solving
- let cool down on ice (ca. 1 h)

- filtrate cooled PFA
- add 100 ml 10x PBS
- adjust pH to 7.4
- fill up volume to 1 l with double-destilled water

Poly-L-Lysine
- 1:2 dilution of Poly-L-Lysine 0.1 % in double destilled water

0.9 % Saline
- solve 4.5 g sodium chloride in 500 ml double-destilled water
- autoclave

30 % Sucrose
- solve 30 g sucrose in ca. 80 ml double-destilled water
- add 10 ml 10x PBS
- fill up to 100 ml with double-destilled water

Tamoxifen (for i.p.injections of 2/ 4/ 8 mg in 100 ml vehicle solution)
- solve 40/ 80/ 160 mg Tamoxifen powder in 200 µl 96 % Ethanol,
- Add corn oil to 2 ml, vortex vigorously
- Sonicate 2-3x 15 min
- Store at -20 C

Tyrode buffer
- solve 4.000 g NaCl
- 0.100 g KCl
- 0.050 g MgCl2
- 0.500 g NaHCO3
- 0.100 g CaCl2
- 0.025 g NaH2PO4
- 0.500 g Glucose
- in 500 ml double-destilled water
- stire until clear solution
- store at 4° C

aCSF
- 21mM NaHCO3
- 129 mM NaCl
- 1.6 mM CaCl2
- 3 mM KCl
- 1.25 mM NaH2PO4
- 1.8 mM MgSO4
- 10 mM glucose

A6 Kits and assays

Ambion Cells-to-cDNA Kit II	Life Technologies, Darmstadt, Germany
Dream Taq polymerase	Fermentas, St. Leon-Rot, Germany
RNeasy FFPE kit	Qiagen, Hilden, Germany
RNeasy Micro Plus kit	Qiagen, Hilden, Germany
SensiscriptReverse Transcription kit	Qiagen, Hilden, Germany
TaqPolymerase	Qiagen, Hilden, Germany
QuickTite™ Lentivirus Titer Kit	Cell Biolabs, USA

A7 Antibodies

Primary Antibodies

HA-tag	Cell Signaling #3724, Frankfurt am Main, Germany
anti-NPY	Abcam, Cambridge, UK
anti-SST	Santa Cruz Biotechnology #13099, Heidelberg, Germany
anti-cFos	Cell Signaling #2250, Frankfurt am Main, Germany

Secondary antibodies

Alexa Fluor 488	Life Technologies, Germany
Alexa Fluor 555	Life Technologies, Germany
Cy2	Jackson ImmunoResearch Labs, UK

A8 Consumables and instruments

Animal care

LignocelBK 8/15	J. Rettenmaier & Sohne, Rosenberg, Germany
Macrolon standard cages (type II long)	Techniplast, Hohenpeissenberg, Germany
	Bioscape, Castrop-Rauxel, Germany
Ssni_ R/M-H V-1534	Ssni_ Spezialitaten, Soest, germany

Autoclave

Systec DB-23 & VA120	Systec Labortechnik, Wettenberg, Germany

Behavioral test systems

TSE Fear Conditioning System	TSE, Bad Homburg, Germany
Open field	Stoelting Co., Wood Dale, IL, USA

Elevated plus maze   Stoelting Co., Wood Dale, IL, USA

Cryostat

CM 1950   Leica, Nussloch, Germany

Freezers and Fridges

Liebherr KU 2407   Liebherr Hausgerate, Ochsenhausen,
                                            Germany

Liebherr GU 4506   Liebherr Hausgerate, Ochsenhausen, Germany

Sanyo Ultra Low   Ewald Innovationstechnik, Bad Nenndorf,
                                            Germany

Glass ware

Glass bottles   Carl Roth, Karlsruhe, Germany

Beaker   Carl Roth, Karlsruhe, Germany

Graduated cylinder   Carl Roth, Karlsruhe, Germany

Staining cuvettes   Carl Roth, Karlsruhe, Germany

Slide holder   Carl Roth, Karlsruhe, Germany

Object slide box   Carl Roth, Karlsruhe, Germany

Membrane slides 1.0 PEN   Carl Zeiss, Jena, Germany

Laser capture system

Laser capture micro dissection system   PALM MicroBeam Carl Zeiss, Jena, Germany

Pipettes

Pipettes   Brand, Wertheim, Germany

Pipette tips   Brand, Wertheim, Germany

Plastic ware

Adhesive cap 500 clear   Carl Zeiss, Jena, Germany

Micro-Amp Fast Reaction Tubes   Life Technologies, Darmstadt, Germany

Micro-Amp 8-cap strips   Life Technologies, Darmstadt, Germany

Micor   -Amp Fast Optical 96-well plate   Life Technologies, Darmstadt, Germany

Micro-Amp Optical Adhesive Film   Life Technologies, Darmstadt, Germany

Real-time PCR

StepOne Plus Real-Time PCR system   Applied Biosystems, Darmstadt, Germany

Software

Anymaze Video tracking system   Stoelting Co., Wood Dale, IL, USA

SPSS Statistics	IBM, Ehningen, Germany
Micorsoft Office	Mircosoft, Redmond, WA, USA
Palm Robosoftware	Carl Zeiss, Jena, Germany
StepOnev2	Life Technologies, Darmstadt, Germany
Graph pad	GraphPad Software, Inc. USA
Adobe Photoshop CS4 Extended	Adobe Systems, San Jose, CA, USA
MATLAB-based analysis tools	MathWorks, Natick, MA, USA

Stereotactic surgery

Stereotactic frame	World precision instruments, Berlin, Germany
Surgical instruments	Carl Roth, Karlsruhe, Germany
Non-absorbable suture material	5-0/PS3, Perma-Hand. silk suture
Micro drill	World precision instruments, Berlin, Germany
5% isoflurane in O_2/N_2O mixture	Rothacher Medical GmbH., Switzerland
Digital microsyringe pump	World precision instruments, Berlin, Germany
NanoFil microsyringe 10 µl	World Precision Instruments, Berlin, Germany
Guide cannula, 26G	Plastics One, Roanoke, VA, USA
Dummy for guide cannula	Plastics One, Roanoke, VA, USA
Internal cannula, 33G	Plastics One, Roanoke, VA, USA
Jeweler's screw	Plastics One, Roanoke, VA, USA

Thermocycler

Veriti Thermal Cycler	Applied Biosystems, Darmstadt, Germany

Others

Scale-Sartorius TE 2101	Sartorius AG, Gottingen, Germany
Centrifuge-Heraeus Pico 17	Thermo Scientific, Germany
Vortexer-VWR Lab dancer	S40 VWR International, Darmstadt, Germany
Water bath-LAUDA A103	Lauda Dr. R. Wobser, Lauda-Konigshof, Germany
Sonicator	VWR International, Darmstadt, Germany
Hot plate	Medite OTS 40.2530 Medite, Burgdorf, Germany